1-1-2014

Solubility Enhancement and Precipitation Inhibition of Poorly Water Soluble Compounds Utilizing Hot Melt Extrusion Technology

Jiannan Lu
University of Mississippi

SOLUBILITY ENHANCEMENT AND PRECIPITATION INHIBITION OF POORLY WATER SOLUBLE COMPOUNDS UTILIZING HOT MELT EXTRUSION TECHNOLOGY

A Dissertation
presented in the Partial Fulfillment of Requirements
for the Doctoral of Philosophy Degree
in the Department of Pharmaceutics
The University of Mississippi

Jiannan (Henry) Lu

Oxford, Mississippi

March 2014

ABSTRACT

Soluplus® (SOL), a graft amorphous copolymer, composed of polyethylene glycol, vinyl acetate and vinylcaprolactam in a ratio of 13: 30: 57, was utilized to prepare solid dispersions containing felodipine (FEL) or ketoconazole (KTZ) using hot-melt extrusion technology. The melting point depression approach was utilized to determine the miscibility and solubility of the model compounds within Soluplus®, of which felodipine demonstrated higher solubility when compared to ketoconazole (14% vs 4.3% w/w) at room temperature (298K). Moreover, the solubility parameters of FEL, KTZ and SOL were calculated as 21.76, 26.51 and 21.64, respectively.

Polarized light microscopy, Fourier transform infrared spectroscopy (FT-IR), Raman microscopy, differential scanning calorimetry (DSC), X-Ray diffraction (XRD), and scanning electron microscopy (SEM) were explored to characterize the FEL-SOL solid dispersions, and FEL was found to be molecularly dispersed in the matrix at a concentration of 10% w/w, which also demonstrated a higher solubility.

A central composite design (CCD) was applied to optimize the processing parameters for KTZ-SOL solid dispersions and the final formulation containing 29.8% drug was extruded at a temperature of 140°C and screw speed of 31 rpm. The robustness of the design was also examined.

A solid dispersion system of paclitaxel (PTX) was also developed to increase the aqueous solubility in order to overcome the side effects of its commercial products Taxol®, which was accomplished with the addition of a non-ionic surfactant, Cremophor® EL. PolyOx™ WSR N-80

(Molecular weight: 200,000 Da) was utilized as the matrix carrier, in which the concentration of PTX was determined as 30%. Various surfactants and solubilizers, including sodium lauryl sulfate (SLS), Lutrol® F68 (F68) and polyethylene glycol (PEG) 3350 were incorporated into the formulation. Of these, PEG 3350 was found to increase the solubility of PTX to 9.29 µg/ml (9-fold); however, the formulation started to precipitate after 2 hours due to the high energy amorphous state of PTX. 5% hydroxypropyl methylcellulose acetate succinate (HPMCAS-LF) successfully postponed the precipitation and maintained the solubility up to 12 hours by forming hydrogen bonds with PTX. This finding was confirmed by FT-IR analysis.

ACKNOWLEDGEMENT

I wish to express the sincere appreciation to my supervisor, Dr. Michael A. Repka, Chair and Professor in the Department of Pharmaceutics, for his continuous support, encouragement, patience and guidance over the last five years. I have learned not only the scientific facts but the art of thinking and how to be a man.

I would like to thank Dr. Soumyajit Majumdar and Dr. Seongbong Jo of Department of Pharmaceutics and Dr. John O'Haver of Department of Chemical Engineering, for being my committee members, thanks for your valuable expertise and suggestions for my studies; I could not have completed my thesis without your help.

I would also like to thank all the faculty and staff in Pharmacy School, especially Dr. Michael Repka, Dr. Soumyajit Majumdar, Dr. Seongbong Jo, Dr. Christy M. Wyandt and Dr. Walter Chambliss. I am thankful to Ms. Deborah King for her patience and assistance in handling the daily issues in the Department of Pharmaceutics. I thank Dr. Sejal Shah for her expertise and advice on my research during her Postdoc period in the department. I also want to thank Dr. Vijayasankar Raman of National Center for Natural Products Research for his time and assistance in the study of polarized light microscopy and scanning electron microscopy. I appreciate the assistance of Dr. Nathan Hammer and his graduate student Kristina Cuellar in the Department of Chemistry and Biochemistry for the use of Raman microscopy.

In addition, I am deeply thankful to all my colleagues and friends for their support and help in all aspects, especially Dr. Feng Zhang, Dr. Huiju Liu, Dr. Yidan Lan, Dr. Jin Xu, Dr. Yanbin Huang, Xin Feng, Joe Morott, Ying Wang, Ketaki Patwardhan, Sindhuri Maddineni,

Manjeet Pimparade, Xingyou Ye, Zhen Guo and Jian Gong. My life is exciting and fulfilled because of you.

I also want to recall with gratitude the mentor, suggestions and help from my supervisors Dr. Deliang Zhou in Abbott Laboratories, Inc. and Mr. Sakae Obara in SE Tylose USA, Inc. respectively, during my internships. I learned a lot from them about how to become a pharmaceutical scientist.

Finally and most importantly, I am very much grateful to my family members, whom this dissertation is dedicated to, for their unwavering love, endless encouragement and support. I could not make the journey this far without you.

TABLE OF CONTENTS

LIST OF TABLES

TABLE **PAGE**

LIST OF FIGURES

FIGURE **PAGE**

CHAPTER 1.

INTRODUCTION

1. 1 Solid dispersion

Currently, many new chemical entities are synthesized by high throughput screening and computational chemistry which results in good biological activity but poor aqueous solubility. This ultimately results in poor oral bioavailability and limits further development of final dosage forms [1, 2]. To address this issue, various techniques have been developed and explored, including formation of salts[3], polymorphs[4], co-crystal[5], solubilized formulations[6-9], nanoparticles[10, 11], and more recently, solid dispersion technology which has attracted increasing interest from both industry and academia[12-18]. Solid dispersions were initially defined as a solid system in which one or more active pharmaceutical ingredients (APIs) are dispersed into one inert carrier by Chiou and Riegelman[19]. The carrier could be amorphous or crystalline, while the API(s) could be either molecularly dispersed into the matrix or dispersed as aggregates. According to the molecululer arrangement of the API within the matrix and the physical state of carriers, solid dispersion could be further classified into three categories, crystalline solid dispersion, amorphous solid dispersion and amorphous solid solution[20-22] (Figure 1-1). In a crystalline solid dispersion system, multiple phases will exist simultaneously, which can be identified by differential scanning calorimetry (DSC) with a glass transition temperature (T_g) corresponding to the carrier and a melting endotherm (T_m) representing the crystalline drug. Therefore, a solid crystalline dispersion is also referred to as a solid crystalline suspension[20]. The solubility of a drug substance can be enhanced by the approach of breaking

down the size of drug particles into micro or nano region[23]. The amorphous solid dispersion is generated when the drug is converted into an amorphous state and dispersed throughout the carrier matrix; however, they have a tendency to revert to their more stable, lower energy crystalline forms from a thermodynamic standpoint. At the same time, a kinetically induced recrystallization will also occur since the amorphous solid dispersion often contains a drug-concentrated region [22, 24]. In a solid solution, which can be defined as a particular subgroup of amorphous solid dispersion, the drug substance is molecularly dispersed into the carrier with only one single glass transition temperature observed in DSC.

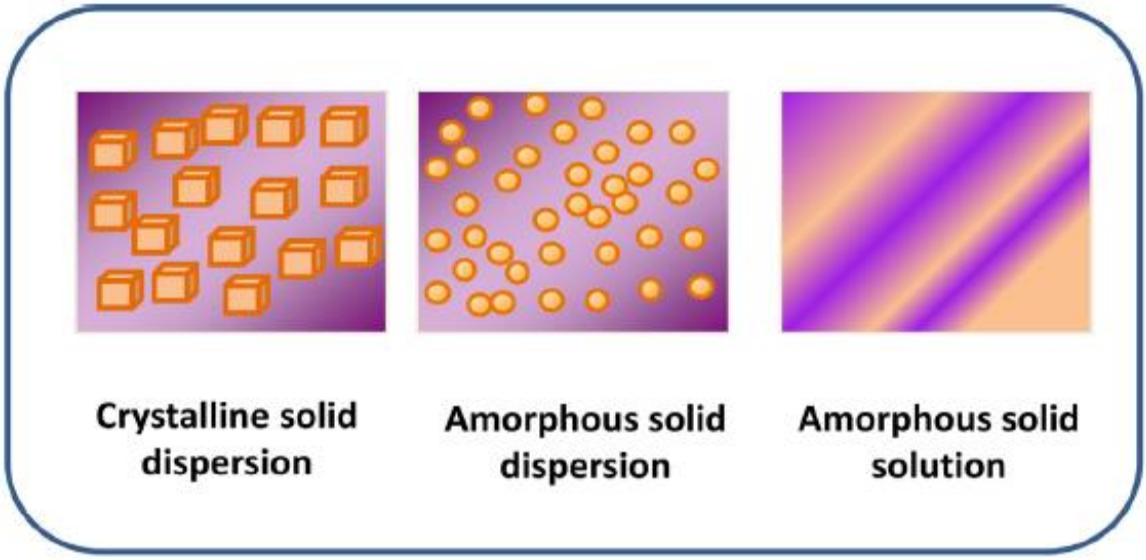

Figure 1-1 State of Solid Dispersion[20]

Basically, there are two types of approaches to produce solid dispersions, fusion-based method and solvent-based method [22, 24, 25]. A solid dispersion can be prepared by a fusion-based method simply by heating the drug-carrier mixture along with other formulation additives to a temperature above their glass transition temperature, melting point or eutectic point, and then followed by cooling at a controlled rate[26-32]. A prerequisite for any material to be processed by this method is thermal stability [24, 25, 33]. Moreover, the miscibility and

compatibility between drug and carrier needs to be seriously considered. The high viscosity of a molten carrier can lead to phase separation and result in an inhomogeneous dispersion which will further threaten the stability of the final products[34]. In terms of a solvent-based method, the hydrophobic drug substances will dissolve with the hydrophilic carriers into their common solvent which will be evaporated [35-47]. Compared to a fusion-based method, this type of technology is often operated at a lower temperature which is more suitable for heat sensitive compounds. However, it is not very straightforward to find a common solvent for the rapidly increasing NCEs and carriers[22]. Moreover, it is always a hurdle to eliminate the solvent residue in the solid dispersions. The common methods to produce solid dispersions are listed in Table 1-1.

Table 1-1: List of methods to produce solid dispersions

Fusion-based methods	Solvent-based methods
Traditional heating and cooling [26, 29, 30]	Traditional evaporation[35-38]
Spray congealing[31]	Spray drying[39, 40]
Hot melt extrusion[28, 32]	Freeze drying[41]
Meltrex^{TM}[48]	Supercritical anti-solvent[43]
Melt agglomeration[27]	Co-precipitation[44]
	Electrostatic spinning[45]
	Fluid-bed coating[42]
	Cryogenic processing techniques[46, 47]

1. 2 Hot melt extrusion

Hot melt extrusion (HME) is one of most widely applied technologies in the plastic industry which dates back to the late 1930s, and was introduced to pharmaceutical industry approximately three decades ago[20, 21, 49-51]. Over the traditional technologies, it offers several unique and distinctive advantages, for instance, continuous process with limited steps, solvent free process and ease to scale up. In addition, the HME process has very low dead-volume, which results in less material loss, if the proper screw design, process parameters and formulation were selected, which is eco-effectively. The applications of HME primarily include solubility/bioavailability enhancement of poorly water soluble compounds [28, 32], taste-masking[52, 53], controlled/sustained release[54, 55] and solid state stability enhancement[56, 57].

The main drawbacks associated to hot-melt extrusion technology is similar to other fusion based methods to produce solid dispersions as previously mentioned[14, 20, 22, 24, 25, 33, 49]. Processing at a high temperature may induce thermal degradation of the materials used[58], which will possibly exclude some of the heat sensitive substances, proteins or peptides, for instance, to HME applications. Finally, although the number of the suitable polymers for HME is increasing, it is still not proportional to the needs of the pharmaceutical industry.

1. 2. 1. Equipment and process

For over three decades, extruders have been well developed to meet the demands of pharmaceutical industry and manufacturing companies have made great effort to design an extruder that is well adapted to the current good manufacturing practices (cGMPs)[20, 50]. Several fundamental characteristics can be utilized to classify hot melt extruders, for instance, the number of screws, direction of screw rotation (co-rotating or counter-rotating), degree of

intermeshing and length of screw barrel (ratio of length/diameter)[21]. A twin screw extruder is often comprised of the following parts: drive, feed, barrel with screw elements, heating/cooling device, control panel, torque transducer, assorted dies and downstream processing equipment (Figure 1-2).

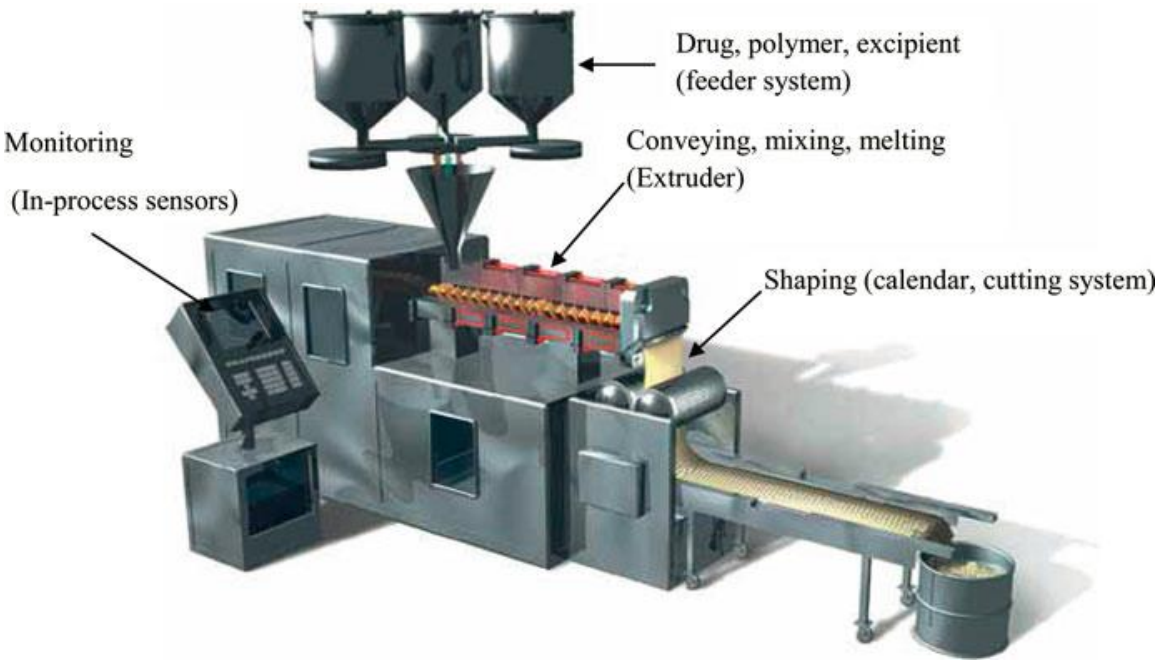

Figure 1-2: Schematic representation of a typical pharmaceutical twin-screw extruder[59]

Generally speaking, a hot melt extrusion process can be defined as process in which the APIs, carriers and other formulation additives will be mixed and extruded under a high temperature and shear condition into a specific shape. From the processing prospective, HME can be theoretically divided into five steps, i) feeding, ii) melting and plasticizing, iii) conveying and mixing, iv) venting and v) stripping and downstream processing[60, 61]. Each elementary section may affect the properties of the final extrudates.

1. 2. 2. Materials

The materials used in a hot melt extrusion process beyond the APIs can be classified into three categories, matrix carriers, plasticizers and other formulation additives. All of components used in HME process are of pharmaceutical grade and thermally stable.

1. 2. 2. 1 Carriers

Carrier materials can be divided into two groups: polymeric and non-polymeric. It is important to select the proper carrier materials which will affect the formulation and final dosage forms in many aspects. The commonly used carriers in HME process are listed in Table 1-2.

Table 1-2: List of carrier materials used in HME

Chemical Name	Trade Name	T_g (°C)	T_m (°C)
Ammonio methacrylate copolymer[62, 63]	Eudragit® RS/RL	64	
Polyvinyl caprolactam– polyvinyl acetate–polyethylene glycol graft copolymer[64]	Soluplus®	70	
Polyvinyl pyrrolidoneco-vinyl acetate[65, 66]	Kollidon® VA64	101	
Hypromellose acetate succinate[66, 67]	Aqoat®	~120	
Hydroxypropyl cellulose[68]	Klucel™	Soften at 130	
Poly(vinyl pyrrolidone)[69]	Kollidon®	90-156	
Polyethylene oxide [70] (Molecular weight>100,000 Da)	PolyOx™	-57 to -50	62-67
Polyethylene glycol[69] (Molecular weight<100,000 Da)	Carbowax™		37-63
Hydroxypropyl methylcellulose[54]	Methocel®	160-210	
Glyceryl palmitostearate [71]	Precirol® ATO 5		52-55
Polyvinyl alcohol–polyethylene glycol copolymer[72]	Kollicoat IR®	45	208
Poly(dimethylaminoethylmethacrylateco-methacrylic esters)[66]	Eudragit® E	50	
Glyceryl trimyristate[71]	Dynasan® 114		55-58
Triglyceride tripalmitin[73]	Dynasan® 116		61-65
Carnauba wax[74]	---		81-86
Ethyl cellulose[75, 76]	Aqualon®	130-133	
Polyvinyl acetate[77]	Sentry® Plus	35-40	
Polyvinyl acetate-polyvinylpyrrolidone copolymer[78]	Kollidon® SR	~35	
Poly(lactide-co-glycolide)[79]	PLGA		

1. 2. 2. 2 Plasticizers

In order to improve the processing conditions of HME, plasticizers are often incorporated into the formulation. Theoretically, any low molecule weight substances which can reduce the secondary bonding between polymer chains and further improve their mobility may be used as plasticizers. The glass transition temperature and melt viscosity of the polymer can be reduced due to the enhanced free volume between polymer chains[80]. The selection of suitable plasticizers for HME is generally on a case-by-case basis, and the study of compatibility with matrix carrier as well as the plasticization effect should be conducted before the HME process, which can be easily achieved on DSC. Several substances have already been demonstrated as plasticizers in extrusion, which include citric acid monohydrate[81], methy paraben[82], low molecular PEG[83], surfactants[84], triethyl citrate[62, 83], acetyltributyl citrate[83], Vitamin E succinate[58], and Vitamin E TPGS[58, 85]. In addition to the traditional plasticizers, drugs were reported to function as plasticizers themselves in many cases [70, 83]. Moreover, supercritical carbon dioxide (CO_2) was recently introduced as a gas plasticizer with some unique benefits. Beyond the reduction of glass transition temperature of polymer and the operating temperature of the extrusion process, the incorporation of CO_2 can increase the porosity of polymer resulting in a faster drug release of the dosage forms[76, 86]. It can also be easily removed at the end of the process without any residue which retains the simplicity of the formulation.

1. 2. 2. 3 Other formulation additives

In order to achieve the desired final dosage forms or prevent the degradation from the high processing temperature, it is common to incorporate other additives into the formulation, which include release modifier[87], antioxidants[58], forming agents[76] and swelling agents[85].

1. 2. 3 Current commercial products produced by HME

As aforementioned, hot-melt extrusion has demonstrated great versatility in pharmaceutical applications with its solvent-free and continuous processing, Additionally, HME readily lends itself to process analytical technology (PAT) and Quality by Design (QbD), which makes it even more suitable for the pharmaceutical industry. As a result, the contract manufacturing companies using HME technology are spreading around US and the world [50]. To date, there are already several HME products in the current market (Table 1-3), and many pharmaceutical companies are making great effort to develop solid dispersion products via HME technology[20].

Table 1-3: Current commercial products produced via HME[21]

Product	Indication	Company
Lacrisert®	Dry eye syndrome	Merck
Zoladex™	Prostate cancer	AstraZeneca
Implanon®	Contraceptive	Organon
Gris-PEG	Antifungal	Pedinol Pharmacal Inc.
NuvaRing®	Contraceptive	Merck
Norvir®	HIV	Abbott Laboratories
Kaletra®	HIV	Abbott Laboratories
Eucreas®	Diabetes	Novartis
Zithromax®	Antibiotic	Pfizer
Orzurdex®	Macular edema	Allergan
Fenoglide™	Dyslipidemia	Life Cycle Pharma
Noxafil®	Antifungal	Merck

1. 3 Material Properties

Certain general pharmaceutical criteria have to be met for all of the materials used in hot-melt extrusion processing, which includes the basic safety and toxicity requirement[49]. In addition, thermal stability is also a prerequisite for all the components. However, with the incorporation of suitable plasticizers, proper screw configuration/design and proper selection of feeding portion, the mean residence time of extrusion process can be shortened, which leaves open the possibility of processing some thermally sensitive compounds.

1. 3. 1 Properties of APIs

The physico-chemical properties of APIs, including T_g, T_m, phase solubility, hydrogen bonding, ionic nature, partition coefficient, and polymorphism, etc., have to be carefully determined during the pre-formulation period before the hot-melt extrusion process, which also pilot the preliminary screening of carriers[21, 49, 88].

1. 3. 2 Properties of Polymers

The polymers play an important role in the hot-melt extrusion process. It is, therefore, also necessary to consider the polymer-related properties to select the proper carriers or determine the suitable processing parameters. Several important parameters of polymers are listed as below.

1. 3. 2. 1 Glass transition temperature

Glass transition temperature (T_g) is one of most important characteristics of any polymer. At a temperature above the T_g, there is only short range or asymmetry order in the pattern of polymer molecules and the chains of polymers have partial flexibility. When the temperature is below the T_g, the polymer are rigid with poor molecular mobility[89]. At this temperature, polymers will undergo a glass transition from amorphous (glassy) to crystalline (rubbery) state

when the polymer liquids are cooled from its melting temperature. Two competitive transitions might occur during the process. The polymers will turn into amorphous state, if the polymer monomer has an irregular structure. On the other hand, part of polymers with regular structure will crystallize. However, from a kinetic standpoint, the process to identify a correct packing pattern is slow, resulting in a remaining amorphous part of the polymer. Consequently, this type of polymer is defined as a semi-crystalline polymer and the amorphous part of which will also undergo a glass transition; however, less pronounced changes in the properties will be observed for semi-crystalline polymers relative to amorphous polymers[89, 90].

As a matter of fact, the T_g is closely related to hot-melt extrusion process. Normally, the processing temperature of hot melt extrusion is set up as 15-60°C above the melting point of semi-crystalline polymers or the T_g of amorphous polymers to reduce the torque required to rotate the screws[91, 92]. From a processing prospective , a polymer with low glass transition temperature, for instance, Soluplus® (approximately T_g =70°C[93]), will be beneficial, since extrusion of polymers with higher T_g often requires a higher processing temperature might lead to degradation of either the polymer or the APIs.

1. 3. 2. 2 Viscosity

Theoretically, viscosity represents the resistance of a fluid to the flow. Unlike the liquid materials, whose viscosity is an intrinsic property, only affected by temperature and pressure, the viscosity of a polymer melt inside the hot-melt extruder is more complicated since the polymer melt is viscoelastic, resulting in a combination of viscosity and elastic effect on its flow[94]. The viscosity of the polymer melts will depend on the polymer properties as well as the processing conditions. The following equation can express the viscosity of a pseudoplastic fluid which most of polymer will behave as during the hot-melt extrusion process[60].

$\eta = K \times \gamma^{n-1}$ .....Equation 1-1

Whereas, η is the viscosity of the polymer melt, γ is the shear rate, K is an exponential function of the temperature and related to the properties of the polymer, and n is the power law constant (typically $0.25 \leq n \leq 0.9$ for polymer melts).

The viscosity of the polymer at a fixed shear rate can be expressed as the following Arrhenius equation[51]:

$\eta = K' \times e^{Ea/RT}$ .....Equation 1-2

Whereas, η is the viscosity of polymer melts, K' is a constant depending on the structure and molecular mass of the polymer, Ea is the activation energy of the polymer for the flow process and is constant for the same type of polymer, R is the gas constant and T is the temperature in Kelvin degree.

1. 3. 2. 3 Hygroscopicity

As previously mentioned, water can function as a plasticizer itself and tremendously affect the physical stability of amorphous solid dispersions. This is particularly true during storage, therefore, the hygroscopicity of polymer needs to be paid close attention to when selecting suitable carriers. It has been reported that water can threaten the physical stability of solid dispersions through numerous pathways, for instances, weakening the drug-polymer intermolecular interactions, decreasing the solubility/miscibility of the drug within polymers resulting in phase separation, or reducing the glass transition temperature leading to enhanced molecular mobility. In terms of stabilization of amorphous solid dispersions, hydrophobic polymers with ionic groups in the structure, for instance, HPMC-AS or Eudragit® L/E 100, have been demonstrated a better capacity[95].

1. 3. 2. 4 Solubility parameter

Solubility parameter δ is one of the approaches to quantify the cohesive energy, which represents the strength of attraction between constituent molecules in the substance. In other words, it determines the energy input required to remove one molecule from its adjacent molecule to an infinite distance, from a thermodynamic standpoint [88, 94, 96]. All kinds of intermolecular interactions, including Van der Waals, covalent bonding, hydrogen bonding, ionic and electrostatic interactions, will contribute to the cohesive energy[96]. It has been broadly applied to estimate the likelihood of drug-polymer miscibility since it was first introduced by Hildebrand[69, 70, 97-100]. The solubility parameter was initially defined as[100]:

$$\delta = (\frac{E_T}{V})^{1/2} \quad \text{Equation 1-3}$$

Where, E_T is the cohesive energy and V is the molar volume.

It was pointed out by Hansen that not only the contribution from dispersion forces E_d, but also from the polar forces E_p and the hydrogen bonding E_h should be accounted when predicting the cohesive energy of substances[101]. Hence, the overall cohesive energy can be written as:

$$E_{T=}E_d + E_p + E_h \quad \text{Equation 1-4}$$

The solubility parameter can be further expressed as:

$$\delta_T^2 = \delta_d^2 + \delta_p^2 + \delta_h^2. \quad \text{Equation 1-5}$$

Two group contribution methods, the Hoy method and Hoftyzer/Van Krevelen method, were developed to determine the solubility parameter based on the Hansen's assumption[94, 102].

In Hoy method, for small molecular weight substances:

$$\delta_T = (F_i + B)/\text{V} \quad \text{Equation 1-6}$$

For amorphous polymers:

$\delta_T = (F_i + B/N)/\mathrm{V}$…….. Equation 1-7

Where F_i is the summary of molar attraction of each component in the structure; B, as a constant, is the base value, N is the number of repeating units in each effective chain and can be calculated as:

$N = 0.5/\Delta_T^{(P)}$……. ……Equation 1-8

Where the Δ_T is the Lydersen correction for non-ideality.

In Hoftyzer/ Van Krevelen method:

$\delta_d = \frac{\sum F_{di}}{V}, \delta_p = \frac{\sqrt{\sum F_{pi}^2}}{V}, \delta_h = \sqrt{\frac{\sum E_{hi}}{V}}$…… Equation 1-9

Where, F_{di}, F_{pi}, and E_{hi} are the different component group contributions in the chemical structure[94].

1.4 Thermodynamic aspects and melting point depression

As mentioned before, APIs will be mixed with carriers and other formulation ingredients in hot-melt extrusion processing. For the mixing of two or more components at a constant temperature and pressure, the change of free energy of mixing could be expressed as the followed equation:

$\Delta G=\Delta H-T\Delta S$……...Equation 1-10

Where ΔG is the Gibbs free energy of mixing, ΔH is the enthalpy of mixing, ΔS is the entropy of mixing and T is the temperature at which the mixing occurs.

The entropy of mixing represents the combination of arrangements of molecules in the lattice according to the Flory-Huggins theory which is a statistical treatment of the polymer solution. For blends of small molecular weight substances, the combinatorial entropy, which represents the number of arrangements of each component in the lattice, mainly determines whether they are miscible, immiscible or partially miscible; however, with increasing molecular

weight, the substance would occupy more positions in the lattice resulting in a decrease of combinatorial entropy. Therefore, other than combinatorial entropy, factors like the non-combinatorial entropy and the enthalpy of mixing would dominate the miscibility of the mixture[103].

The phenomenon of melting point depression was broadly observed in the field of polymer blends [104-107], and was further introduced into study the miscibility/compatibility of drug-polymer systems based on the assumption that the drug-polymer system is analogous to the solute-solvent system in the Flory-Huggins theory which is a lattice based, statistical model[108] [109-112]. It is illustrated that the chemical potential of the drug would diminish during the melting process if the drug was miscible with polymer and could dissolve in it which would lead to the drop-off of melting point. The drug-polymer interaction parameter $\chi_{drug\text{-}polymer}$ could be calculated by Equation 4:

$$\frac{1}{T_m} - \frac{1}{T_m^0} = -\frac{R}{\Delta H_{fusion}}\left[ln\emptyset_{drug} + \left(1 - \frac{1}{m}\right) * \left(1 - \emptyset_{drug}\right) + \chi_{drug-polymer}(1 - \emptyset_{drug})^2\right] \quad \text{Equation 1-11}$$

Where T_m and T_m^0 are the melting point of drug in the binary mixture and pure crystalline drug, respectively, R is the gas constant, ΔH_{fusion} is the heat of fusion of the pure drug, ϕ is the volume fraction of drug, and m is volume ratio of polymer to the lattice and can be estimated as:

$$m = \frac{M_W(polymer)/\rho(polymer)}{M_w(drug)/\rho(drug)} \quad \text{Equation 1-12}$$

At the same time, $\chi_{drug\text{-}polymer}$ is variable with temperature and can be mathematically expressed as[103]:

$$\chi\,(T) \cong A + \frac{B}{T} \quad \text{Equation 1-13}$$

Where both of A and B are constants.

Another approach to estimate the interaction parameter is by using the solubility parameter which was development by Hildebrand and Scott[100]:

$$\chi = \frac{\nu(\delta_{drug} - \delta_{polymer})^2}{RT} \quad \text{Equation 1-14}$$

Where ν is the volume per lattice site, δ is the solubility parameter, R is the gas constant and T is the temperature. The Hildebrand method only considers the dispersion force and was suitable for the nonpolar mixtures. Further modification of this method was conducted with the involvement of the polar forces and hydrogen bonding, resulting in a more precise prediction. However, in the current study, to simplify, the authors only took the established values from peers as the solubility parameter and hence the calculated χ value was used only as a reference. For more details about the group additive methods, the readers are encouraged to reference the valuable textbook[94].

A complete phase diagram of the drug-polymer binary system could be generated according to the highly temperature dependent Gibbs free energy of mixing:

$$\Delta G_{mix} = RT[\emptyset_{drug} ln \emptyset_{drug} + \frac{1-\emptyset_{drug}}{m} \ln(1 - \emptyset_{drug}) + \chi_{drug-polymer} \emptyset_{drug}(1 - \emptyset_{drug}) \quad \text{Equation 1-15}$$

Therefore, the binodal curve (T_b-$\emptyset_{drug}$), which represents the coexistence of two components in one phase without phase separation, could be extrapolated by the common tangent method.

$$(\frac{\partial \Delta G}{\partial \emptyset})_{\emptyset=\emptyset_1} = (\frac{\partial \Delta G}{\partial \emptyset})_{\emptyset=\emptyset_2} \quad \text{Equation 1-16}$$

The above equation (9) can be solved by numerical analysis using Matlab or other computational softwares. It is worth pointing out that for any composition between $\emptyset_1$ and $\emptyset_2$

(the difference is called as miscibility gap), the binary system can be spontaneously stabilized by separation into $\emptyset_1$ and $\emptyset_2$.

The following spinodal curve (T_s--$\emptyset_{drug}$), which is the boundary of metastable and unstable region, could be plotted by equalizing the second derivation of ΔG_{mix} to zero, hence:

$$T_s = \frac{2B}{\frac{1}{\emptyset_{drug}} + \frac{1}{m(1-\emptyset_{drug})} - 2A} \quad \text{Equation 1-17}$$

1. 5 Supersaturating drug delivery system

According to the Fick's first law, the drug absorption depends on the permeability coefficient and concentration in the gastrointestinal tract (GIT)[113]. Therefore, to achieve good solubility is a crucial factor for achieving acceptable bioavailability of biopharmaceutical classification system's (BCS) class II or IV drugs. Solid dispersions can enhance the solubility of poorly water soluble compounds through converting the drug from its crystalline form to its amorphous form, which is a relatively higher energy state. As a result, the concentration of drug in solution may be higher than its saturated concentration when the formulation is entering the gastrointestinal tract and a supersaturated solution is obtained. However, the amorphous state is usually thermodynamically unstable, and it has the tendency to lower the energy through a precipitation pathway during dissolution, which will possibly limit the absorption [114, 115]. More time for drug absorption will be provided if the precipitation step is delayed or prohibited. Various pharmaceutical excipients, including polymers[116-119], surfactants[120, 121]and cyclodextrins [122, 123], have been applied for this purpose.

1. 6 Design of Experiment (DoE)

Design of experiments (DOE) has been recently introduced to pharmaceutical development and recommended by the US Food and Drug Administration (FDA) from a quality by design (QbD) prospective, which was thoroughly discussed in ICH guidelines Q8, Q9 and

Q10. In addition to process analytical technologies (PAT), multivariate data-analysis and/or prior knowledge, a robust process or product with good qualities can be achieved. Response surface methodology (RSM) is an approach comprised of mathematical and statistical techniques for the development, improvement and optimization of processing or product development which can model the responses of dependent variables from the alteration of the independent variables by using a sequence well-designed experiments[124]. It has been utilized in many aspects of industry and is now applied in pharmaceutical product development.

1. 7 Materials

1. 7. 1 Polymeric carriers

Soluplus®

Soluplus® (SOL), kindly gifted from BASF SE (Ludwigshafen, Germany), is a graft amorphous copolymer of polyethylene glycol, vinyl acetate and vinylcaprolactam at a ratio of 13: 30: 57. The low glass transition temperature and good flowability make Soluplus® suitable for hot melt extrusion process. In addition, due to its amphiphilic structure, it can be used as a surfactant to improve the solubility of poorly water soluble compounds. Moreover, it is soluble in many solvents which also provides the possibility to be used in spray drying technique. The chemical structure and properties of Soluplus® are listed as below (Figure 1-3).

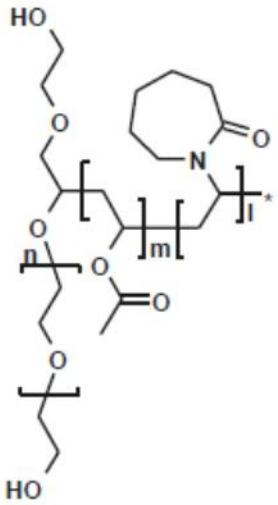

Figure 1-3: Chemical structure of Soluplus®

Table 1-4: Properties of Soluplus®[93]

Properties	Determination Method	Value
Average Molecular Weight	Gel Permeation Chromatography	118, 000 g/mol
Particle Size	Laser Diffraction	340 µm
T_g	DSC	70°C
Critical Micelles Concentration (CMC)		7.6 mg/L
Solubility Parameter	Gas Chromatography	19.4 $MP^{1/2}$

PolyOx™ WSR N-80

Polyethylene oxide (PolyOx™, PEO) is a semi-crystalline, non-ionic, hydrophilic polymer with a low melting point temperature, ranged from 57 to 73°C, which is suitable for the hot melt extrusion process. In addition, based on the molecular weight, it has different gelling/swelling properties and has been utilized to regulate the drug release from the matrix. It is

believed that the larger the molecular weight is, the longer diffusion pathway the drug will undergo, which will result in a sustained release[125]. Therefore, PolyOx^{TM} WSR N-80 (MW: 200,000 Da), kindly supplied by Dow Chemical Company (Midland, MI, USA), is expected to enhance the solubility of poorly water soluble compounds while maintaining the solubility due to its gelling property.

1. 7. 2 Model drugs

Felodipine (FEL), a long-acting 1,4-dihydropyridine-calcium channel blocker used for hypertension[126], with a poor aqueous solubility, was purchased from Ria International LLC (East Hanover, NJ). Ketoconazole (KTZ), for the treatment of the systemic fungal infections[127], was supplied by Afine Chemicals Ltd. (Hangzhou, Zhejiang, China).

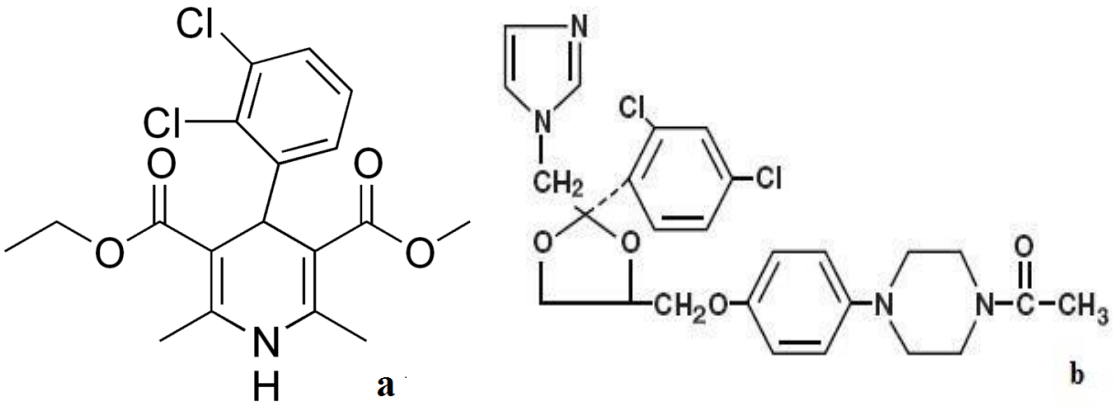

Figure 1-4: a. Structure of Felodipine; b. Structure of Ketoconazole

Currently, cancer has become one of the greatest threats to people's health, and hence anti-cancer agents are a focus of research by many investigators. Paclitaxel (PTX, Figure 1-5) is one of the most useful anticancer agents, originally derived from the bark of the western yew tree, *Taxus brevifolia*, with an extremely low aqueous solubility, reported as less than 1 μg/ml[128, 129]. It has been used for various cancers, including ovarian, breast, lung, and brain

and neck cancers[130]. The current marketed product of paclitaxel is Taxol®, using a mixture of Cremophor® EL and ethanol as a vehicle for the delivery of paclitaxel. However, this product has been reported to have serious adverse effects, for example, neutropenia and peripheral neuropathy, which limits the use of paclitaxel for cancer chemotherapy [131, 132]. These side-effects have been mainly attributed to Cremophor® EL[133], which is a non-ionic solubilizer and surfactant, produced by reaction between ethylene oxide and castor oil of German Pharmacopoeia (DAB 8) quality in a molar ration of 35:1[134], although, paclitaxel has some side-effects itself. Thus, new drug delivery systems for paclitaxel without Cremophor® EL are needed and great efforts have been made, however, very few formulations were prepared using solid dispersion technique[129, 135, 136].

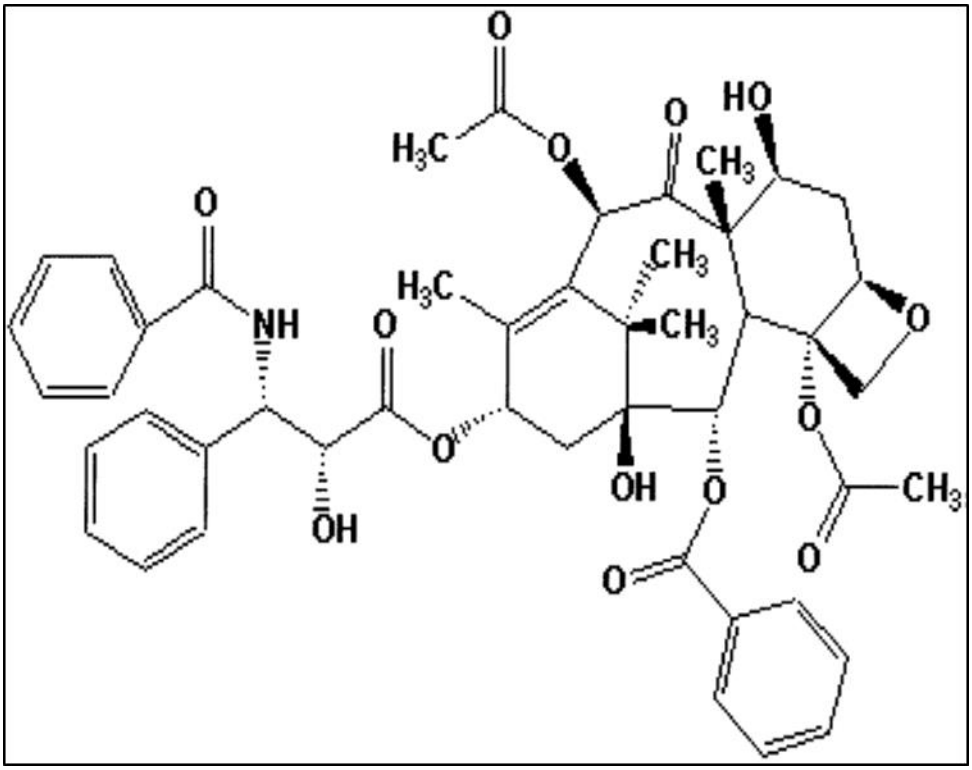

Figure 1-5: Structure of PTX (5β, 20-Epoxy-1, 2α, 4, 7β, 13α-hexahydroxytax-11-en-9-one4, 10-diacetate2-benzoate13-ester with (2R, 3S)-N-benzoyl-3-phenyllisoserine)

1. 7. 3 Other excipients, chemicals and reagents

Hydroxypropyl methylcellulose E5 (Methocel™, HPMC E5) was supplied by Colorcon, Inc (West Point, PA, USA), hydroxypropylmethylcellulose acetate succinate (HPMCAS HF and LF grades) was supplied by Shin-Etsu Chemical Co., Ltd (Tokyo, Japan), polyvinylpyrrolidone (Kollidon® 17PF) and Pluronic® F68 were provided by BASF SE (Ludwigshafen, Germany), polyethylene glycol 3350 (PEG 3350), sodium hydroxide, monobasic potassium phosphate and tribasic sodium phosphate were purchased from Sigma-Aldrich LLC. (St. Louis, MO, USA). Sodium lauryl sulfate (SLS) was purchased from Fisher Scientific (Fair Lawn, NJ, USA). All the organic solvents and water used in the study were high performance liquid chromatography (HPLC) grade.

1.8 Objectives

- To investigate the phase diagram of drug-polymer solid dispersion
- To investigate Soluplus® as a polymeric carrier for solubility enhancement of poorly water-soluble compound
- To investigate the influence of formulation factor and processing parameter on solid dispersions produced via HME
- To develop a solid dispersion formulation of paclitaxel with enhanced solubility
- To investigate the precipitation inhibition effect of different excipients

CHAPTER 2

INVESTIGATE THE PHASE DIAGRAM OF DRUG-POLYMER SOLID DISPERSIONS

2. 1 Methods

2. 1. 1 Physical mixtures preparation

The FEL-SOL or KTZ-SOL physical mixtures were prepared using drug concentration of 100, 95, 90, 85, 80, 70, 60, 50 and 40% (w/w). The two components were geometrically mixed and triturated using a mortar and pestle. All of the materials were sieved with USP 60 mesh prior to mixing. The physical mixtures were then stored in a vacuum desiccator with silica at room temperature until further use.

2. 1. 2 Preparation of solid dispersions

Physical mixtures were prepared in 50 g batches containing 10, 30, 50, 60, and 70% drug loadings, and were initially sieved and mixed in a V-cone blender (MaxiBlend^{TM}, GlobePharma,North Brunswick, NJ, USA) at 50 rpm for 15 min. The physical mixtures were then extruded with a co-rotating twin-screw extruder (16 mmPrism EuroLab, ThermoFisher Scientific, Stone, UK) into uniform rods at an extrusion temperature of 140°C and a screw speed of 100 rpm. The extrudates were milled into fine powders using a laboratory grinder and further sieved with USP Mesh No. 60.

2. 1. 3 Differential scanning calorimetry (DSC)

DSC studies were conducted on the physical mixtures using a differential scanning calorimeter (Diamond DSC, PerkinElmer) equipped with Pyris software (Shelton, CT, USA). Approximately 5-7 mg of the physical mixture samples were packed into a hermetically sealed

aluminum pan. Upon analysis, the samples were initially heated from 30-120°C at a rate of 10°C/min and further heated to 170°C at a rate of 1°C/min, respectively. Extrudates were heated from 30-170°C at a rate of 10°C/min during the overall heating cycle to detect the glass transition temperature. The glass transition temperature of the individual components was determined by heating from 30-170°C at a rate of 10°C/min, cooling down to 30°C at a rate of 40°C/min, and reheating to 170°C at a rate 10°C/min. The instrument was calibrated with indium and zinc before testing. Nitrogen was used as purge gas at a flow rate of 20 mL/min. All the experiments were performed in triplicate.

2. 1. 4 Theoretical prediction of glass transition temperature (T_g).

The T_gs of the solid dispersions were theoretically predicted according to three equations, 1), Fox equation[137]:

$$\frac{1}{Tg_{mix}} = \frac{w_1}{Tg_1} + \frac{w_2}{Tg_2} \quad \text{.....Equation 2-1}$$

2), Gordon-Taylor equation[138] and 3), Couchman-Karasu equation[139]:

$$Tg_{mix} = \frac{w_{1*}Tg_1 + k*w_2*Tg_2}{w_1 + k*w_2}, where, k_{G-T} = \frac{Tg_1*\rho_1}{Tg_2*\rho_2}, k_{C-K} = \frac{\Delta Cp_1}{\Delta Cp_2} \quad \text{.....Equation 2-2}$$

Where the $T_{g\ mix}$ is the theoretical Tg of the binary system, $Tg_{1,\ 2}$ were the Tgs of each individual component, and the $w_{1,\ 2}$ were the weight fraction of each component, $\rho_{1,\ 2}$ were the true density of each component which were measured in Micromeritics AccuPyc 1330 Pycnometer, $\Delta Cp_{1,\ 2}$ was the heat capacity of each of the components, and the $K_{G\text{-}T}$ and $K_{C\text{-}K}$ were the constant for the Gordon-Taylor and Couchman-Karasu equation, respectively.

2. 2 Results& Discussion

2. 2. 1 Melting Point Depression

Generally, a melting point depression is often observed when the substance is melting with impurities. For a pure crystalline drug at the melting point temperature, the chemical

potential of both the solid state and molten state is equals[140], and for the drug polymer mixtures, the melting point temperature of the drug could be reduced if the drug can dissolve in the polymer due to the thermodynamics of mixing. A large depression would be expected if the mixing is strongly exothermic, while weekly exothermic, athermal or endothermic mixing would lead to noticeably decreased reductions of the melting point[110]. Recently, many pharmaceutical scientists were trying to determine a rational choice of heating rate when investigating the drug-polymer solid dispersion systems: however, no consensus has been reached, and the debate is still continuing. The heating rate varies from 0.1 to 400°C/min [109-112, 141, 142]. A slow scan rate is assumed to provide sufficient time to achieve molecular level mixing [141], hence, the heating rate used was 1°C/min in the current study. Another issue regarding the melting point depression measurement is whether to use the onset, midpoint or offset values to predict the interaction parameter. A thorough discussion was conducted by Marsac and co-researchers[110]. The offset values were recommended to be applied when studying the melting point depression since they represent the complete melting of the systems[104]. However, it still requires more effort to understand the details. In the current study, both the onset and offset values were compared. Both systems demonstrated a similar degree of melting point depression (~5°C) when utilizing the offset values. Interestingly, a discrepancy between the two systems was observed when the onset values were applied. With an increase of Soluplus® concentration, the onset of endothermic peak of felodipine was obviously depressed, which illustrated the felodipine is at least partially miscible with Soluplus® (Fig 2-1a). Instead, the melting peaks corresponding to ketoconazole were slightly shifted towards the lower temperature, which is an evidence of immiscibility of the binary mixture (Fig 2-1b).

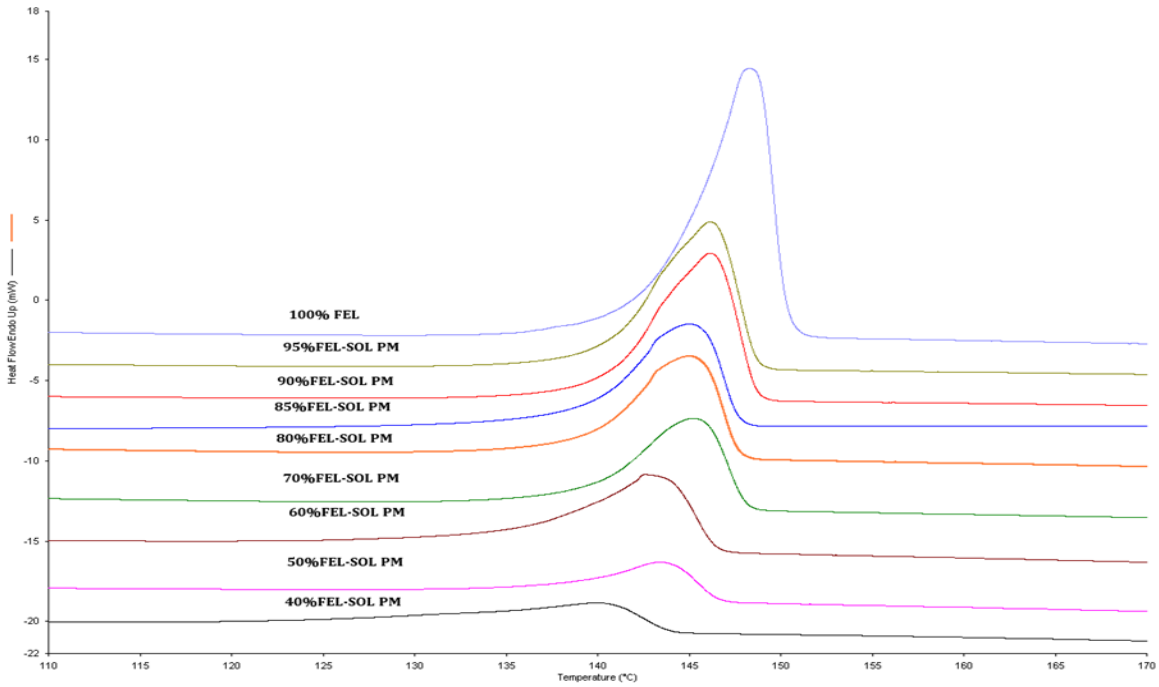

Figure 2-1a: Melting point depression of FEL-SOL physical mixtures

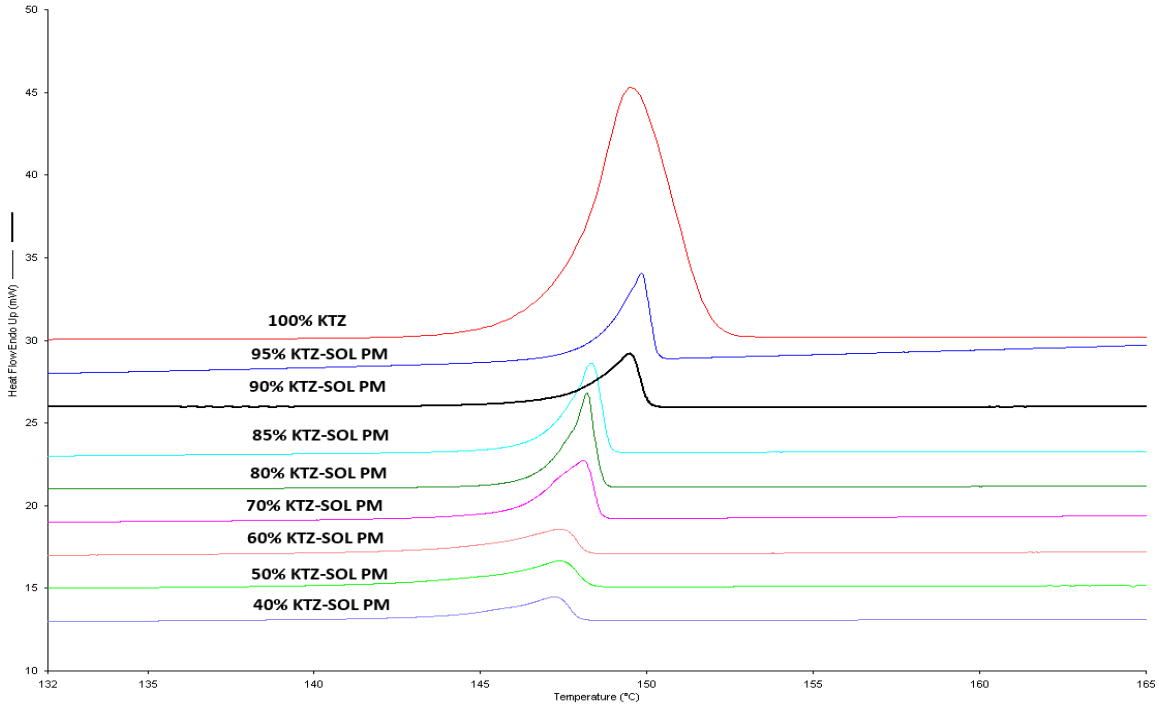

Figure 2-1b: Melting point depression of KTZ-SOL physical mixtures

It is clearly shown in Fig 2-2a and 2-2b that the onset melting temperature of both felodipine and ketoconazole decreased with an increase in the concentration of Soluplus®. However, a much larger reduction of the melting point from the FEL-SOL systems was observed compared to the KTZ-SOL system, which indicated that felodipine was possibly more miscible with Soluplus® than ketoconazole was. This phenomenon was similar with the study reported by Marsac et. al. that felodipine demonstrated a larger melting point depression than ketoconazole when mixing with polyvinylpyrrolidone K12[110]. Our observation is that the onset value of the melting point is referred to the start point of the melting event, and there would be more Soluplus® molecules surrounding the felodipine molecules due to the smaller molecular weight/size compared to the ketoconazole molecules which would further lead to a larger depression of the onset values.

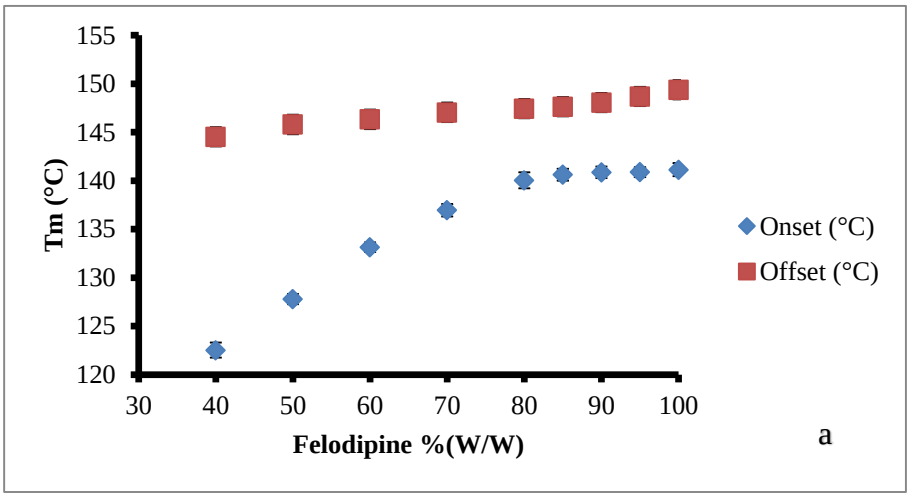

Figure 2-2a: Plot of melting temperature vs concentration of FEL-SOL system

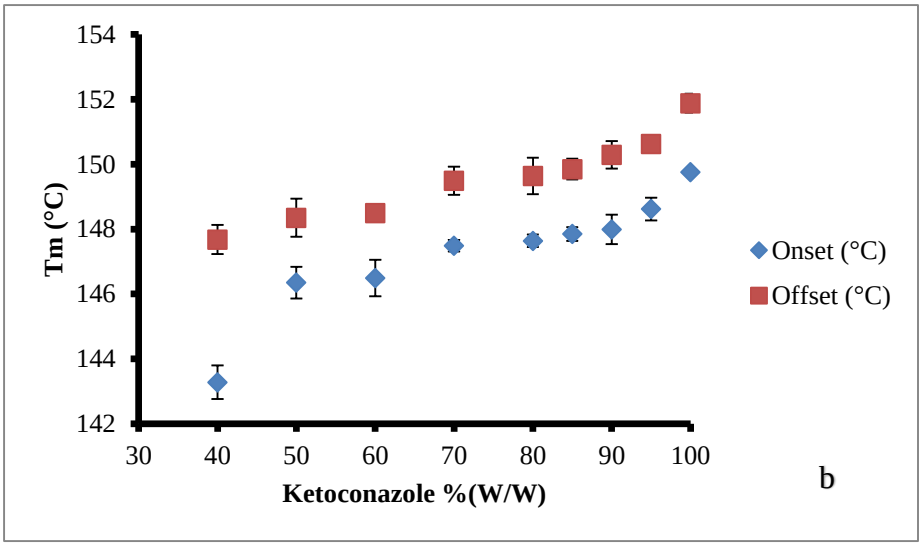

Figure 2-2b: Plot of melting temperature vs concentration of KTZ-SOL system

2. 2. 2 Interaction parameter χ

The interaction parameter χ values for the FEL-SOL and KTZ-SOL systems were calculated as 3.57/15.48 and 12.21/20.03 according to the F-H equation, (onset/offset, respectively) which indicates the system is not favorable for mixing at the room temperature and a strong repulsive force exists between the drug and polymer molecules, however, the calculated χ values are consistent with the assumption that felodipine would be more miscible with Soluplus® compared with ketoconazole. Meanwhile, the solubility parameter was also used to estimate the miscibility of drug-polymer systems as it is broadly accepted that the binary system is miscible if the difference of solubility parameter is less than 7 $MP^{1/2}$, and immiscible while the difference is larger than 10 $MP^{1/2}$[98]. To simplify, the solubility parameter of Soluplus® was taken as 19.4 according to technical information from BASF[93], the solubility parameter of felodipine is 25.0 referred the previous work from Marsac[109], and the solubility parameter of ketoconazole is calculated as 19.45[97] (Table 2-1).

Table 2-1: Properties of Soluplus®, Felodipine and Ketoconazole

	Soluplus®	Felodipine	Ketoconazole
MW (g/mol)	118000	384.26	531.43
T_g (°C)	68	42.95	44.92
ΔH_{fusion} (KJ/mol)	_____	30.83	56.65
δ ($MP^{1/2}$)	19.4[93]	25.0[109]	19.45[97]
ν (cm^3/mol)	98819.19	271.04	372.89
ρ (g/cm^3)	1.1941	1.4177	1.4332
ΔC_p (J/(g*°C))	0.155	0.376	0.44

The differences indicated that both of the drug-polymer systems are likely to be miscible, however, this was in contradiction with the prediction from the Flory-Huggins theory. The interaction parameter χ of FEL-SOL and KTZ-SOL systems were further calculated as 3.429 and 0.00037, respectively. Although both of the positive χ values also indicated the possible partial miscibility, if not immiscibility, of the two binary systems, it was interesting to find out the significant difference between the χ values of ketoconazole calculated from two methods while the χ values of felodipine were close to each other. This result was might be due to the various algorithmic strategies employed when calculating the solubility parameter[101, 143], since the parameters used here were taken from different sources. Another possibility is due to the limits of lattice-based theory which does not account for the free volume change during the mixing process or the intermolecular interactions [90, 103, 140]. Moreover, the depression of the melting point is not only related to the thermodynamic effect of mixing, but also associated with other factors, for instance, the morphology of the polymer. It has been reported that the crystalline lamellar thickness affected the depression and the authors suggested using the equilibrium melting temperature instead of the apparent melting point[144]. Lastly, since the melting point temperature of KTZ-SOL system only slightly altered in a large weight fraction range from 50-95%, the solid-liquid boundary could be above the melting point of ketoconazole, and in that case, the assumption of the Flory-Huggins theory would not exist. However, since the solubility parameters were only used here as a reference, the further discussion would not be conducted and the interaction parameter χ values calculated from the melting point depression were used to construct the overall phase diagrams for both systems.

2. 2. 3 Construction of the F-H phase diagram

Figure 2-3a and 2-3b shows the linear fit of χ value (obtained from offset values) versus $1/T_m$ at different compositions, a good linearity was achieved for both of the two systems. In equation 1-13, the constant A is representing the non-combinatorial entropic part, while B/T is the contribution from the enthalpy of mixing[103]. Janssens[22] and Qian[145] recently illustrated that χ is a function of temperature instead of a constant as it was proposed in the Flory theory. Hence, a series of χ values at different temperature could be obtained.

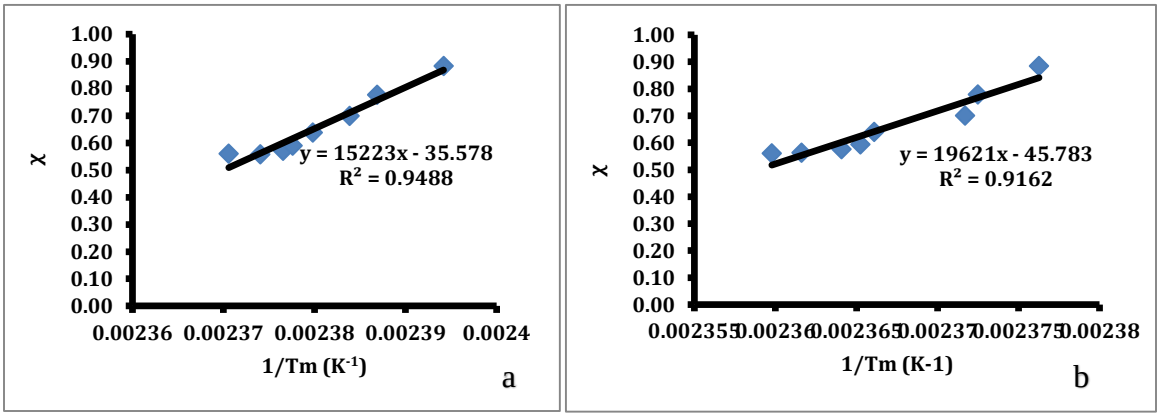

Figure 2-3:Plot of χ vs 1/Tm of FEL-SOL system (a), Plot of χ vs 1/Tm of KTZ-SOL system (b)

The Gibbs free energy of mixing-drug composition diagrams of felodipine and ketoconazole were further generated by fitting the χ values into equation 1-15, and were shown as Figure 2-4a and Figure 2-4b, respectively.

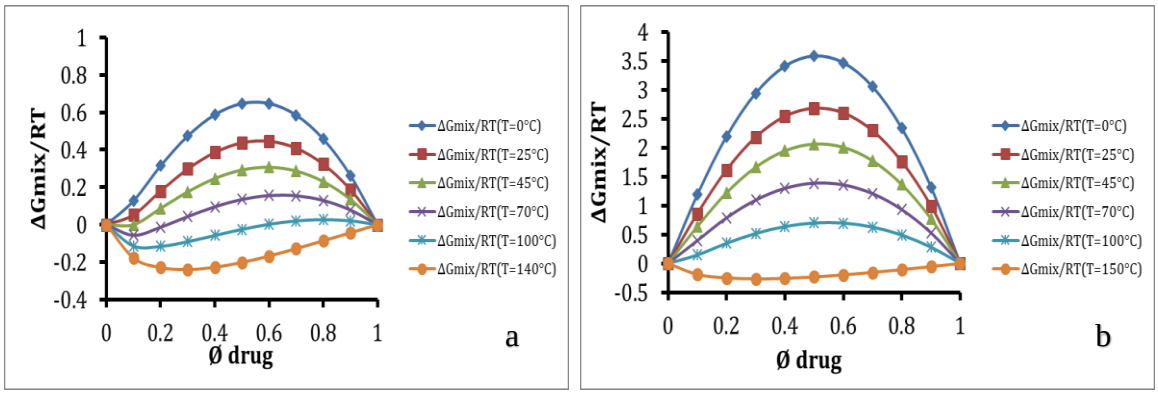

Figure 2-4: Free energy of mixing vs concentration of FEL-SOL system (a), Free energy of mixing vs concentration of KTZ-SOL system (b)

A negative ΔG value indicates that the mixing is thermodynamically favored and miscibility could be achieved, while a positive value indicates a likely partial miscible or immiscible system. The different miscibility of felodipine and ketoconazole in Soluplus® was observed since FEL-SOL system demonstrated a less ΔG value. According to the traditional thermodynamics theories, the Gibbs free energy of mixing is dependent on the temperature; therefore, a phase diagram could be generated to offer an overall understanding of the solid dispersion under the treatment of temperature. A typical phase diagram consists of two curves[90, 103]; one is the binodal curve, which represents the phase boundary between single phase and two phases, in which the drug-rich domain and polymer-rich domain could coexist and the binary system is a metastable state; another curve is called as spinodal, which discriminates the unstable and metastable regions. For any points between the binodal and spinodal curves, the systems can stand for a small fluctuation and phase separation happens only if the fluctuation is

large enough to create a nuclei with a critical size. On the other hand, phase separation would be expected to occur spontaneously if the drug composition in the solid dispersion located below the spinodal curve[103, 146]. It is important to point out that for any binary mixtures, the binodal and spinodal curve will always meet at one critical point. It is very valuable to be able to construct the phase diagram when formulating solid dispersions for poorly water-soluble compounds, since it frequently promotes the compounds to a high energy, metastable state, for instance, converting the compounds from crystalline to amorphous, and a recrystallization during the storage is associated most often. The points between binodal and spinodal curves provides information to the formulation scientists about the achievable drug loading, processing and storage temperature [109, 111, 112]. The phase diagrams of FEL-SOL and KTZ-SOL systems were shown as Figure 2-5a and 2-5b, respectively.

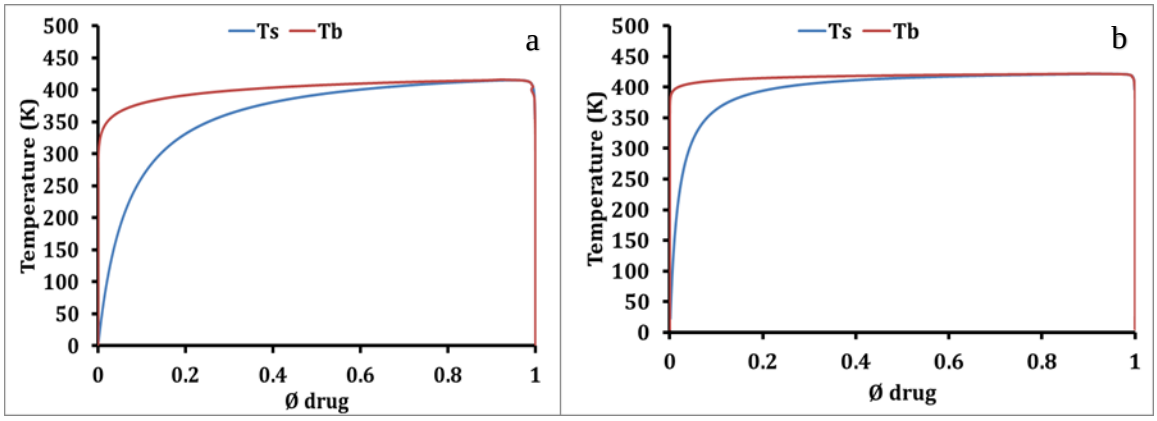

Figure 2-5: Phase diagram of FEL-SOL system (a), Phase diagram of KTZ-SOL system (b)

At the temperature of 298K, the FEL-SOL solid dispersions could contain approximately 14% (w/w) drug in the metastable state while the KTZ-SOL solid dispersions could only contain approximately 4.3% (w/w). However, the solubility of felodipine and ketoconazole in Soluplus® are expected be less than 1% (w/w). With the increasing of temperature to 410K, both of systems showed a homogeneous mixing with one single phase for almost the overall range, hence, 413K (140°C) was set up as the processing temperature for the hot melt extrusion.

2. 2. 4 Estimation of miscibility and solubility of drugs in polymers

The term "solubility" here is referred to the concept in the basic thermodynamics theory, which is the equilibrium parameter at a state where the chemical potential of solute equals to the chemical potential of solvent. On the other hand, miscibility is termed in polymer physics for polymer blends[103], which are usually in a stable amorphous state, and was further applied in small molecule and polymer systems. It is worth to point out that if the drugs are in a meta-stable amorphous state, they will always tend to recrystallize to the stable crystalline state, in other words, to reach the equilibrium solubility of drugs in the polymer. From the last decade, numerous approaches, including melting point depression[109-112], solubility parameters[98], determining the solubility of drugs in the monomers[109], have been proposed to theoretically or practically predict the miscibility and solubility of poorly water-soluble compounds in different types of polymers. However, it is still difficult to measure the solubility of drugs in polymers at normal storage temperature, especially the temperature close or below Tg, since it involves not only the thermodynamic concerns but also the kinetics of phase separation and molecular mobility[145]. It is commonly accepted that the equilibrium solubility of drug within polymers only could be extrapolated or calculated by modeling. Most of the studies that tried to study the miscibility or solubility of solid dispersions are based on thermal analysis, generally using DSC,

while few drawbacks are associated with this technique. 1), any separated domain size below about 30nm could be not discriminated by DSC[147]; 2) the miscibility may be affected by the experimental condition during the heating process in DSC[148]. Beyond the traditional thermal analysis, few other methods were applied to predict the miscibility of solid dispersion. Pair Distribution Function (PDF), a computational method which is extrapolated from XRD pattern, has been introduced by several research groups [149-152]. It represents the interatomic distance which is the fingerprint of a certain solid and has been demonstrated capable to predict the miscibility by comparison of the PDF pattern of individual amorphous component with their final dispersion. It could be inferred that two components are miscible if the PDF pattern of the solid dispersion cannot be derived from their individual patterns. Recently, solid state nuclear magnetic resonance (SSNMR) was utilized to assess the miscibility of solid dispersions [153-157]. It is pointed out that the phenomena, short-range dipolar coupling and longer-range spin diffusion, are the fundamentals of feasibility of this techniques[154]. Rheological method was also utilized to investigate the solubility of drug in polymer. Yang and the co-researchers successfully determine acetaminophen's solubility in poly(ethylene oxide) by a combination of rheological method and thermal analysis.[158].

2. 2. 5 Comparison of theoretical and practical Tg of solid dispersions

The glass transition temperature is an important characteristic of polymers, and it is generally recognized that the Tg is not a real thermodynamic parameter, neither a first-order nor second-order transition[90, 94]. Instead, it represents a temperature region by a single value similar to the melting point temperature (T_m)[159]. The molecular mobility and the molecule relaxation are condensed at the temperature below Tg, in contrast, the viscosity of polymer will increase. Beyond the commonly used thermal analysis, other techniques, based on various

mechanisms, were also applied to measure the glass transition temperature, including dilatometry[90], thermo-mechanical analysis (TMA)[160], dynamic mechanical analysis (DMA)[161], and dielectric analysis (DEA)[162], resulting in the different Tg values. Information like miscibility could be extrapolated from the Tg value, thus, it is meaningful to be able to theoretically predict the Tg for the early development of solid dispersion. To date, a few empirical methods are proposed to estimate the Tg of binary mixture[137-139, 159, 163], and among of which, Fox equation[137], Gordon-Taylor equation[138] and the Couchman-Karasz equation[139] were applied most often. The glass transition temperature of Soluplus, felodipine, and ketoconazole was determined as 68, 42.95 and 44.92°C, respectively (Table 2-1). Figure 2-6 illustrated the difference between theoretical and practical T_g of felodipine-Soluplus® solid dispersions.

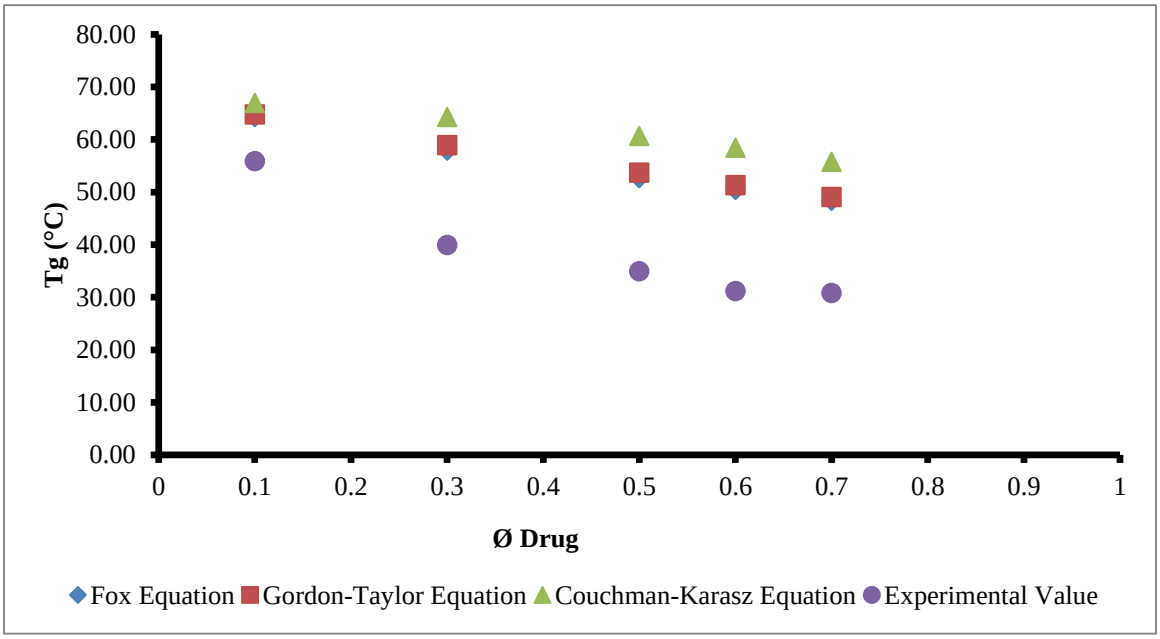

Figure 2-6: Experimental vs theoretical Tg of FEL-SOL system

All of the felodipine-Soluplus® solid dispersions demonstrated a single T_g (Figure 2.7), which indicates a possible homogeneous miscible system. However, it is not robust enough to conclude as a miscible system [152, 164].

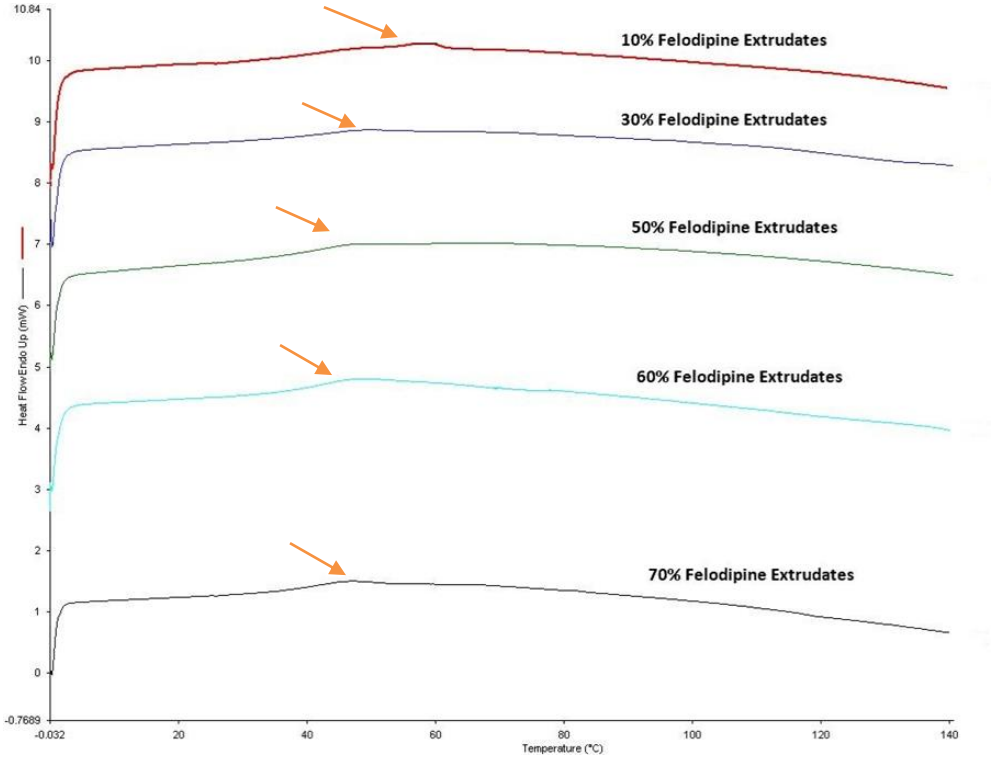

Figure 2-7: DSC of FEL-SOL solid dispersions

The practical Tgs of felodipine-Soluplus® solid dispersions are significantly below the theoretical ones. The discrepancy may be due to the limitation of the empirical methods which are based on volume additivity and assumes no interactions between drug and polymer. Strong intermolecular interactions, for instance, hydrogen-bonding, hydrophobic interactions, polar interactions, and ionic interactions, would attribute to the difference between predicted and practical values. A recently published review from Pinal[165]pointed out that in addition to the drawbacks mentioned above, the contribution from the entropy of mixing was also ignored in

those empirical equations. Moreover, it is also noteworthy considering the fact that T_g is a kinetically controlled phenomenon, in other word, the experimental condition will have an effect on the final Tg obtained. The readers are recommended to refer the recent review from Baird and Taylor for more details[166]. Contrast to felodipine-Soluplus® systems, two separated Tgs were detected in all the ketoconazole-Soluplus® systems except the 10% KTZ loading solid dispersion (listed as Table 2-2), indicating a phase separation occurred. As expected, the first T_g corresponding to the amorphous ketoconazole was decreasing while the second Tg corresponding to the melting point of ketoconazole was increasing with the increasing of KTZ loading.

Table 2-2: Theoretical and experimental T_gs (°C) of ketoconazole-Soluplus® solid dispersions

KTZ (%)	Fox	G-T	C-K	Experimental
10	64.68	65.16	67.13	53.94
30	58.92	59.90	64.97	51.66, 123.90
50	54.10	55.13	61.99	42.33, 128.79
60	51.98	52.90	60.02	38.01, 137.44
70	50.01	50.77	57.59	35.83, 137.99

CHAPTER 3

SOLUPLUS® AS A POLYMERIC CARRIER FOR SOLUBILITY ENHANCEMENT OF POORLY WATER-SOLUBLE COMPOUNDS

3. 1 Methods

3. 1. 1 Solubility Parameter Calculation

The solubility parameter δ was calculated using Hoy and Hoftyzer/Van Krevelen method, respectively, since both methods provide the same accuracy level (10%). The average value from the two methods was used to estimate the drug-polymer miscibility as recommended[94]. To determine the solubility parameter of Soluplus®, which is comprised of polyvinyl caprolactam - polyvinyl acetate - polyethylene glycol in a ratio of 57:30:13, the number average of the three monomers was calculated.

3. 1. 2 Differential Scanning Calorimetry (DSC)

The solubility of felodipine in Soluplus® matrix was predicted by DSC using a Perkin-Elmer Diamond DSC instrument (Norwalk, CT). Approximately 5-7 mg binary physical mixtures containing felodipine varied from 10-100% were weighed and sealed into an aluminum pan. Samples were heated from 30 to 180°C at various rump rates of 10, 20, 50 and 100°C/min. The enthalpy of fusion of felodipine was recorded and plotted versus the concentration. The extrudates were only subjected to a heating rate of 10°C/min. The instrument was calibrated with indium and zinc before test. Nitrogen was used as purge gas at a flow rate of 20 mL/min. All the experiments were triplicated.

3. 1. 3 Hot-Melt Extrusion

A batch size of 50 g physical mixtures containing 10, 30 and 50% FEL were initially sieved with USP 60 mesh and mixed in a V-cone blender (MaxiBlendTM, GlobePharma, North Brunswick, NJ, USA) at 50 rpm for 15 min and further extruded with a co-rotating twin-screw extruder (16 mm Prism EuroLab, ThermoFisher Scientific, Stone, UK) into uniform rods at an extrusion temperature of 140°C and a screw speed of 100 rpm. Afterwards, part of the rods was milled into fine powders using a laboratory grinder, and the rest was kept in refrigerator properly until further study.

3. 1. 4 Phase Solubility Determination

Excess amount of felodipine (approximately 20 mg) was added to 20 mL vials containing either purified water or pH 6.8 phosphate buffer (with or without pre-dissolved Soluplus®), the concentration of Soluplus® varied from 0-1000 µg/mL (0, 10, 50, 100, 250, 500 and 1000 µg/mL, respectively). The samples were placed into a Precision Reciprocal Shaking Bath (ThermoFisher Scientific, Stone, UK) at 37°C and shaken at a speed of 80 rpm for 24 hours to achieve the equilibrium. Afterwards, the samples were filtered through a 0.45 µm Nylon filter membrane (Whatman, Piscataway, NJ) and further analyzed using HPLC at a λ_{max} of 238 nm.

3. 1. 5 Particle Size Analysis

The samples from the phase solubility study were further subjected to particle size analysis using a Zetasizer Nano ZS Zen3600 (Malvern Instrument, Inc. UK). Mean particle size and the polydispersity index (PdI) were determined at 37°C backscatter detection in disposable folded capillary clear cells. A He–Ne laser of 633 nm was utilized to obtain the data, and the particle size analysis data was evaluated using volume distribution.

3. 1. 6 Drug Release Studies

All the extrudates were subjected to in vitro dissolution studies utilizing a Hanson SR8-plus™ dissolution test station (Hanson Research Corporation, Chatsworth, CA) operated at 100 rpm paddle speed. The extrudates were weighed precisely equivalence to 20mg FEL and filled into size#1 gelatin capsules. These capsules were placed in sinkers and added to the dissolution vessel. Two types of dissolution medium were utilized: 1) 500 mL pH 6.8 phosphate buffer, 2) 500 mL pH 6.8 phosphate buffer with pre-dissolved Soluplus® (250 and 500 μg/mL, respectively). At pre-determined time intervals, 1.5 mL samples were removed from the dissolution vessels and replaced with an equal volume of fresh dissolution medium. These collected samples were immediately filtered using 13 mm PTFE membrane filters (Whatman, Piscataway, NJ) with a pore size of 0.2 μm and analyzed using HPLC at a λmax of 238 nm. Experiments were performed in triplicate and the mean values were compared.

3. 1. 7 Polarized Light Microscopy (PLM)

The optical properties of pure felodipine, Soluplus®, and extrudates were observed at room temperature using a Nikon Eclipse E600 Pol microscope equipped with a Nikon DS-Fi 1 camera. Images were analyzed using NIS-Elements BR 3.2 software. In addition, the extrudates were also exposed to dissolution medium (pH 6.8 phosphate buffer with or without pre-dissolved Soluplus®), and observed under polarized light to understand the dissolution behavior.

3. 1. 8 FT-IR Spectroscopy (FT-IR)

The spectra of FEL, SOL, and extrudates were obtained on a PerkinElmer Spectrum 100 FT-IR Spectrometer, equipped with the universal ATR accessory, in the range of 4000-650 cm^{-1}, using a resolution of 1 cm^{-1}.

3. 1. 9 Raman Spectroscopy

The excitation sources employed for Raman spectroscopy were the 514.5 nm line and 647 nm line from a Stabilite 2018 Kr/Ar mixed-gas ion laser. The spectra were collected in the range of 50-3600 cm^{-1} using a Jobin-Yvon Ramanor HG2-S Raman spectrometer with two 1800 grooves/mm gratings and a thermoelectrically cooled (-30°C) photomultiplier tube detector as previously reported[167]. A scan speed of 2 cm^{-1}/s was employed for spectra shown. Spectra were obtained for the solid state of felodipine and Soluplus® as well as the extrudates.

3. 1. 10 Theoretical Methods

Calculations were performed using the Gaussian 09 package (Revision A.1 ed.; Gaussian, Inc.: Wallingford CT, 2009). The optimized equilibrium geometry, vibrational frequencies, and Raman intensities of Felodipine were determined using the B3LYP density functional with the 6-311+g (d, p) basis set. Simulated spectra were constructed with a custom program developed with National Instruments LabView as reported[167].

3. 1. 11 X-ray diffraction (XRD)

XRD studies were performed on a powder X-ray diffraction apparatus (Bruker AXS, Madison, WI) using CuKα radiation at 40 mA and 40 kV. The samples of interest were analyzed in the diffraction angles range of 5–35° (2θ) at a scan rate of 2°/min, with a scanning step of 0.05°. All of experiments were triplicated.

3. 1. 12 Scanning Electron Microscopy (SEM)

The morphology of samples was determined using a JEOL JSM-5600 SEM at an accelerating voltage of 5kV equipped with JSM 5000 software. Samples of interest were coated with gold utilizing a Hummer 6.2 sputtering system for 10min before observation.

3. 2 Results and Discussion

3. 2. 1 Solubility parameter calculation

It is crucial to measure the solubility/miscibility of drug in polymer when developing amorphous solid dispersions since it will provide useful information regarding the proper selection of drug loading along with the prediction of the stability of solid dispersions[88]. Solubility is generally recognized as a thermodynamic parameter at which moment the chemical potential of the substance in the solvent equals to the chemical potential of substance precipitated and the same concept could be used in drug-polymer systems[145]. The term of miscibility is firstly introduced in the polymer blends[168], and further extrapolated to small molecule systems. However, unlike the polymer blends, the amorphous drugs are usually metastable and tend to recrystallize, resulting in a more complex situation to predict the miscibility. As mentioned before, solubility parameter was applied to predict the miscibility of felodipine-Soluplus® in the current study. The group contribution values of felodipine and the three monomers of Soluplus® were listed in Table 3-1 to 3-8[94]. Consequently, the solubility parameter of felodipine was calculated as 20.78 and 22.74, according to the Hoy and Hoftyzer/Van Krevelen method, respectively. Meanwhile, the solubility parameter of Soluplus® was determined as 21.49 and 21.79, respectively. The solubility parameter of Soluplus® obtained by gas chromatography was 19.4[93], which is close to the average value 21.64 in this study, indicating the accuracy of this method. It is well accepted that two substances are not miscible if the solubility parameter

difference is larger than 10 $MP^{1/2}$; to the contrast, good miscibility is expected when the difference is less than 7 $MP^{1/2}$, especially when the difference is less than 2 $MP^{1/2}$[98]. However, it is worth mentioning that solubility parameter only provides a simple theoretical pathway to predict the miscibility of drug-polymer systems from the initial assessment standpoint, it is always necessary to perform practical experiments to identify the miscibility of the drug-polymer systems for formulation development. Nevertheless, it is clearly shown that the solubility parameters of felodipine and Soluplus® are very close to each other (Table 3-9), which indicated the likelihood of drug-polymer miscibility.

Table 3-1: Group contribution of felodipine using Hoftyzer/Van Krevelen method

Structure group	No.	F_{di} $(MJ/m^3)^{½}$* mol^{-1}	F_{pi} $(MJ/m^3)^{½}$ *mol^{-1}	E_{hi} (J/mol)	V (cm^3*mol^{-1})
$–CH_3$	4	420	0	0	33.5
$–CH_2–$	1	270	0	0	16.1
>CH–	1	80	0	0	-1
=C<	4	70	0	0	-5.5
–Cl	2	450	550	400	26
–COO–	2	390	490	7000	18
–NH–	1	160	210	3100	4.5
Ring	1	190	0	0	16
Phenylene (o, m, p)	1	1270	110	0	33.4

Table 3-2: Group contribution of felodipine using Hoy method

Structure group	No.	$F_{T,i}$ $(MJ/m^3)^{½}$ *mol^{-1}	$\Delta_{T,i}^{*}$	V (cm^3*mol^{-1})
$–CH_3$	4	303.5	0.023	21.55
$–CH_2–$	1	269	0.02	15.55
>CH–	1	176	0.012	9.56
=C<	4	173	0	7.18
–Cl	2	330	0.017	19.5
–COO–	2	640	0.047	23.7
–NH–	1	368	0.031	11
Ring (6 membered)	1	-48	0	----
Phenylene (o, m, p)	1	20.2	0	----
$CH_{ar.}$	3	241	0.011	13.42
$C_{ar.}$	3	201	0.011	7.42

Table 3-3: Group contribution of PEG6000 using Hoftyzer/Van Krevelen method

Structure group	No.	F_{di} $(MJ/m^3)^{½}$ *mol^{-1}	F_{pi} $(MJ/m^3)^{½}$ *mol^{-1}	E_{hi} (J/mol)	V (cm^3*mol^{-1})
$–CH_2–$	2	270	0	0	16.1
–OH–	2	210	500	20000	10

Table 3-4: Group contribution of Vinyl Acetate using Hoftyzer/Van Krevelen method

Structure group	No.	F_{di} $(MJ/m^3)^{½}$ $*mol^{-1}$	F_{pi} $(MJ/m^3)^{½}$ $*mol^{-1}$	E_{hi} (J/mol)	V (cm^3*mol^{-1})
$–CH_3$	1	420	0	0	33.5
–COO–	1	390	490	7000	18
=CH–	1	200	0	0	13.5
$=CH_2$	1	400	0	0	28.5

Table 3-5: Group contribution of Vinyl Caprolactam using Hoftyzer/Van Krevelen method

Structure group	No.	F_{di} $(MJ/m^3)^{½}$ $*mol^{-1}$	F_{pi} $(MJ/m^3)^{½}$ $*mol^{-1}$	E_{hi} (J/mol)	V (cm^3*mol^{-1})
>N–	1	20	800	5000	-9
–CO–	1	290	770	2000	10.8
=CH–	1	200	0	0	13.5
$=CH_2$	1	400	0	0	28.5
$–CH_2–$	5	270	0	0	16.1
Ring	1	190	---	---	16

Table 3-6: Group contribution of PEG6000 using Hoy method

Structure group	No.	$F_{T,i}$ $(MJ/m^3)^{½}$ $*mol^{-1}$	$\Delta_{T,i}^{(P)}$	V (cm^3*mol^{-1})
$–CH_2–$	2	269	0.02	15.55
–OH–	2	675	0.049	12.45

Table 3-7: Group contribution of Vinyl Acetate using Hoy method

Structure group	No.	$F_{T,i}$ $(MJ/m^3)^{½}$ *mol^{-1}	$\Delta_{T,i}^{(P)}$	V (cm^3*mol^{-1})
$–CH_3$	1	303.5	0.022	21.55
–COO–	1	640	0.05	23.7
=CH–	1	249	0.0185	13.18
$=CH_2$	1	259	0.018	19.17

Table 3-8: Group contribution of Vinyl Caprolactam using Hoy method

Structure group	No.	$F_{T,i}$ $(MJ/m^3)^{½}$ *mol^{-1}	$\Delta_{T,i}^{(P)}$	V (cm^3*mol^{-1})
>N–	1	125	0.008	12.14
–CO–	1	538	0.04	17.3
=CH–	1	249	0.0185	13.18
$=CH_2$	1	259	0.018	19.17
$–CH_2–$	5	269	0.02	15.55
Ring (7-membered)	1	92	0.007	---

Table 3-9: Summary of the calculated parameters of felodipine, monomers and Soluplus®

	FEL	*PVC*	*PVA*	*PEG*	*SOL*
Hoy	20.78	19.45	19.48	35.08	21.49
H-V	22.74	20.43	18.16	36.14	21.79
Ave.	21.76	---	---	---	21.64

3. 2. 2 Differential Scanning Calorimetry (DSC) Analysis

Figure 3-1 demonstrated the thermal behavior of pure felodipine under different heating rate. The peak magnitude increased with the heating rate, which is due to the alternation of flow of energy measured by DSC [142, 169].

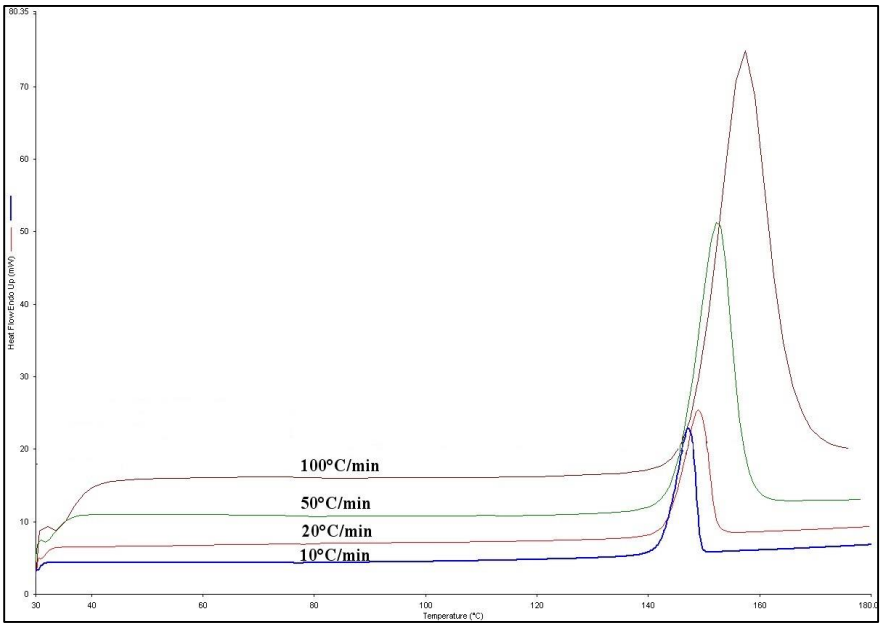

Figure 3-1: DSC of felodipine at different heating rate

Numerous approaches have been proposed to determine the solubility of drug within polymer in solid state, either theoretically or practically, based on different mechanisms, and one of them is to utilize the enthalpy of fusion[109, 142, 158, 170-176]. The enthalpy of fusion is generally defined as the heat needed to convert the substance from solid to liquid state without temperature increasing[177], and it was introduced to calculated the drug solubility by Theeuwes et al. based on the mechanism that the dissolved drug has no contribution to the endothermic event[174]. Therefore, by plotting the enthalpy of fusion versus the drug loading concentration, the intercept in X-axis would be theoretical solubility of the drug within the polymer[174]. Moreover, the scan rate of DSC is reported to affect the thermal events by several studies [142,

176], as a faster scan rate will improve sensitivity while losing resolution and *vice versa*. The values of enthalpy of fusion of felodipine were recorded and plotted versus concentration in Figure 3-2; a good linear correlation was obtained for each scan rate. Subsequently, the predicted solubility of felodipine in Soluplus® matrix was determined as 9.24, 9.86, 6.23 and 6.28%, respectively. The solubility measured at a higher scan rate is lower to which determined at a slower scan rate, this phenomenon is similar as the study reported by Gramaglia et.al[142], which is possibly due to that a slow scan rate will provide more time for the two components to achieve completely mixing.

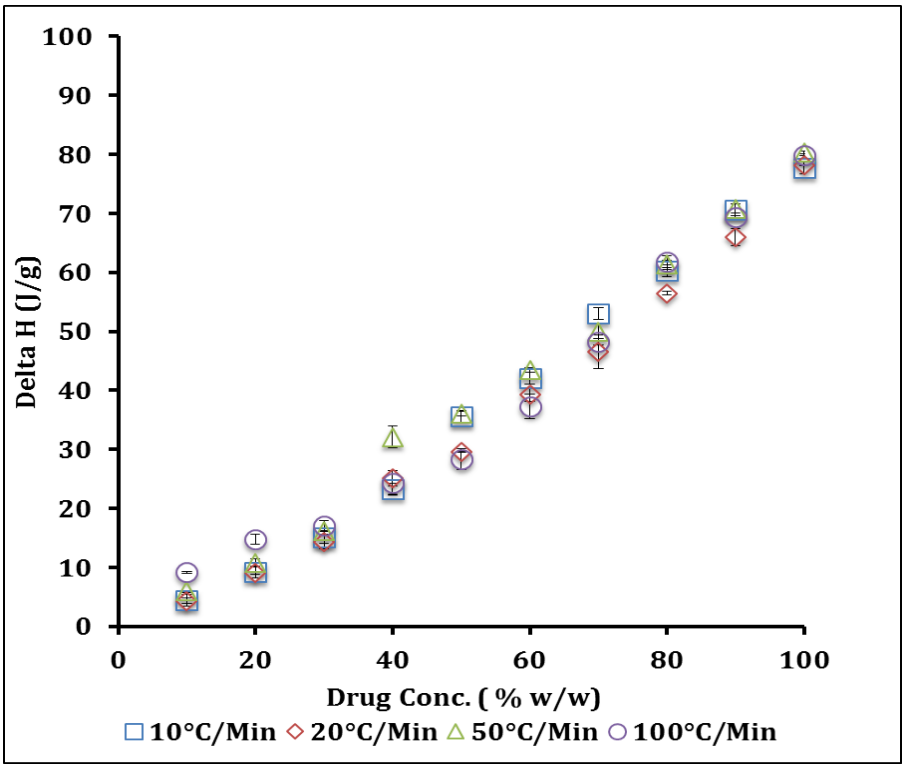

Figure 3-2: Plot of Δ_H versus concentration at different heating rate

3. 2. 3 Phase Solubility Determination

Figure 3-3a demonstrated the phase solubility of felodipine in aqueous solutions with or without pre-dissolved Soluplus®. The solubility of felodipine could not be detected in neither medium without pre-dissolved Soluplus® which is due to the low aqueous solubility of crystalline felodipine. With the increasing of concentration of Soluplus® in water, the solubility of felodipine was enhanced up to 20.44 μg/ml which is attributed to the solubilizing effect of the amphiphilic structure of Soluplus® and the formation of drug polymer conjugate, however, the solubility of felodipine in the phosphate buffer with Soluplus® was comparatively lower than the ones in water. Moreover, the particle size analysis of the blank Soluplus® solution demonstrated that Soluplus® can form micelles in both water and phosphate buffer in the range of 70-80 nm, and the particle size of the micelles kept constant once its concentration was above 10 μg/ml, which is consistent with the reported critical micelles concentration (CMC) of Soluplus® in water at 37°C as 7.9 μg/ml [93] (Table 3-10). Interestingly, with the addition of felodipine, the particle size was observed to reduce to 50-60 nm associated with a very narrow particle size distribution indicating felodipine was embedded into the micelles. Therefore, it would not be surprised to observe solubility enhancement with nano-sized particles, and the reduction of particle size is most probably due to the intermolecular interaction, for instance, hydrogen bonding, between the two components, which can attract each other.

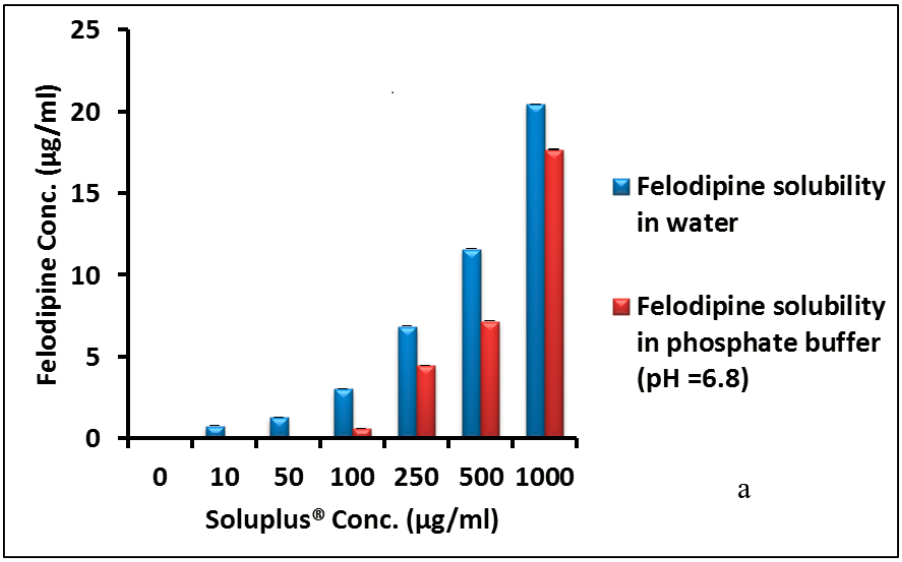

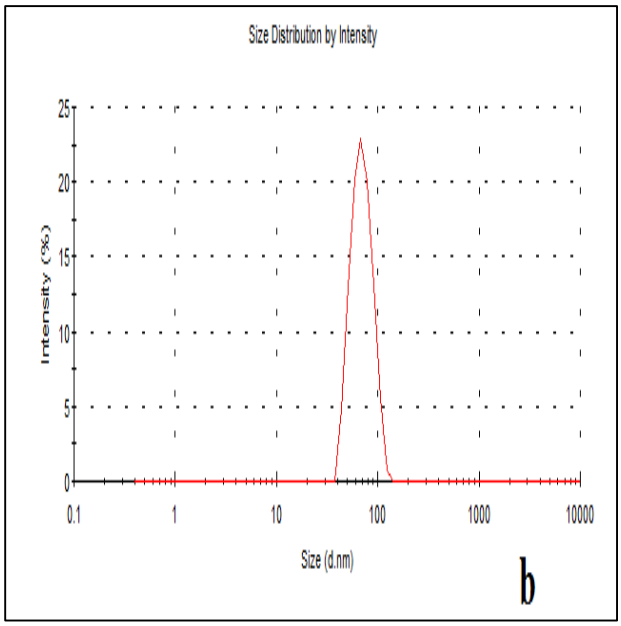

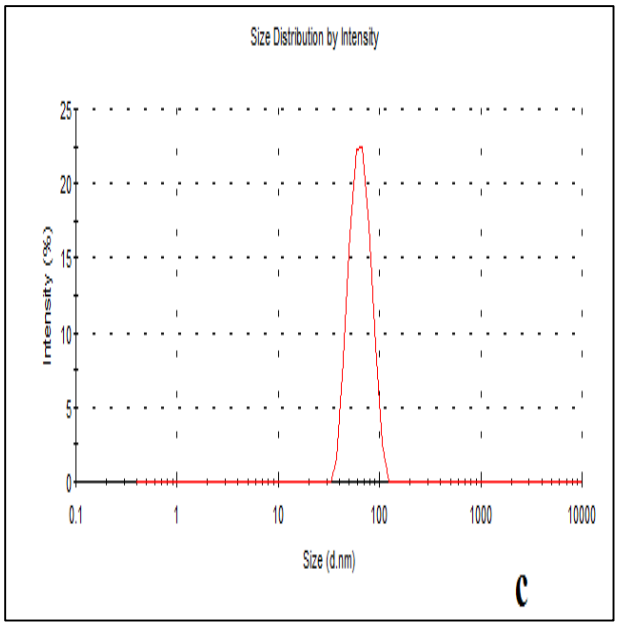

Figure 3-3: Phase solubility of felodipine in aqueous solutions (a), Particle size distribution of felodipine in water with 1000 µg/ml Soluplus® (b), Particle size distribution of felodipine in phosphate buffer (pH=6.8) with 1000 µg/ml Soluplus® (c)

Table 3-10: Particle size analysis (Mean ± SD, d.nm) Solution A: phosphate buffer with Soluplus®, solution B: water with Soluplus®, solution C: felodipine in phosphate buffer with Soluplus®, solution D: felodipine in water with Soluplus®

Conc. of Soluplus® (μg/mL)	Solution A	Solution B	Solution C	Solution D
0	---	---	---	---
10	78.75±1.23	67.12±1.31	65.32±1.65	62.29±2.01
50	78.98±2.19	62.89±1.45	67.58±2.01	62.17±1.98
100	73.47±1.87	64.30±1.21	67.19±1.11	61.16±1.78
250	70.74±2.23	65.25±1.63	66.60±1.32	61.56±1.89
500	71.25±0.98	63.06±1.99	63.30±1.47	60.87±1.45
1000	72.29±1.34	63.17±1.12	62.80±1.32	60.98±1.89

3. 2. 4 Dissolution Results

The dissolution profiles of felodipine-Soluplus® solid dispersions as well as the pure felodipine were shown in Figure 3-4. The drug loading has a clear effect on the solubility profile, and supersaturation was generated in the formulation containing 10% felodipine. The solubility of felodipine was increased to approximately 12 μg/ml in 30min followed a precipitation which is possibly attributed to the metastable amorphous state of felodipine in the matrix. Meanwhile, SDs with 30% and 50% felodipine showed a slight enhancement of solubility. It was illustrated by Friesen et al, that the physical properties of drug substance, for instance, the melting point temperature, glass transition temperature and LogP value, would affect the drug loading in the formulations[178]. If T_m/T_g value larger than 1.4 associated with a LogP value less than 6, the compounds would have a tendency to recrystallize from the amorphous state and limit a drug loading between 10-35% in the formulation. In this case, the T_m/T_g value of felodipine was determined as 1.87 and the LogP value is 4.83[179], therefore, the dissolution behavior of

felodipine is expected. Formulation scientists have been made great efforts to inhibit the precipitation of supersaturated drug delivery systems and maintain a sufficient period of high solubility by many approaches and one of the most important method is to form intermolecular interaction with the aids of different excipients, for instance, polymers[180, 181], surfactants[182], and cyclodextrins[183]. Typically, the precipitation of drug from supersaturation system consists two steps, nucleation and the following crystal growth process. It is important to point out that the dissolved drug molecules have to overcome an energy barrier, which is due to the interfacial tension between drug particles and dissolution medium, to form aggregates (nucleation process), which can further grow to crystals, although the precipitation is thermodynamically driven by supersaturation. Therefore, the energy barrier provides the possibility to delay or prevent the nucleation process if it could be promoted high enough to overcome and the supersaturation could remain in the metastable state for longer time. Pharmaceutical excipients like polymers have been widely employed to stabilize the supersaturation systems based on the mechanism of direct interaction between polymers and drug particles and hydrogen bonding is the one observed most often. The active energy is increased with the formation of hydrogen bonding, and furthermore, the polymers will compete with the drug particles to absorb on the crystals or postpone the absorption by means of steric effect, which will finally lead to a retarded crystal growth rate[114]. Clearly, the apparent solubility of felodipine in all three solid dispersions was promoted and maintained in the phosphate buffer with pre-dissolved Soluplus® (Figure 3-5). This phenomenon could be explained that the pre-dissolved Soluplus® formed micelles itself which can embed the felodipine resulting in a further enhancement of solubility. Moreover, the pre-dissolved Soluplus® could also form intermolecular interaction with the dissolved felodipine molecules, which can delay

the precipitation process. However, the amount of pre-dissolved Soluplus® studied here did not make significant difference on the solubility enhancement effect.

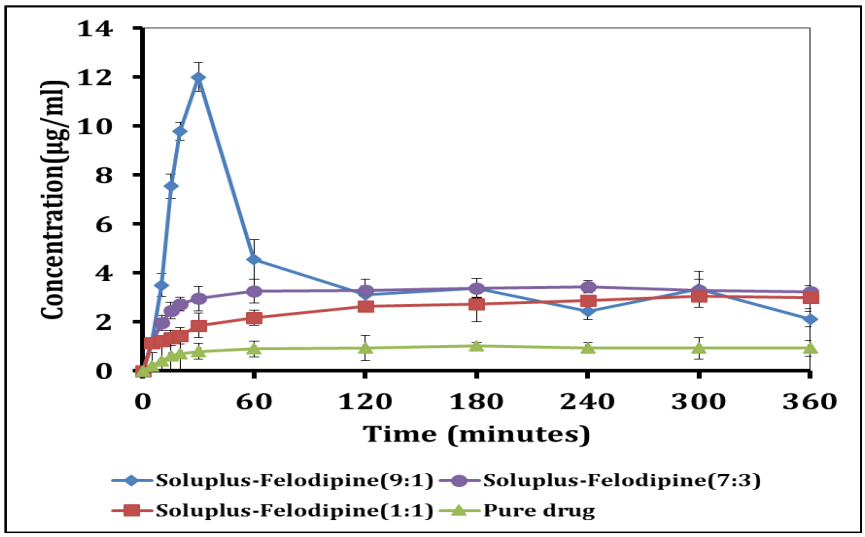

Figure 3-4: Dissolution profile of felodipine-Soluplus solid dispersions in 500 mL pH 6.8 phosphate buffer

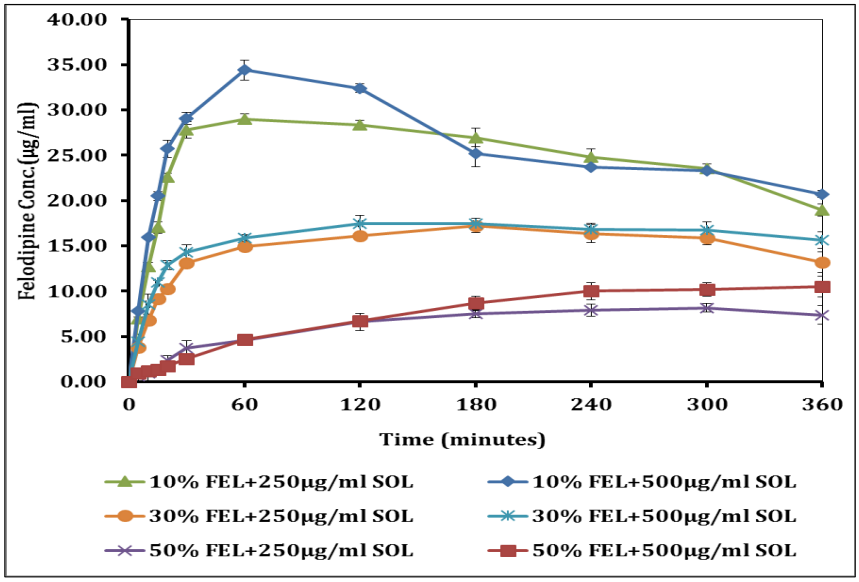

Figure 3-5: Dissolution profile of felodipine-Soluplus solid dispersions in 500 mL pH 6.8 phosphate buffer with pre-dissolved Soluplus® (250 and 500 µg/mL, respectively)

3. 2. 5 DSC and XRD

The DSC thermograms of individual components along with solid dispersions of three ratios were reported in Figure 3-6. No characteristic endothermic melting peak of felodipine was observed which illustrated the amorphous state of felodipine in the structure. Moreover, in addition with the single glass transition temperature (T_g), homogeneous solid dispersions were obtained and which is expected to further benefit the physical stability of extrudates, however, exceptions were also reported[152, 164]. Therefore, it is necessary to characterize the solid dispersions utilizing other techniques.

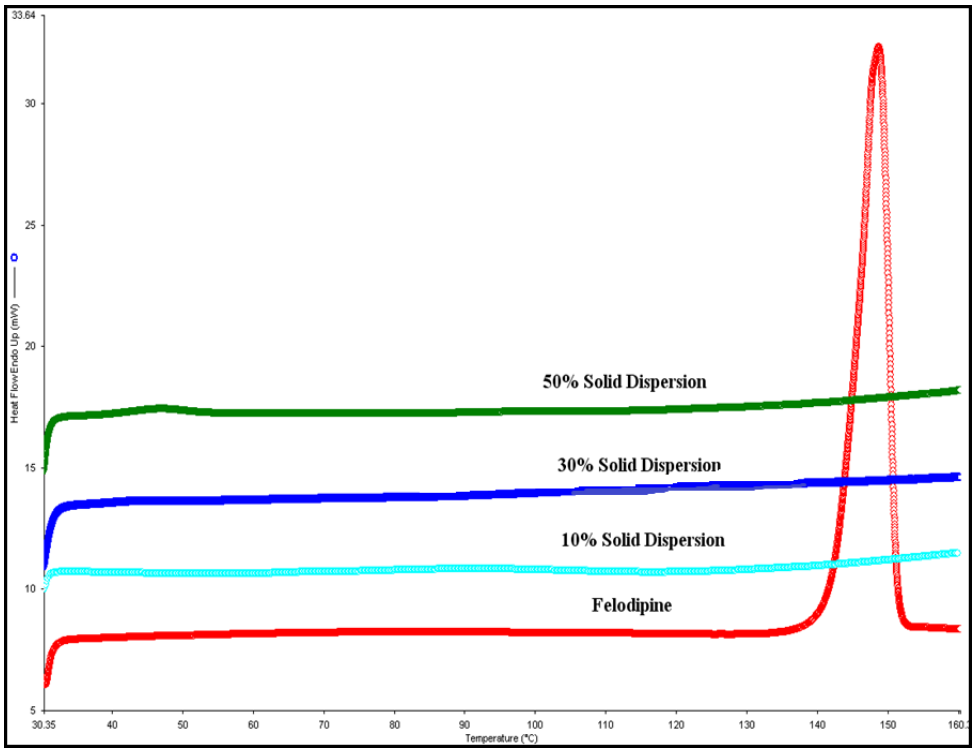

Figure 3-6: DSC of felodipine-Soluplus solid dispersions

XRD has been the thumb of rule to characterize the solid dispersion in the pharmaceutical industry due to its excellent capacity to provide fingerprints and quantitative analysis of substance[184]. No crystalline peaks were detected in the solid dispersions compared to the pure felodipine indicating the possible amorphous state of drug (Figure 3-7).

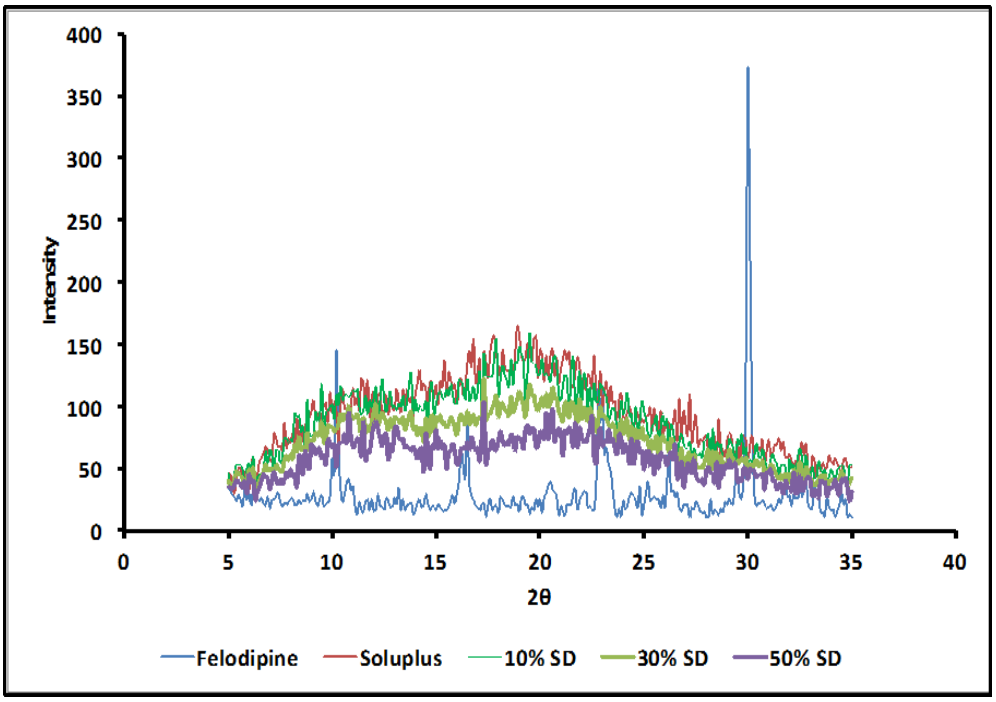

Figure 3-7: XRD of pure felodipine, Soluplus® and FEL-SOL solid dispersions

3. 2. 6 Polarized light microscopy

For crystalline materials, the molecules are regularly arranged, which usually results in various refractive indices and finally turns into the exhibition of vivid color when the substances are observed under polarized light. On the other hand, the molecules in amorphous substance are randomly oriented, and only one principle refractive index is corresponded. Although cubic crystals such as sodium chloride also have the same property as amorphous substance, they rarely exist in organic materials. Therefore, the crystalline and amorphous states of substances can be differentiated by polarized light due to the different optical properties and the absence of birefringence is a strong evidence of the existence of amorphous state[185, 186]. In Figure 3-8b, none of the SDs exhibited birefringence as contrasted to the crystalline felodipine (Figure 3-8a), and the observation was also obtained for 10 and 50% SDs, which confirmed the amorphous state of felodipine in the formulations. In addition, the SDs were also exposed to pH 6.8 phosphate buffer and observed to simulate the dissolution process. Interestingly, the particles of 10% felodipine solid dispersion slightly extended with a deduction of thickness during the period of observation, which likely demonstrated that the solid dispersions already started to dissolve into the medium, while no similar phenomenon was observed for 30% or 50% solid dispersion (Figure 3-8c and 3-8d). This would be attributed to the higher apparently solubility of 10% solid dispersions compared to the others.

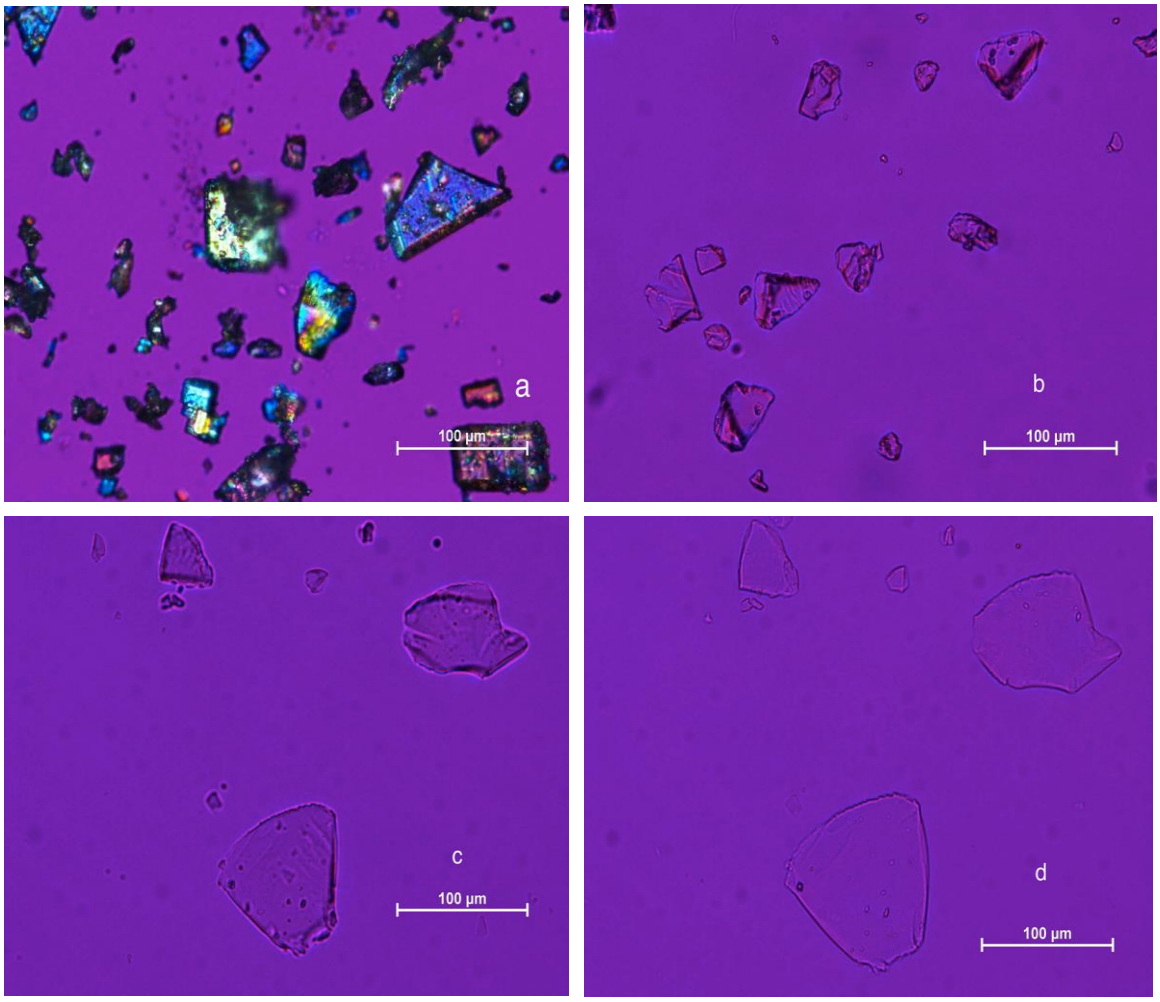

Figure 3-8: PLM images of crystalline felodipine (a), 30% felodipine-Soluplus® SD (b), 10% felodipine-Soluplus® SD exposed to phosphate buffer at 0min (c), 10% felodipine-Soluplus® SD exposed to phosphate buffer at 30min (d)

3. 2. 7 Fourier transform infrared spectroscopy (FT-IR)

Felodipine was reported to be able to form hydrogen bonding with several types of polymers containing hydrogen acceptor group while felodipine itself functions as a donor [187-190]. As previously mentioned before, the delay of the precipitation of felodipine solid dispersions was probably due to the intermolecular interaction with Soluplus®, therefore, FT-IR and Raman Spectroscopy were conducted to prove the proposal. Crystalline felodipine demonstrated a characteristic N-H stretch peak at around 3371 cm^{-1} (Figure 3-9), however, no N-H stretch peak was detected solid dispersions of all three ratios which would possibly due to the formation of hydrogen bond with the ketone group in Soluplus® structure.

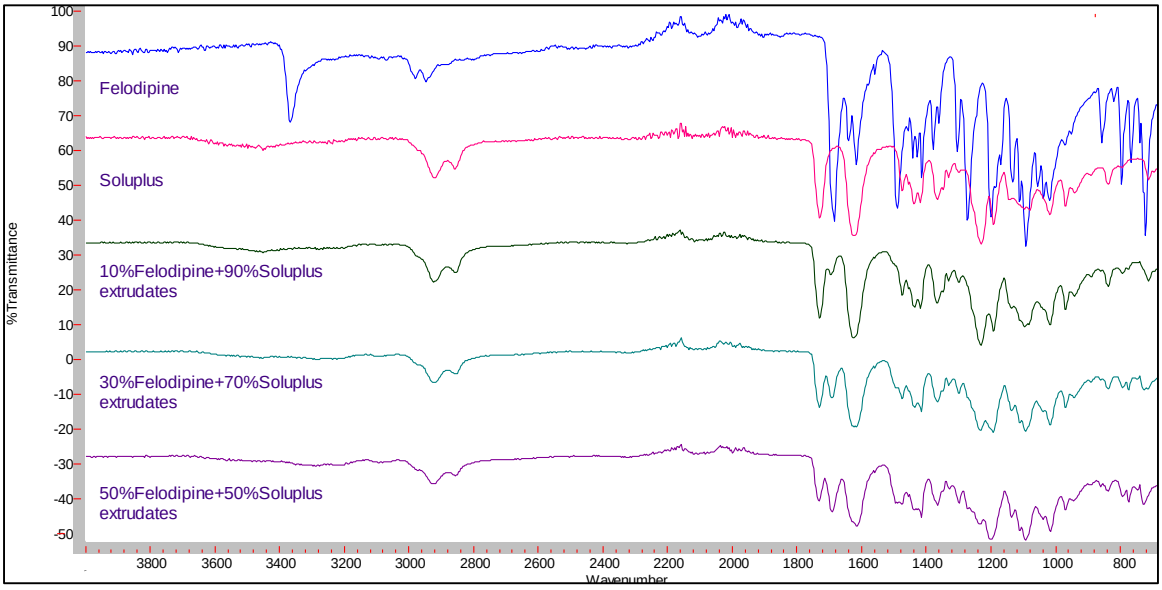

Figure 3-9: FT-IR spectra of felodipine, Soluplus® and SDs

3. 2. 8 Raman spectroscopy

To date, Raman spectroscopy has been extensively applied in pharmaceutical researches for both qualitative and quantitative purposes, and it was successfully utilized to determine the hydrogen bonding [34, 151, 191-193]. Nollenberger et al. reported that felodipine has a characteristic N-H stretch peak at 3375 cm^{-1} as well as a characteristic peak at 1639 cm-^{1} due to the free carbonyl stretching[151]. Although the N-H stretch peak in felodipine was not obvious in the Raman study here, attributed to the higher intensity of other molecular vibrations (Figure 3-10a), a Raman peak shift was clearly observed in the range of 1200-1700 cm^{-1}, which is an indication of potential intermolecular interaction (Figure 3-10b). Therefore, a theoretical calculation of felodipine molecular vibration was conducted to further identify the corresponding shifted peaks and consequently, C-H bending, N-H bending and an combination of C-C stretching with N-H bending peak were confirmed associated with 8, 7 and 5 cm^{-1} wavelength peak shift, respectively, which is indicative of the formation of hydrogen bonding (Figure 3-10c).

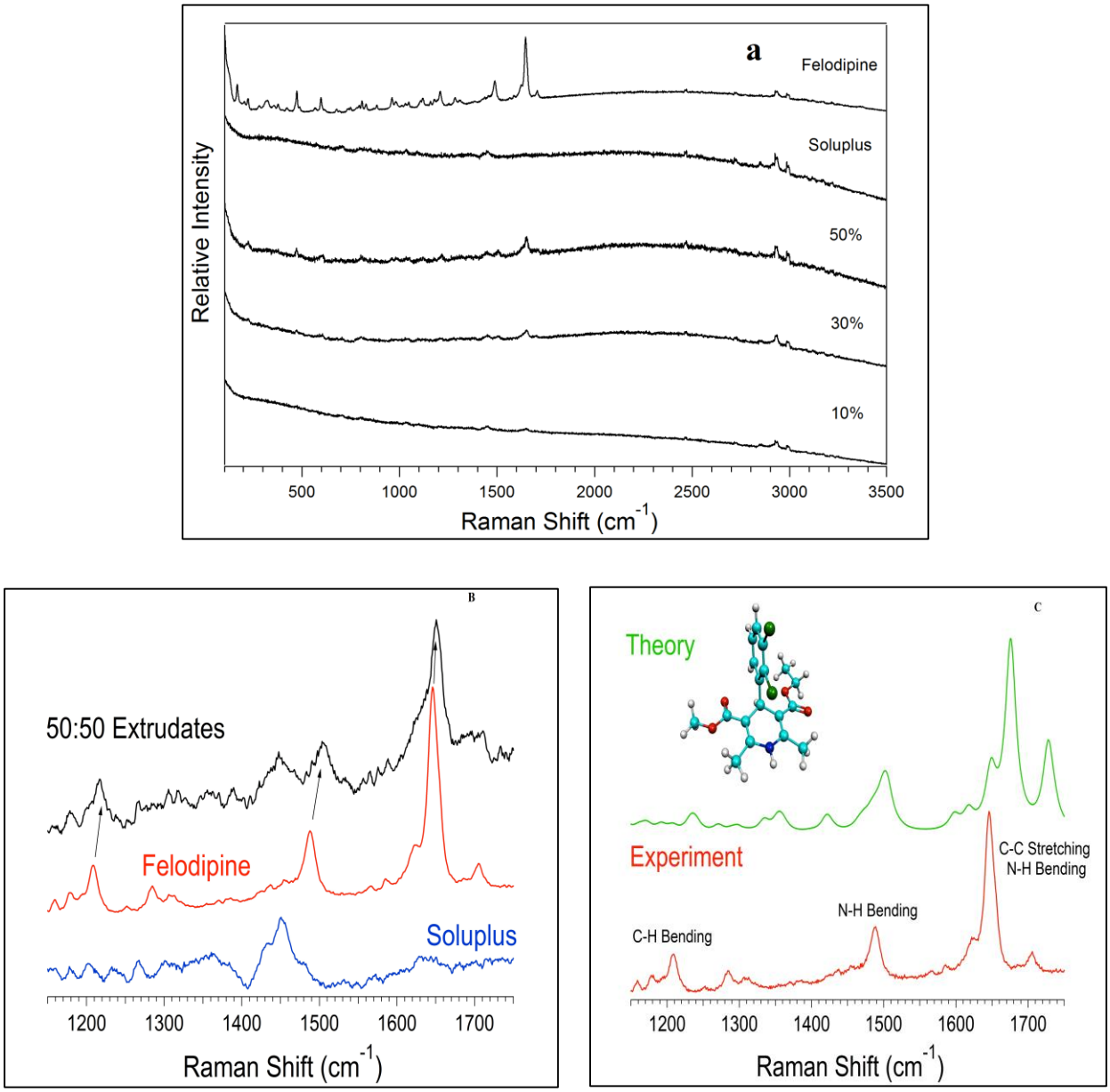

Figure 3-10: Raman spectra of felodipine, Soluplus® and SDs in the range of 50-3600cm^{-1} (a), Raman spectra of felodipine, Soluplus® and 50% SD in the range of 1200-1700 cm^{-1} (b), Theoretical and practical Raman spectra of felodipine in the range of 1200-1700 cm^{-1} (c)

3. 2. 9 Scanning Electron Microscopy

SEM has been widely applied to characterize solid-state properties of substances in pharmaceutical industry due to its high magnification and resolution[185]. The morphology of the selected samples was evaluated in SEM studies. Soluplus® powders demonstrated spherical shapes with smooth surface which indicates the amorphous state of the polymer (Figure 3-11a). To the contrast, pure felodipine powders revealed a plate-like shape with edged surfaces, attributed to the crystalline form (Figure 3-11b) [97]. For 10% felodipine solid dispersion, the surface was also smooth indicating that the felodipine was in amorphous state and uniformly distributed in the matrix, however, in the solid dispersions which contain 30 and 50% felodipine, few species with the features of crystal felodipine were detected which can possibly contribute to the phenomenon that no significant enhancement of solubility in these two solid dispersions compared to pure felodipine (Figure 3-11c and d). In addition, the cross-section of the extruded rods was also investigated. There is no difference between pure Soluplus® and 10% felodipine-Soluplus® rods, which indicated felodipine molecularly dispersed into the matrix and the formation of solid solution, to the contrary, few small felodipine crystals were also detected in part of the 30 and 50% felodipine-Soluplus® rods, which is consistent with the observation of extrudates surface; these small aggregates in the extrudates might also explain the lower solubility of 30 and 50% extrudates (Figure 3-11e-g). And this discrepancy with XRD studies was probably due to the detection limit of XRD (5% w/w)[88]

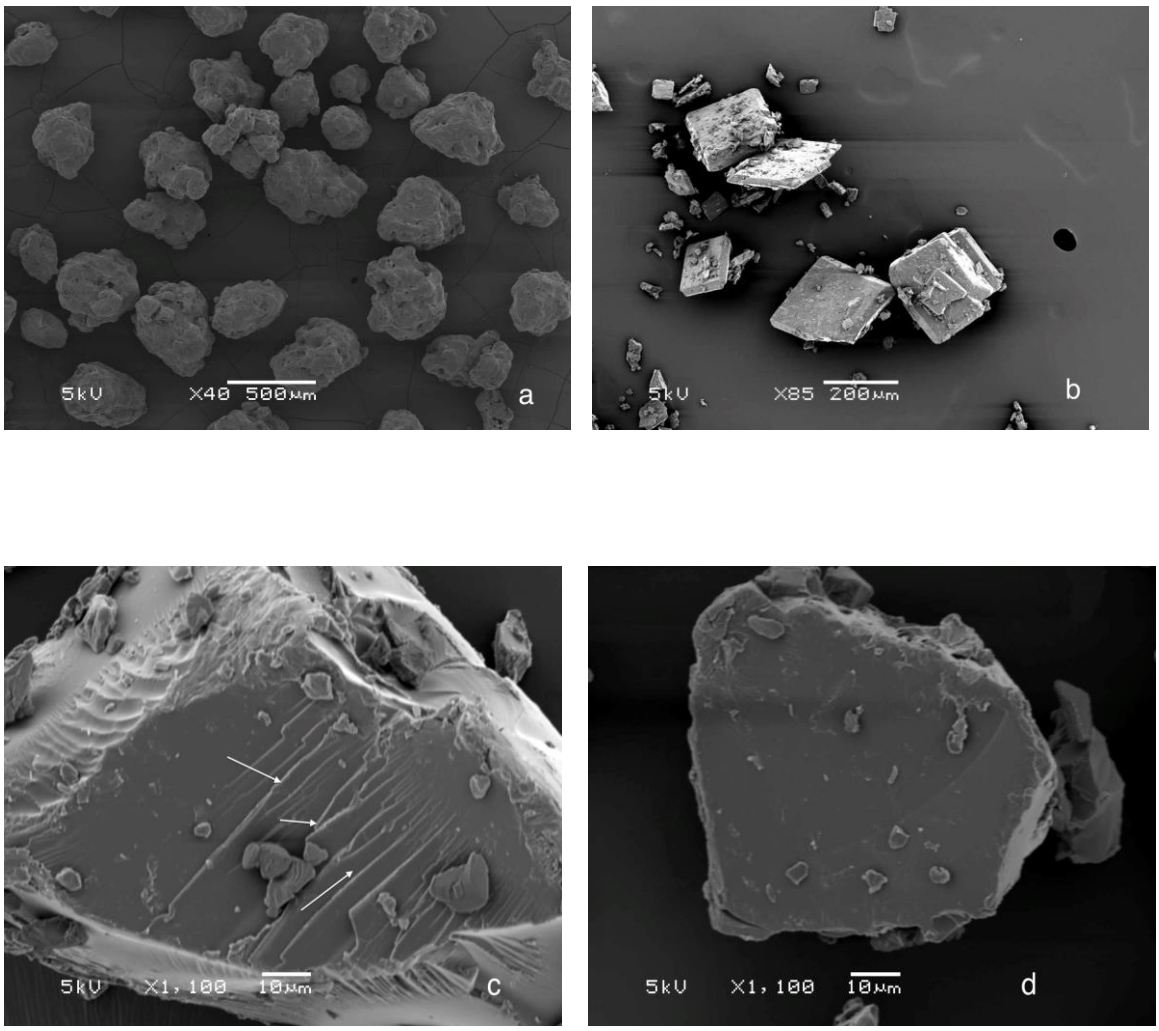

Figure 3-11: SEM of Soluplus® (a), felodipine (b), crystalline features of 30% SD (c), smooth surface of 50% SD (d)

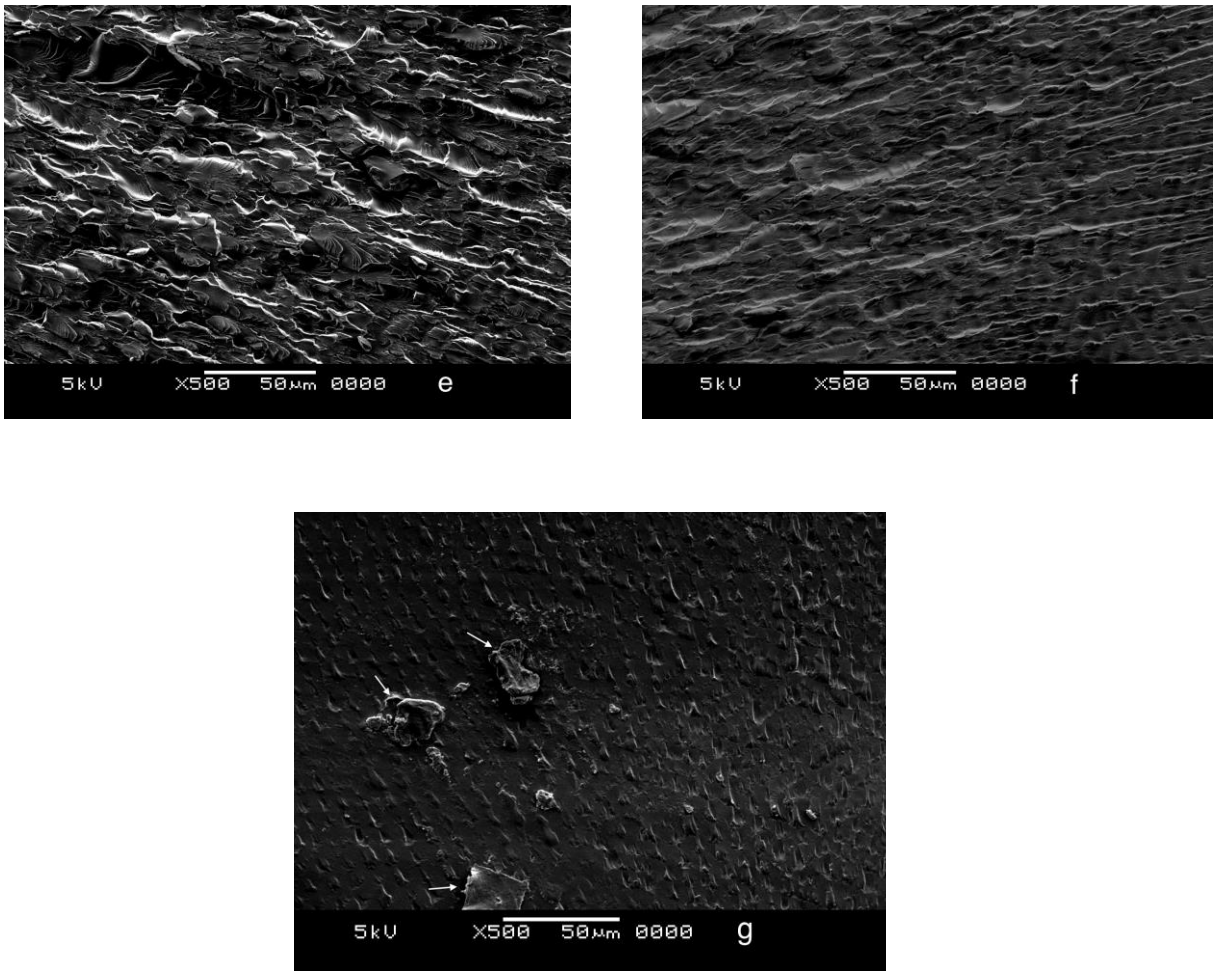

Figure 3-11: cross-section of Soluplus® rods (e), cross-section of 10% felodipine rods (f), cross-section of 30% felodipine rods (g)

CHAPTER 4

INFLUENCE OF FORMULATION FACTORS AND PROCESSING PARAMETERS ON KETOCONAZOLE-SOLUPLUS® MELT EXTRUDATES USING RESPONSE SURFACE METHODOLOGY

4. 1 Methods

4. 1. 1 Solubility Parameter Calculation

The solubility parameter δ was calculated using Hoftyzer/Van Krevelen method, which provides an accuracy level of 10% as mentioned previously[94]. To determine the solubility parameter of Soluplus®, which is comprised of polyvinyl caprolactam-polyvinyl acetate-polyethylene glycol at a ratio of 57:30:13, the number average of the three monomers was calculated.

4. 1. 2 Differential Scanning Calorimetry

The solubility of ketoconazole in Soluplus® matrix was predicted by DSC using a Perkin-Elmer Diamond DSC instrument (Norwalk, CT). Approximately 5-7 mg binary physical mixtures containing 10-100% ketoconazole were weighed and sealed into an aluminum pan. Samples were heated from 30 to 200°C at a ramp rate of 10°C/min, and cooled down from 200 to 30°C at a rate of 40°C/min followed a re-heating cycle to 200°C at a rate of 10°C/min. The enthalpy of fusion of ketoconazole was recorded and plotted versus the concentration. The extrudates were only subjected to the first heating cycle. The instrument was calibrated with indium and zinc before testing. Nitrogen was used as purge gas at a flow rate of 20mL/min. All the experiments were performed in triplicate.

4. 1. 3 Central Composite Design

A central composite design (CCD) based response surface methodology (RSM) was created using Design-Expert® 8.0 (Stat-Ease, Inc.), with three independent variables (% drug load, screw speed and temperature) and two dependent variables (post-extrusion drug content and % drug release at 15min).

4. 1. 4 Hot Melt Extrusion

The drug-polymer physical mixtures were prepared at pre-determined drug concentration. The two components were initially sieved with USP 60 mesh and further mixed in a V-cone blender (MaxiBlend™, GlobePharma, North Brunswick, NJ, USA) at 50 rpm for 15 min. The mixtures were extruded into uniform rods using a ThermoFisher Scientific HAAKE MiniLab II. The extruded rods were milled into powder using a laboratory grinder.

4. 1. 5 Drug Content Analysis

Approximately 20 mg of the physical mixtures or powdered extrudates were weighed and dissolved in 20 mL methanol. The solution was then diluted 10 times with methanol. The samples were filtered through 13 mm PTFE membrane filters (Whatman, Piscataway, NJ) and analyzed utilizing a HPLC at a wavelength of 231 nm. The mobile phase consisted of 25 mM phosphate buffer and acetonitrile at a ratio of 4:6, and the pH was adjusted to 4.5 with phosphoric acid.

4. 1. 6 *In Vitro* Dissolution Studies

Extrudates containing ketoconazole equivalent to 20 mg were filled into capsules and subjected to dissolution studies using a Hanson SR8-Plus dissolution test system according to USP 31 apparatus 2, (0.1N HCl pH 1.2, 75 rpm, 37±0.5°C). 1.5 mL samples were collected precisely at pre-determined interval and replaced with equal amount of fresh dissolution medium.

The withdrawn samples were immediately filtered through a 0.2 µm, 13 mm PTFE membrane filters (Whatman, Piscataway, NJ) and analyzed using the same method utilized for drug content analysis.

4. 1. 7 Fourier Transform Infrared Spectroscopy (FT-IR)

Fourier transform infrared spectroscopy (FT-IR) studies were conducted on a PerkinElmer Spectrum 100 FT-IR Spectrometer, equipped with the universal ATR accessory, in the range of 4000-650 cm^{-1}, using a resolution of 1 cm^{-1}. All the experiments were performed in triplicate.

4. 1. 8 Stability

The extrudates were filled into sealed borosilicate glass vials and stored under 25°C/60% RH and 40°C/75% RH conditions per ICH guidelines. At pre-determined time interval, samples were subjected to DSC, content analysis, and dissolution studies to evaluate the physical and chemical stability.

4. 2 Results and discussion

4. 2. 1 Solubility Parameter Calculation

The group contribution of ketoconazole is listed in Table 4-1, and the solubility parameters was further determined as 26.51. It is well accepted that two materials are likely to be miscible if the difference of solubility parameters is less than 7 $MP^{1/2}$, and in contrast, immiscibility is expected if the difference is larger than 10 $MP^{1/2}$[98]. As calculated before, the solubility parameter of Soluplus® is 21.64, therefore, KTZ and SOL are expected to be partially, if not completely, miscible.

Table 4-1: Group contribution of ketoconazole using Hoftyzer/Van Krevelen method

Structure group	No.	F_{di} $(MJ/m^3)^{½} \cdot mol^{-1}$	F_{pi} $(MJ/m^3)^{½} \cdot mol^{-1}$	E_{hi} (J/mol)	V $(cm^3 \cdot mol^{-1})$
$–CH_3$	1	420	0	0	33.5
$–CH_2–$	6	270	0	0	16.1
=CH–	3	200	0	0	13.5
>C<	2	-70	0	0	-19.2
–Cl	2	450	550	400	26
–CO–	1	290	770	2000	10.8
–N<	3	20	800	5000	-9
–O–	3	100	400	3000	3.8
–N=	1	0	0	0	5
Ring	3	190	0	0	16
Phenylene (o, m, p)	2	1270	110	0	33.4

4. 2. 2 Differential Scanning Calorimetry

As previously mentioned, it is challenging to estimate the solubility of a drug within a polymer in the solid state; however, several approaches have been demonstrated to either theoretically or practically determine the drug's solubility in the polymer. One such method is to utilize the enthalpy of fusion[110, 141, 142, 158, 170-175, 194]. The enthalpy of fusion is generally defined as the heat needed to convert the substance from solid to liquid state without increasing the temperature[177], and it was introduced to calculate the drug solubility by Theeuwes et al. based on the assumption that the dissolved drug has no contribution to the endothermic event. Therefore, by plotting the enthalpy of fusion versus the drug loading concentration, the intercept in the X-axis would be the theoretical solubility of the drug within the polymer [174]. As presented in Figure 4-1a, Ketoconazole has a characteristic melting peak

at 146°C, and a glass transition temperature of 42°C while in the amorphous phase was determined using the second heating cycle (Figure 4-1b). The variation from the T_g value in Chapter 2 is most probably due to experimental related characteristics of T_g. Moreover, with an increase in the concentration of Soluplus®, the height of the melting peak decreased. Interestingly, a small hump around 62°C was also observed when the concentration of ketoconazole reduced to 40% or less, which was possibly attributed to the T_g value of small amount of KTZ-SOL solid dispersion when the physical mixtures prepared. No endothermic peak was observed in the second heating cycle for all binary mixtures, which indicated that the drug was converted into its amorphous phase. Furthermore, the solubility of ketoconazole in Soluplus® matrix was determined as ~5% (Figure 4-2).

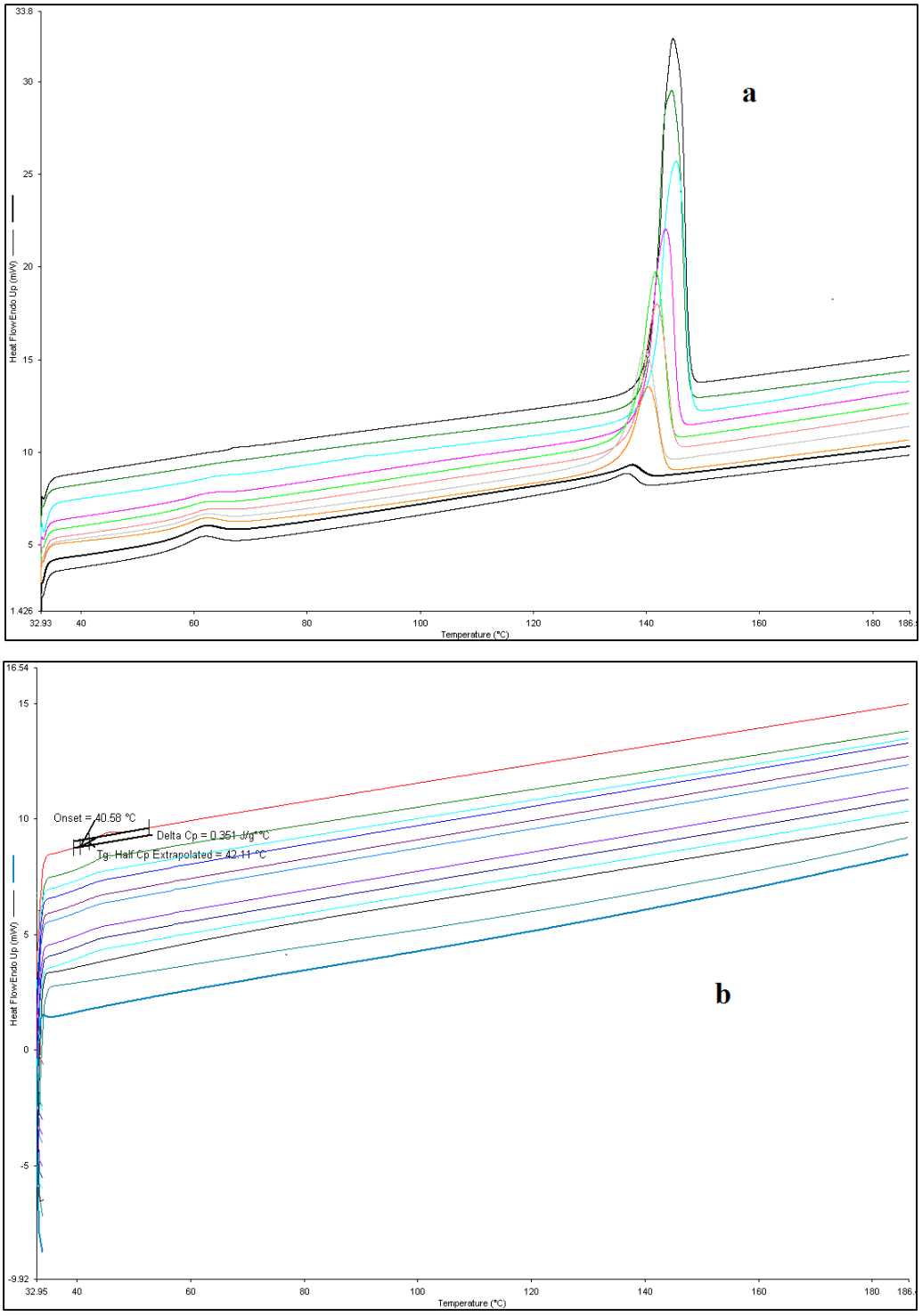

Figure 4-1: First heating cycle of DSC (a), Second heating cycle of DSC (b)

(From the top to bottom: 100, 90, 80, 70, 60, 50, 40, 30, 20, and 10% KTZ or KTZ-SOL physical mixtures)

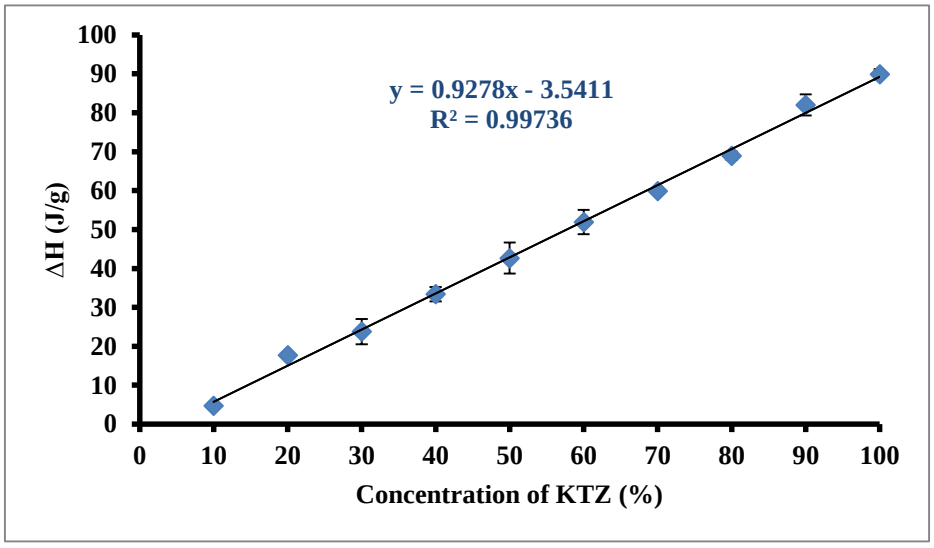

Figure 4-2: Enthalpy of fusion versus ketoconazole concentration

4. 2. 3 Central Composite Design

Processing parameters such as screw design, screw speed, feeding rate or process temperature have been demonstrated to have influences on the properties of extrudates in many studies [195-197]. However, it is also not unusual to find that the processing parameters have little or no effect on the properties of formulation [198]. Therefore, whether these parameters would affect the properties of the formulation needs to be considered on a case-by-case basis. Twenty formulations containing ketoconazole and Soluplus® including six center points (marked in yellow) were generated under a central composite design (Table 4-2), in which, drug loading (A), screw speed (B), and processing temperature (C) are the independent variables, while post extrusion content as well as drug release percentage at 15min are the dependent variables.

Table 4-2: Experimental Design

Std	Run	Factor 1 A: Drug loading (%)	Factor 2 B: Screw speed (RPM)	Factor 3 C: Temperature (°C)
6	1	36	65	112
7	2	24	65	148
1	3	24	35	112
17	4	30	50	130
13	5	30	25	130
16	6	30	50	130
4	7	36	35	148
11	8	30	50	100
19	9	30	50	130
14	10	30	75	130
12	11	30	50	160
3	12	24	35	148
8	13	36	65	148
10	14	40	50	130
5	15	24	65	112
18	16	30	50	130
9	17	20	50	130
2	18	36	35	112
15	19	30	50	130
20	20	30	50	130

4. 2. 4 Statistical analysis

In the dissolution studies, all of twenty formulations demonstrated approximately 100% release at 45min, compared to less than 20% release of the pure drug, which demonstrated solubility enhancement of ketoconazole. The overall results were shown in Figure 4-3, and further subjected to analysis of variance (ANOVA). Both of the two responses (post extrusion content and % drug release at 15min) fit into the response surface quadratic model appropriately. This is indicated by the p-value of the model and lack of fit (0.0002, 0.0647) and (0.0005, 0.0517), respectively.

Select	Std	Run	Factor 1 A:Drug Load %	Factor 2 B:Screw Speed RPM	Factor 3 C:Temperature C	Response 1 Post Extrusion Content %	Response 2 Release@15Min %
	14	1	30.00	50.00	160.00	100.75	68.87
	19	2	30.00	50.00	130.00	98.55	76.36
	10	3	40.00	50.00	130.00	92.75	48.23
	6	4	36.00	35.00	148.00	99.49	64.27
	4	5	36.00	65.00	112.00	89.27	51.78
	15	6	30.00	50.00	130.00	99.9	71.81
	5	7	24.00	35.00	148.00	90.05	81.4
	3	8	24.00	65.00	112.00	67	42.27
	2	9	36.00	35.00	112.00	95.27	58.21
	18	10	30.00	50.00	130.00	103.47	70.38
	1	11	24.00	35.00	112.00	91.62	59.5
	9	12	20.00	50.00	130.00	53.98	60.68
	20	13	30.00	50.00	130.00	97.19	72.84
	11	14	30.00	25.00	130.00	102.19	65.76
	17	15	30.00	50.00	130.00	102.97	76.65
	13	16	30.00	50.00	100.00	89.64	42.83
	12	17	30.00	75.00	130.00	99.28	65.81
	7	18	24.00	65.00	148.00	81.19	59.12
	16	19	30.00	50.00	130.00	104.73	70.82
	8	20	36.00	65.00	148.00	94.57	55.72

Figure 4-3: Overall results of twenty KTZ-SOL formulations

The post extrusion content can be expressed in the equation below,

Post extrusion content = 101.15+8.29*A-3.60*B+2.97*C+2.77*A*B-0.38*A*C+2.07*B*C-9.88A^2-0.20B^2-2.16C^2.....Equation 4-1

Whereas drug loading has the most significant effect ($p<0.0001$) on the post-extrusion content (Figure 4-4). The two opposite coefficients of A and A^2 (8.29 and -9.88, respectively), imply that drug loading has a dual influence on the post extrusion content, and an optimized value will exist. It is not surprising to obtain a high content while the drug loading is high. On the other hand, when drug loading is very low, an acceptable post extrusion content could also be obtained which is possibly attributed to the more homogeneous mixing. Temperature and screw speed also had partial effect on the content. A slower screw speed is associated with a prolonged residence time in the extruder, while a higher processing temperature would reduce the viscosity of polymer which will also be beneficial for mixing.

Response	1	Post Extrusion Content				
ANOVA for Response Surface Quadratic model						
Analysis of variance table [Partial sum of squares - Type III]						
Source	Sum of Squares	df	Mean Square	F Value	p-value Prob > F	
Model	2802.23	9	311.36	12.65	0.0002	significant
A-Drug Load	*947.93*	*1*	*947.93*	*38.52*	*0.0001*	
B-Screw Speed	*178.93*	*1*	*178.93*	*7.27*	*0.0224*	
C-Temperature	*121.94*	*1*	*121.94*	*4.96*	*0.0502*	
AB	*63.62*	*1*	*63.62*	*2.59*	*0.1389*	
AC	*1.20*	*1*	*1.20*	*0.049*	*0.8296*	
BC	*35.45*	*1*	*35.45*	*1.44*	*0.2577*	
A^2	*1420.26*	*1*	*1420.26*	*57.72*	*< 0.0001*	
B^2	*0.61*	*1*	*0.61*	*0.025*	*0.8779*	
C^2	*68.09*	*1*	*68.09*	*2.77*	*0.1272*	
Residual	246.07	10	24.61			
Lack of Fit	*200.56*	*5*	*40.11*	*4.41*	*0.0647*	*not significant*
Pure Error	*45.51*	*5*	*9.10*			
Cor Total	3048.30	19				

Figure 4-4: ANOVA for response surface quadratic model of post extrusion content

Similar to post extrusion content, the % Drug release at 15min can also be expressed by the following equation:

% Drug release at 15min = 73.08-2.42*A-3.98*B+6.74*C+3.01*A*B-3.53*A*C-0.88*B*C-6.29A^2-2.28B^2-5.80C^2 ..... Equation 4-2

Whereas all of the three independent factors affected the % drug dissolution at 15 minutes which is indicated by the p-value of A^2 (0.0005), B (0.0108), C (0.0004) and C^2 (0.0009) (Figure 4-5). The negative coefficient -6.29 of A^2 indicates that a high drug loading will retard the release of ketoconazole, which is due to the reduction of hydrophilic polymer in the formulation. Meanwhile, the negative coefficient -3.98 of B illustrates that slower screw speed will provide a more sufficient time for mixing which will turn into a faster release. However, it is surprising to find out opposite coefficients of C and C^2 which demonstrate that temperature might have a dual effect on the % release at 15min.

Response 2 Release@15Min

ANOVA for Response Surface Quadratic model

Analysis of variance table [Partial sum of squares - Type III]

Source	Sum of Squares	df	Mean Square	F Value	p-value Prob > F	
Model	2109.85	9	234.43	10.47	0.0005	significant
A-Drug Load	*80.63*	*1*	*80.63*	*3.60*	*0.0869*	
B-Screw Speed	*218.37*	*1*	*218.37*	*9.76*	*0.0108*	
C-Temperature	*626.43*	*1*	*626.43*	*27.98*	*0.0004*	
AB	*75.22*	*1*	*75.22*	*3.36*	*0.0967*	
AC	*103.32*	*1*	*103.32*	*4.62*	*0.0572*	
BC	*6.43*	*1*	*6.43*	*0.29*	*0.6038*	
A^2	*575.25*	*1*	*575.25*	*25.70*	*0.0005*	
B^2	*75.82*	*1*	*75.82*	*3.39*	*0.0955*	
C^2	*488.56*	*1*	*488.56*	*21.83*	*0.0009*	
Residual	223.85	10	22.38			
Lack of Fit	*186.30*	*5*	*37.26*	*4.96*	*0.0517*	*not significant*
Pure Error	*37.55*	*5*	*7.51*			
Cor Total	2333.70	19				

Figure 4-5: ANOVA for response surface quadratic model of % release at 15min

The actual values of both post extrusion responses, content and % release at 15 min, laid beside the predicted values (straight line in Figure 4-6 a and b) indicates the robustness of the experimental design.

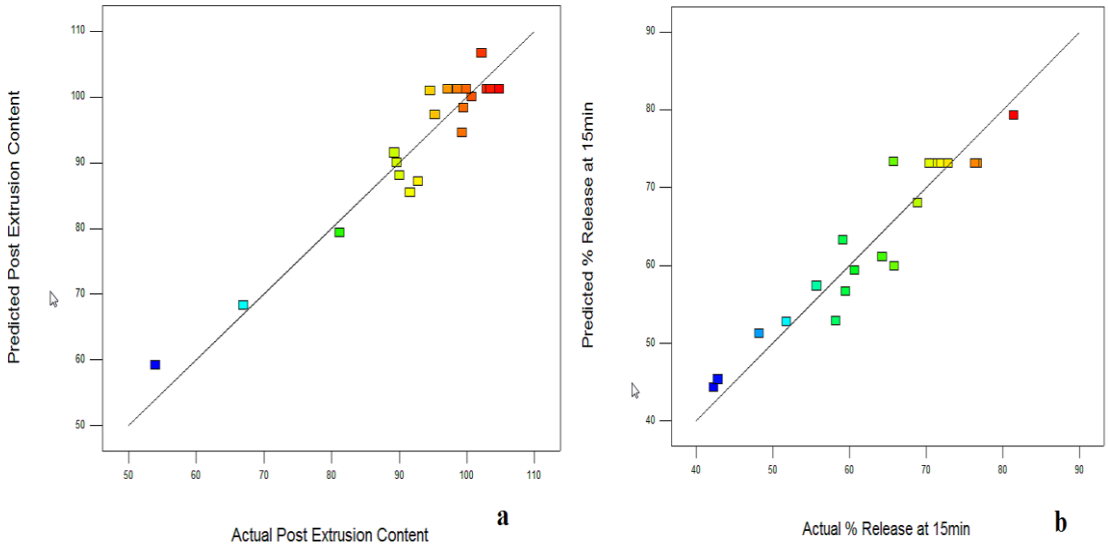

Figure 4-6: Predicted values vs actual values post extrusion content (a), % release at 15min (b)

As a result, the formulation parameters were further optimized as: 29.8% drug loading extruded at a temperature of 140°C and screw speed of 31 rpm with highest desirability of 0.489 (Figure 4-7) a predicted post processing content of 104.86% (Figure 4-8a) and 77.19% (Figure 4-8b) release at 15min on the criteria of maximizing drug loading, post extrusion content and % release at 15min (The cut-off values of post extrusion content and % release at 15 min were set up as 95% and 70%, respectively) while maintaining extrusion temperature and screw speed in the range of the design space.

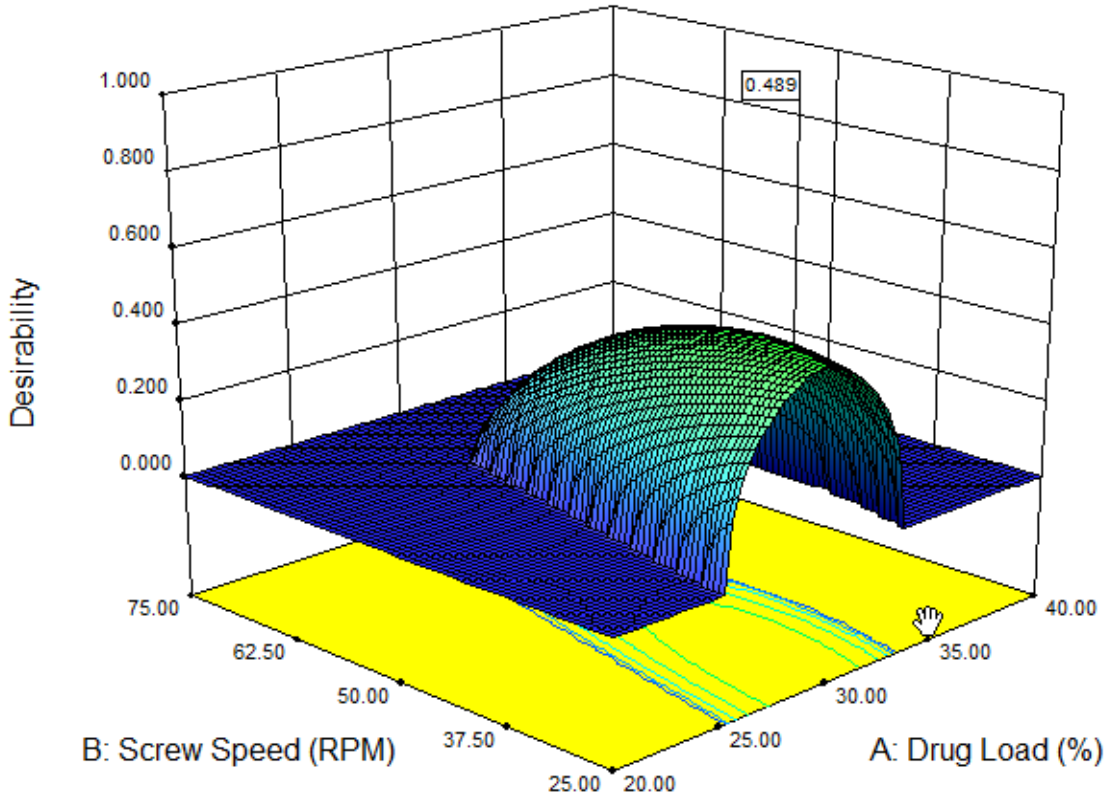

Figure 4-7: 3D contour of desirability

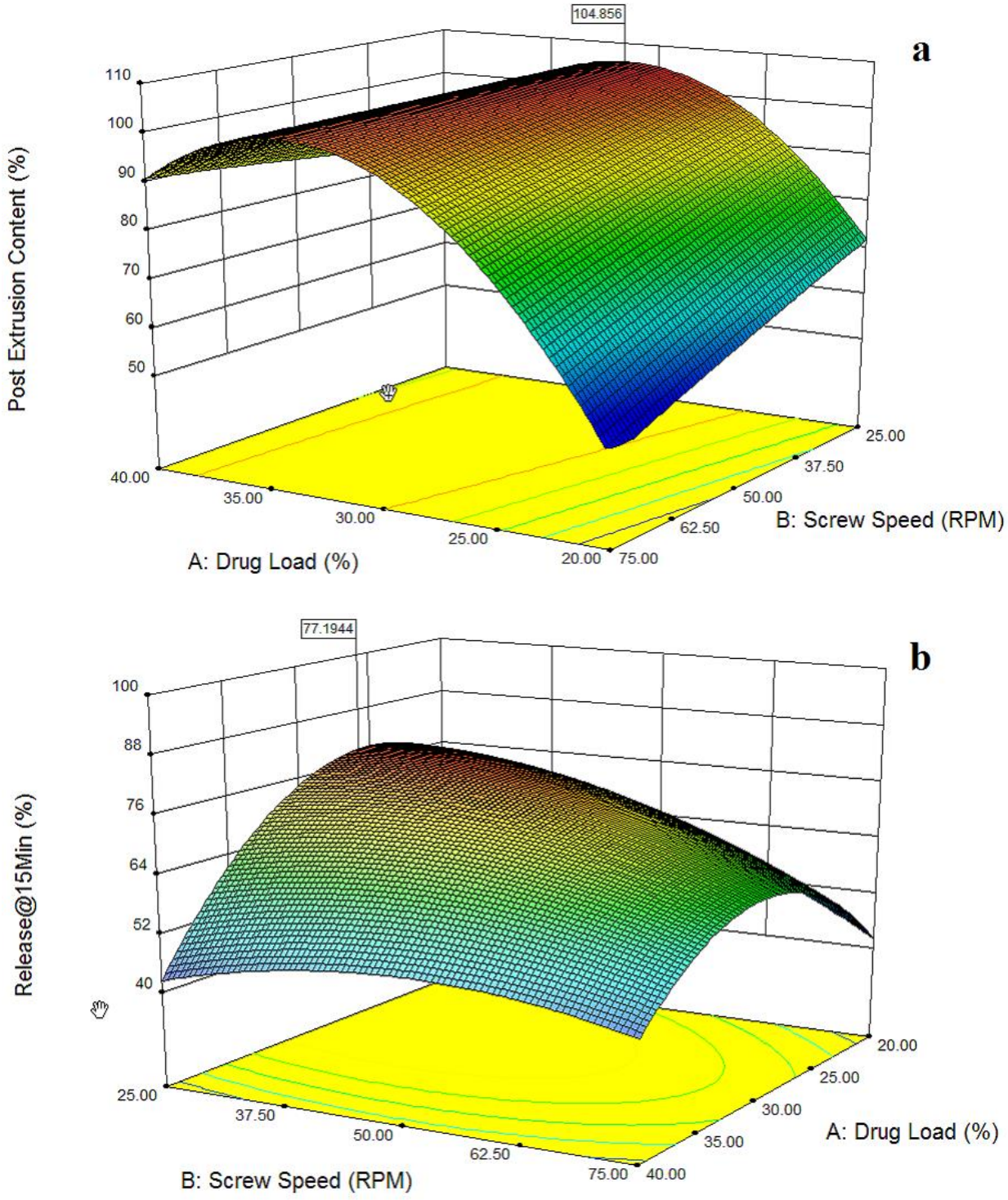

Figure 4-8: 3D contour of KTZ post extrusion content (a), % release at 15min (b)

In order to validate the optimized model, three repeated batches were conducted under the conditions stated above, and the results were consistent with the predicted values which demonstrated the robustness of this model (Table 4-3 and Figure 4-9).

Table 4-3: Predicted value vs actual value of optimized formulation

Response	Predicted Value	Actual Value	Bias (%)
Post extrusion content (%)	104.86	97.68±4.38	6.85
Release at 15min (%)	77.19	72.80±1.31	5.69

Bias= (Predicted Value-Actual Value)/Predicted Value ×100

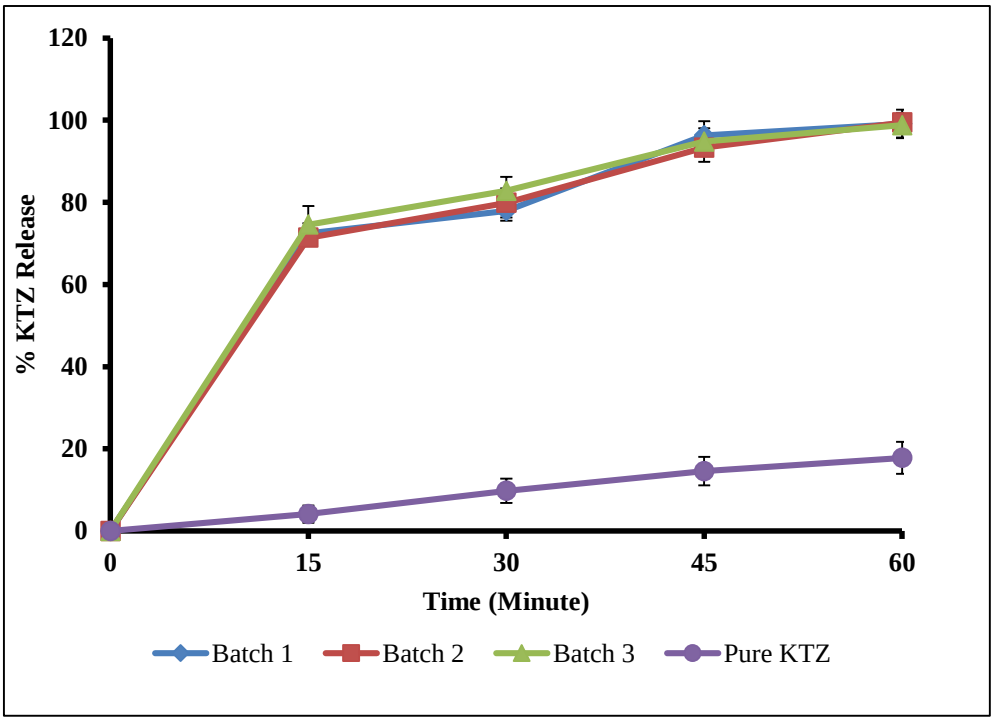

Figure 4-9: Dissolution profile of optimized formulation containing 29.8% KTZ

4. 2. 5 Fourier transform infrared spectroscopy

Intermolecular interactions, for instance hydrogen bonding, are important in solid dispersion systems which have been demonstrated to benefit the physical stability. However, due to the fact that no hydrogen donor is presented in the structure of KTZ, it is not expected that hydrogen bonding would be observed nor other intermolecular interactions between KTZ and SOL. In order to confirm the assumption, FT-IR studies were conducted on individual component and the extrudates. As shown in Figure 4-10, the spectrum of extrudates is a collection of the two components' patterns and no sign of hydrogen bonding was detected.

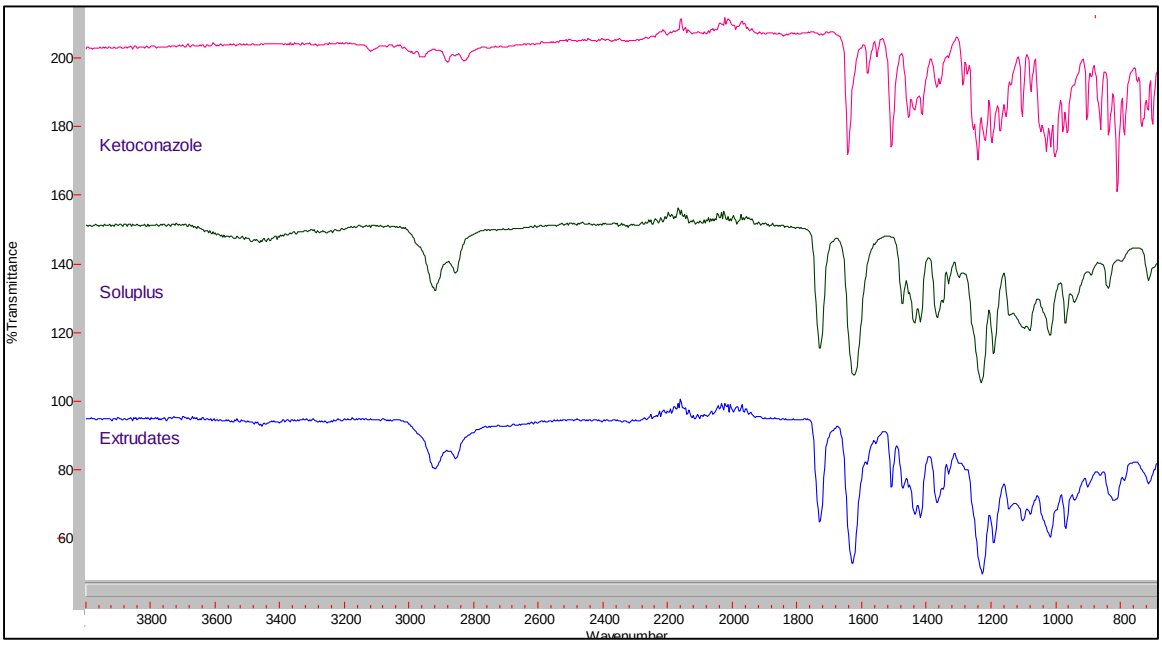

Figure 4-10: FT-IR spectra of KTZ, SOL and Extrudates

4. 2. 6 Scanning electron microscopy (SEM)

The morphology of the Ketoconazole-Soluplus® solid dispersions was examined by SEM study (Figure 4-11a-d). This technique provided direct visual information about the samples. The pure crystalline ketoconazole demonstrated a plate-like shape with rough surfaces, while the Soluplus® particles appeared spherical in shape. Meanwhile, the extrudates revealed a smooth surface which indicated that ketoconazole was in the amorphous state within the matrix [97]. Furthermore, since all the particles under observation demonstrated a similar morphology, it could be extrapolated that the drug was uniformly distributed into the matrix, which indicates good miscibility between drug and polymer.

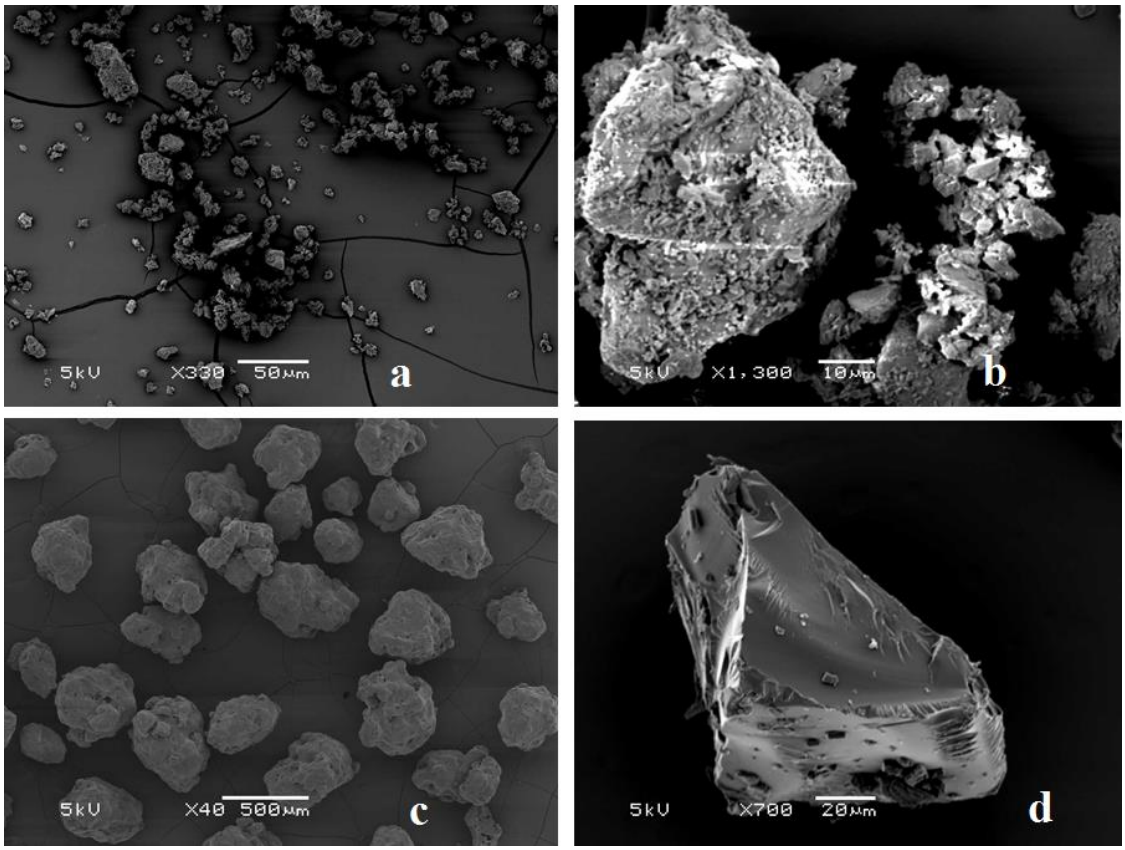

Figure 4-11: SEM of KTZ ×330 magnification (a), SEM of KTZ ×1300 magnification (b), SEM of SOL (c), SEM of optimized extrudates (d)

4. 2. 7 Stability Test

Stability is one of the most crucial concerns for any pharmaceutical development process, and in regards to the amorphous solid dispersions, the drugs could be less physically or chemically stable than crystalline materials due to being in a higher energy state. Moreover, moisture and temperature are the most common factors which can induce the stability issues [199-201]. Hence, the optimized formulation was stored into two temperature/moisture conditions to evaluate both the physical and chemical stability. No sign of re-crystallization or phase separation was determined in the DSC thermograms (Figure 4-12) which was indicative of a good physical stability. Additionly, all the drug content tests performed on the stability samples were above 95% and all the samples demonstrated similar dissolution profile demonstrating the samples chemically stable (Figure 4-13 &14).

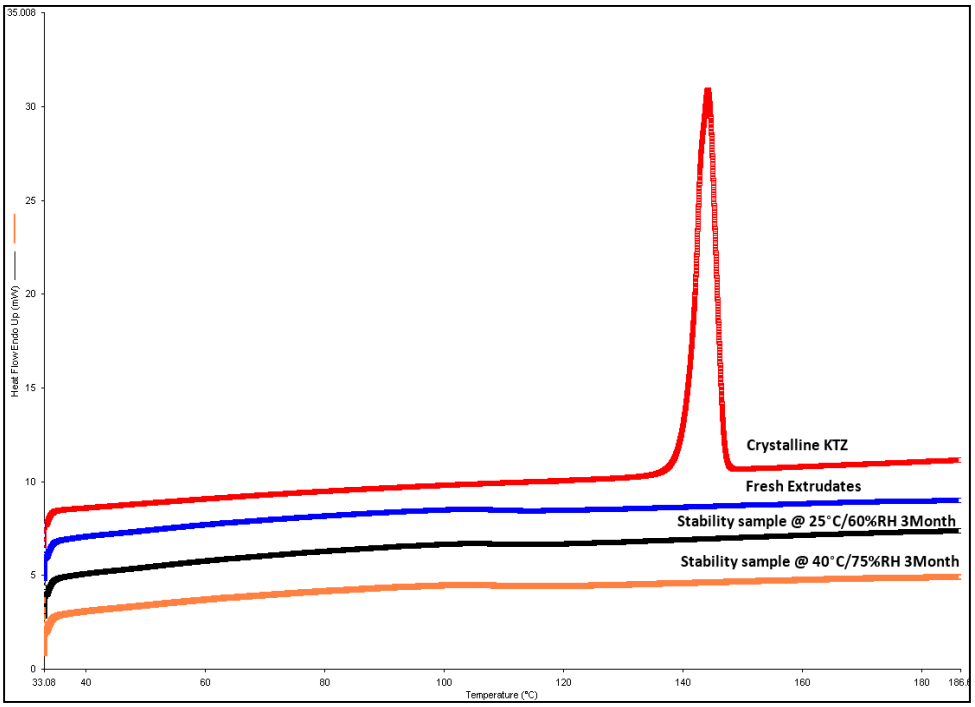

Figure 4-12: DSC of crystalline KTZ, fresh extrudates, stability samples stored at 25°C/60% RH and 40°C/75% RH (3 month point)

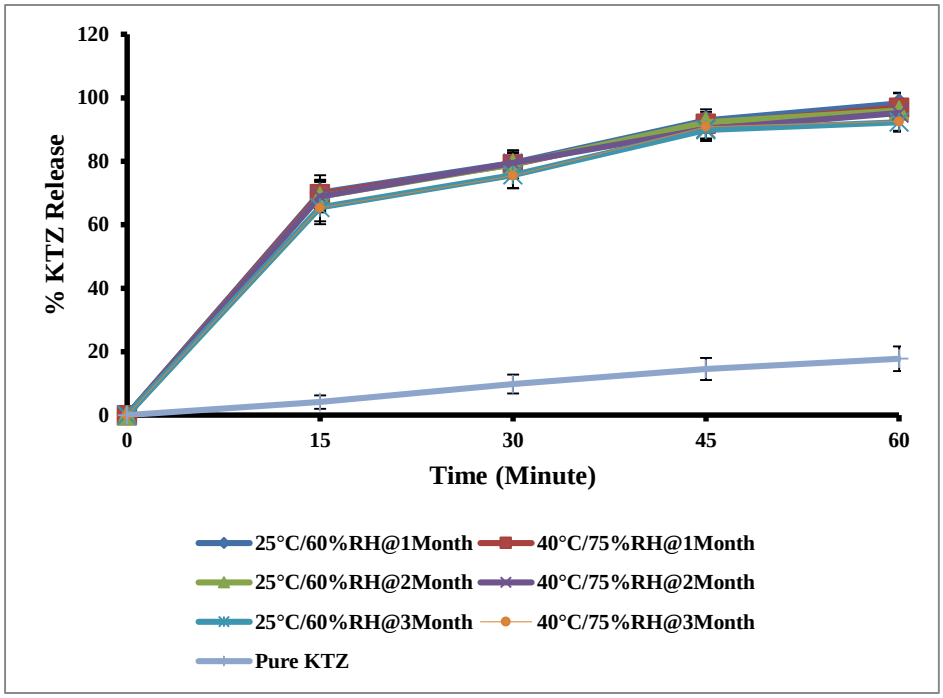

Figure 4-13: *In vitro* dissolution of crystalline KTZ, stability samples stored at 25°C/60% RH and 40°C/75% RH (1, 2 and 3 month point)

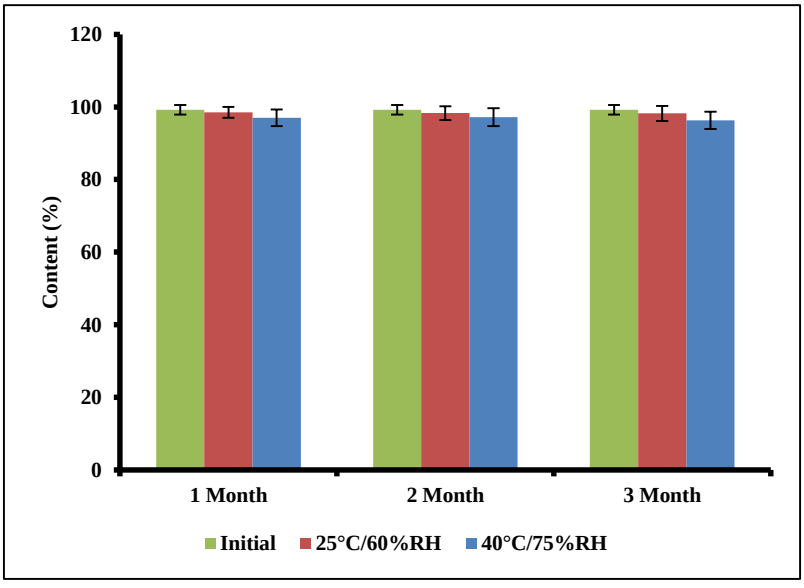

Figure 4-14: KTZ content of fresh extrudates, stability samples stored at 25°C/60% RH and 40°C/75% RH (1, 2 and 3 month point)

CHAPTER 5

SOLUBILITY ENHANCEMENT AND PRECIPITATION INHIBITION OF PACLITAXEL USING HOT MELT EXTRUSION TECHNOLOGY

5. 1 Methods

5. 1. 1 Phase solubility determination

An excess amount of paclitaxel (approximately 1mg) was added to 20mL vials containing pH 1.2 hydrochloric acid, pH 4.0 critic acid buffer, pH 6.8 and 7.4 phosphate buffer, respectively. The samples were placed into a Precision Reciprocal Shaking Bath (ThermoFisher Scientific, Stone, UK) at 37°C and shaken at a speed of 80rpm for 48 hours to achieve equilibrium. The samples were then filtered through a 0.45 μm Nylon filter membrane (Whatman, Piscataway, NJ) and analyzed using HPLC at a λmax of 230 nm.

5. 1. 2 Preparation of solid dispersions

Initially, a hot-melt cast molding method was used to prepare the solid dispersion systems. PTX, concentrations varied from 10-40%, was homogeneously mixed with PolyOx^{TM} WSR N-80 and other excipients and heated at the temperature ranged from 140-150°C for 8-10 min. The final formulation was extruded using a ThermoFisher Scientific HAAKE MiniLab II. The screw speed and processing temperature were set up at 50rpm and 145°C, respectively. Extrudates were further pelletized and filled into capsules (size 1) for dissolution studies.

5. 1. 3 *In vitro* dissolution studies

Dissolution studies were performed on a Hanson SR8-Plus™ dissolution test station (Hanson Research Corporation, Chatsworth, CA) operated at 50 rpm, using four types of

media, 1) 900 mL pH 6.8 phosphate buffer, 2) 900 mL pH 7.4 phosphate buffer, 3) 900 mL 0.1N HCl and 4) 750 mL 0.1N hydrochloric acid (pH 1.2) for 2 hours, followed with additional 250 mL 0.2M tribasic sodium phosphate to adjust pH to 7.4 by adding either 2N HCl or NaOH. All the dissolution studies were conducted for 12 hours. USP apparatus 2 and 5 were utilized for the dissolution of capsules and patches, respectively. At pre-determined time intervals 1.5mL samples were removed from the dissolution vessels and replaced with fresh dissolution medium. These collected samples were immediately filtered using 13mm PTFE membrane filters (Whatman, Piscataway, NJ) with a pore size of 0.2 µm and analyzed. The release studies were performed in triplicate and the average values were compared.

5. 1. 4 Differential scanning calorimetry (DSC)

Approximately 5-7 mg samples were weighed and analyzed at 10°C/min heating rate between 25°C to 250°C using a Perkin-Elmer Diamond DSC instrument (Norwalk, CT) equipped with Pyris software (Shelton, CT, USA). The instrument was calibrated with indium and zinc before testing. Nitrogen was used as purge gas at a flow rate of 20 mL/min. All the experiments were performed in triplicate.

5. 1. 5 Fourier transform infrared spectroscopy (FT-IR)

Fourier transform infrared spectroscopy (FT-IR) studies were conducted on a PerkinElmer Spectrum 100 FT-IR Spectrometer, equipped with the universal ATR accessory, in the range of 4000-650 cm^{-1}, using a resolution of 1 cm^{-1}. All the experiments were performed in triplicate.

5. 1. 6 Stability

The extrudates were placed in sealed bottles and stored in 25°C/60% RH and 40°C/75% RH conditions per ICH guidelines. Samples were taken at every month and subjected to DSC and dissolution studies in the period of storage up to 3 months.

5. 2. 1 Phase Solubility Determination

The aqueous solubility of paclitaxel was determined as 0.7-0.8 µg/ml in different solutions (Figure 5-1), which is confirmed with the reported value[129]. Also, only slight difference was observed with the alteration of pH, due to the lack of functional groups which can be ionized in the structure of paclitaxel. Hence, it is not feasible to improve the solubility of paclitaxel by common approaches like salts formation[202] and the solubility enhancement of paclitaxel was challenging to pharmaceutical researchers. Various methods were developed to promote the solubility of PTX, and the pros and cons of different approaches were thoroughly discussed in several reviews [129, 135, 136, 203-207].

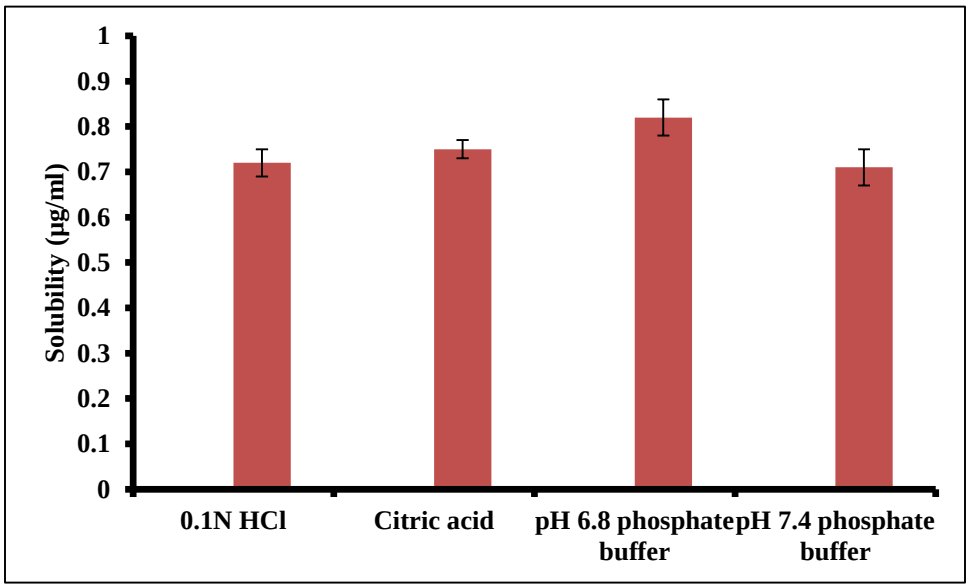

Figure 5-1: Phase solubility of paclitaxel

5. 2. 2 Differential Scanning Calorimetry

An endothermic peak of paclitaxel was observe around 223.14°C, followed with a degradation event, which is consistent with observation from Liggins[208]. No endothermic peak of PTX was observed in DSC thermograms for the binary physical mixtures of PTX and PolyOx^{TM} WSR N-80 up to 40% PTX loading (Figure 5-2), which is a supportive sign of the miscibility/ solubility of PTX in the polymer matrix. Interestingly, no degradation event was detected in the physical mixtures either, which demonstrated the ability of PolyOx^{TM} WSR N-80 to prevent the thermal degradation of PTX.

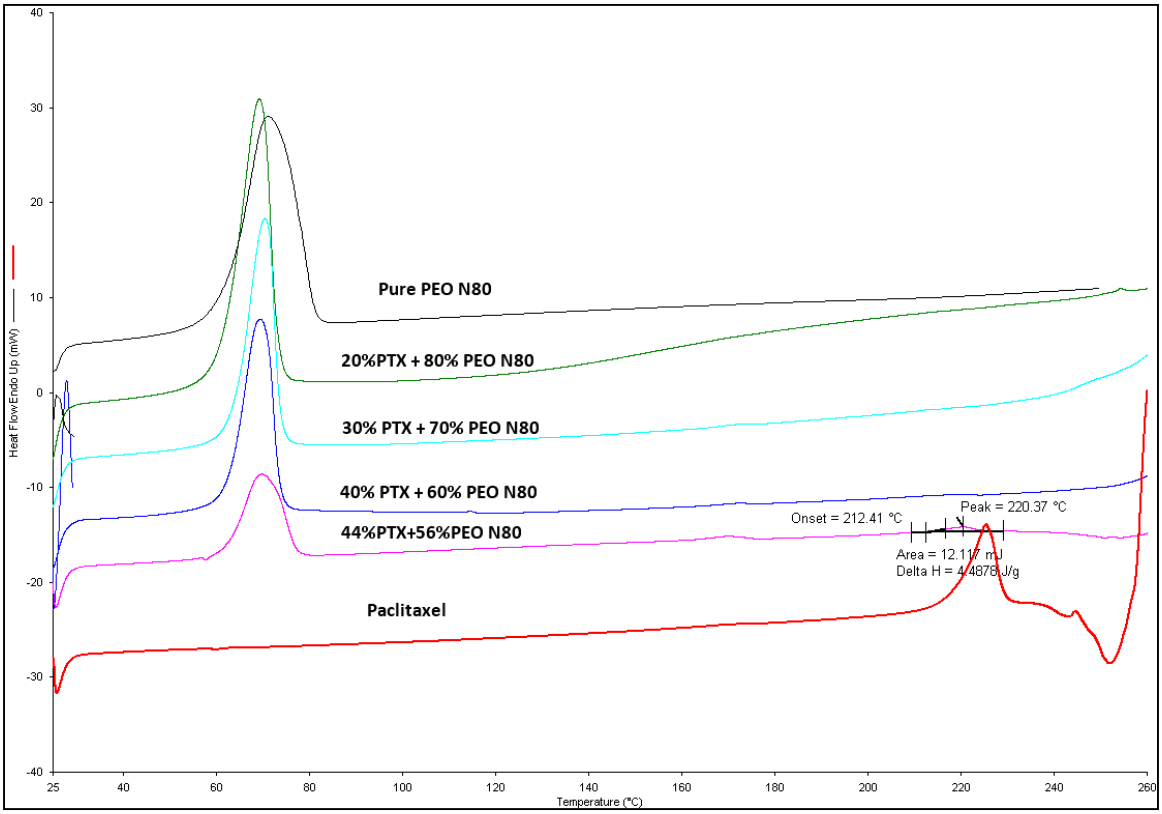

Figure 5-2: DSC thermograms of PolyOx^{TM} WSR N-80, paclitaxel, and physical mixtures

5. 2. 3 *In vitro* release study

A. Effect of drug loading

Polyethylene oxide and its low molecular weight analogs (polyethylene glycol) have been widely employed to improve the aqueous solubility of hydrophobic compounds[209-212], the reason for the rapid release of poorly water insoluble compounds in the formulation is probably attributed to its good wettability and solubilizing effect[213]. It has been demonstrated that the contact angle and the powder surface properties have a significant influence of the dissolution rate [214, 215]. The possible formation of a polymer film around the drug particles due to the swelling property of the polymer would modify the surface morphology of the drug associated with a reduction of contact angle which will further lead to an improved dissolution rate. It is clearly observed in Figure 5-3 that the solubility of PTX was promoted with an increase in PTX loading in the solid dispersion matrix when compared to the crystalline PTX; however, the solubility of PTX in the formulation with 40% loading was only slightly increased and was lower than the other solid dispersions which illustrated the capacity of PolyOx^{TM} WSR N-80 to solubilize PTX was approximately 30%. It is worth to pointing out that for all the formulations demonstrating a solubility enhancement effect, the dissolution medium was clear initially, and became opaque after 2 hours. This finally resulted in a clear solution again at the end of dissolution. This process could be correlated to the solubility profile and possibly corresponded to the precipitation from the supersaturated systems initially, and dissolving into the solution afterwards. However, this dissolution phenomenon is not in agreement with observations in DSC thermograms in which 40% PTX was also solubilized in the matrix.

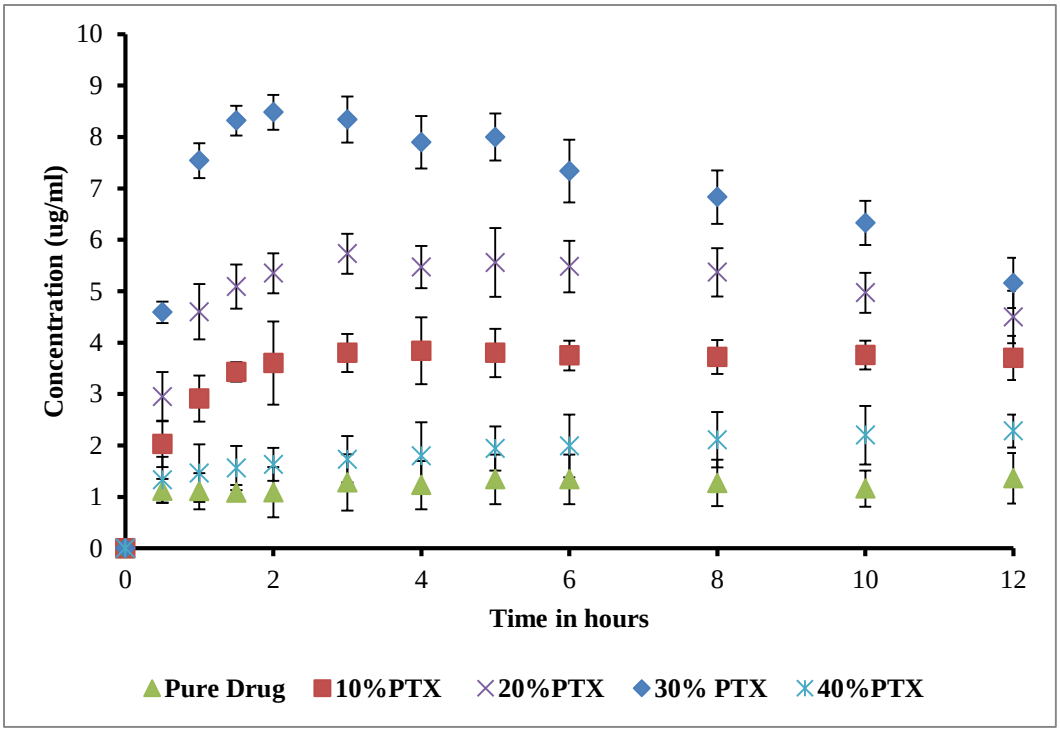

Figure 5-3: Effect of drug loading on solubility enhancement of paclitaxel

B Effect of different additives

The incorporation of surfactants and other solubilizers into solid dispersions to improve the solubility of hydrophobic compounds has received considerable attention over the last two decades [37-40]. The mechanism of solubility enhancement is most probably due to the reduced interfacial tension between drug and dissolution medium resulting from the increased wettability of the system. In addition, when the concentration of surfactant is above the critical micelles concentration (CMC), the solubility of the hydrophobic species will be further enhanced by incorporation into the surfactant aggregates [41]. Various additives were added into the formulations and the effect on the solubility enhancement was investigated. With the addition of sodium lauryl sulfate, an anionic surfactant, the solubility of paclitaxel was higher than the formulation containing F-68, which is probably due to further reduction in the surface tension of

SLS[216]. Moreover, PEG 3350 demonstrated a higher solubility enhancement of the PTX, which is probably due to the good miscibility between PEG 3350 and PolyOx^{TM} WSR N-80.

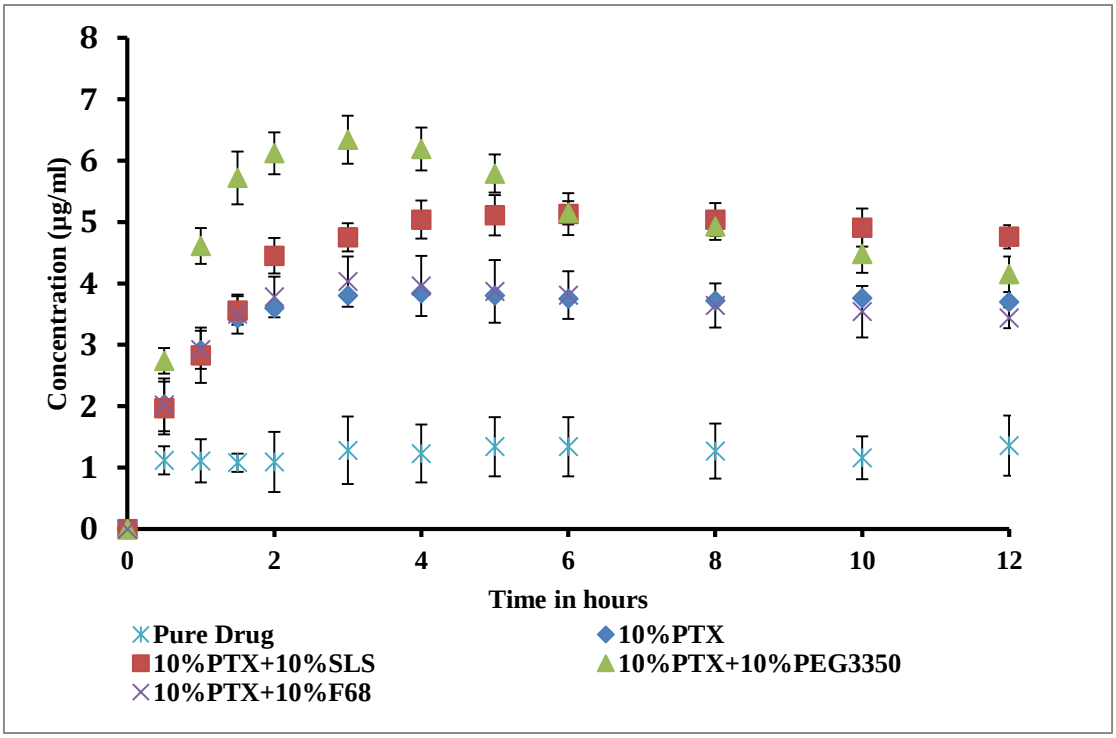

Figure 5-4: Effect of different additives on solubility enhancement of paclitaxel

C. Effect of concentration of PEG 3350

The effect of PEG 3350 concentration on the solubility enhancement of paclitaxel was further investigated (Figure 5-5). The apparent solubility of paclitaxel was increased with the increasing of PEG 3350 percentage up to 15%, however, with the addition of 20% PEG 3350, the solubility of paclitaxel dropped. The solubility enhancement of paclitaxel is most probably due to PolyOx^{TM} WSR N-80 while the addition of PEG 3350 increased the wettability of formulations, however, the reduction of solubility of paclitaxel probably indicated the optimal concentration of PEG 3350 is not beyond 15%.

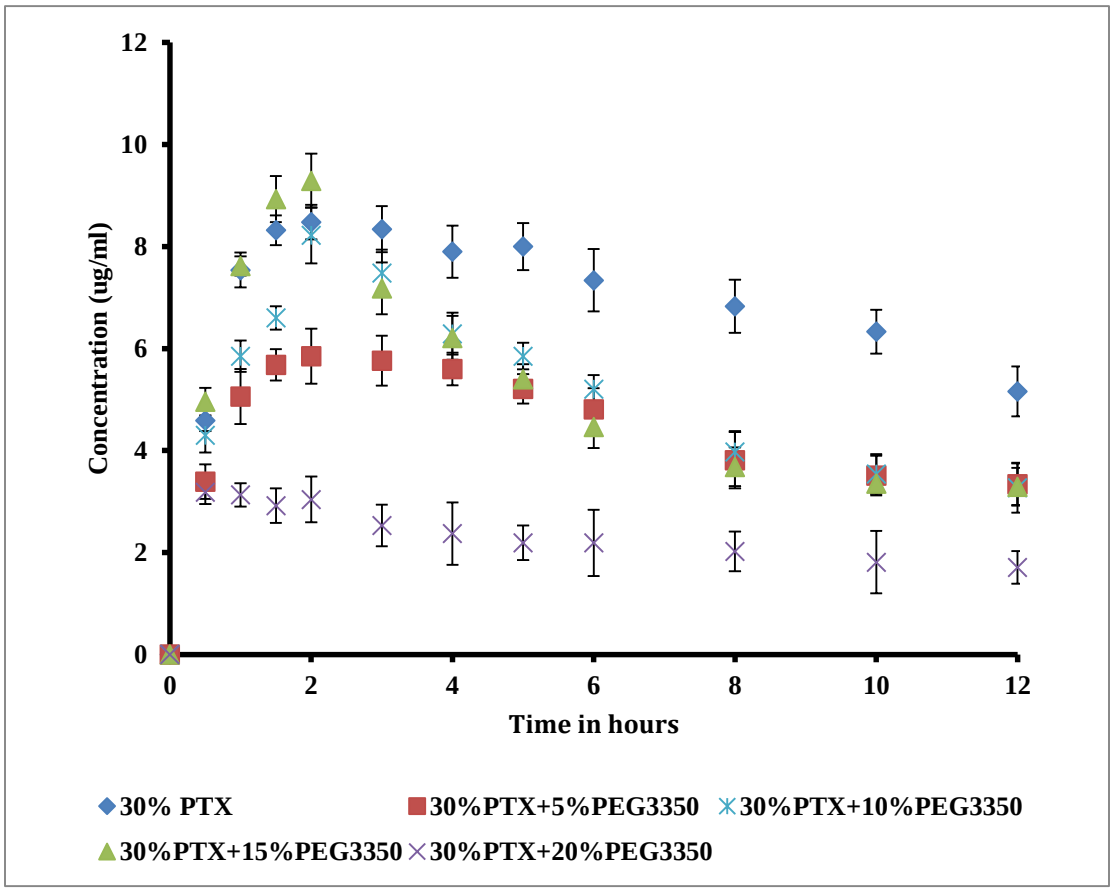

Figure 5-5: Effect of concentration of PEG 3350 on solubility enhancement of paclitaxel

5. 2. 4 Precipitation inhibition with polymers

Supersaturating drug delivery system has been broadly employed to enhance the solubility of hydrophobic compounds. However, apart from its tremendous advantages on solubility enhancement, the supersaturating system has the tendency to precipitate when the formulations are exposed to the dissolution medium, which limits further application. To address this hurdle, a so-called precipitation inhibitor is usually incorporated into the supersaturating drug delivery system. Typically, the precipitation of drug from supersaturating drug delivery system consists of two steps, nucleation and the following crystal growth process. It is important to point out that the dissolved drug molecules have to overcome an energy barrier, which is due to the interfacial tension between drug particles and dissolution medium, to form aggregates (nucleation process), which can further grow to crystals, although the precipitation is thermodynamically driven by supersaturation. Therefore, the energy barrier itself provides the possibility to delay or prevent the nucleation process if it could be promoted high enough and the supersaturation could remain in the metastable state for a longer period of time. Pharmaceutical excipients like polymers have been widely employed to stabilize the supersaturation systems based on the mechanism of direct interaction between polymers and drug particles and hydrogen bonding is the one observed most often. The active energy is increased with the formation of hydrogen bonds and, furthermore, the polymers will compete with the drug particles to absorb on the crystals or postpone the absorption by means of steric effects, which will finally lead to a retarded crystal growth rate[114].

Currently, HPMCAS has been used as a precipitation inhibitor in many studies, and it demonstrated a superior effect on stabilization of the supersaturating drug delivery system. The mechanism is mainly attributed to the two properties of HPMCAS itself, 1) it can be partial

ionized at a pH above 5.5, which results in the stabilization of nano-sized amorphous drug-polymer aggregates; 2) the hydrophobic group in the HPMCAS structure can provide sites for drug association[178, 217]. It was demonstrated in Figure 5-6 that the apparent solubility of paclitaxel was maintained up to 12 hours with the addition of 5% HPMCAS-LF, while the formulation containing 5% HPMCAS-HF showed a lower solubility of PTX, however, the solubility was also maintained. The difference between AS-LF and AS-HF is succinoyl substitution to acetyl substitution ratio, which is 15:8 in AS-LF contrasted with a ratio of 6:12 in AS-HF, leading to that AS-LF can dissolve in solutions of pH 5.5 or higher while AS-HF can only dissolve in a solution of pH 6.5 or higher. Tanno et al. evaluated the properties of solid dispersions using HPMCAS as a matrix carrier. AS-HF was observed to provide a slower but higher and more stable release over the three polymers, however, the dissolution behavior was different with the alternation of the drug-polymer ratio[218]. Jachowicz et al also reported the dissolution behavior of piroxicam solid dispersions using HPMCAS as a carrier [219]. The AS-HF solid dispersion demonstrated a faster release over AS-LF solid dispersion when the drug-polymer ratio is 1:1, on the other hand, the two solid dispersions revealed similar release profile when the drug-polymer ratio was adjusted to 1: 5. The reason for the different dissolution behavior is still not clear and further investigation is necessary; however, it was clear that substitution of HPMCAS structure had played an important role in the phenomenon. Meanwhile, other cellulose derivatives and vinyl polymers are also used as stabilizers and the effect of polymer types was also investigated (Figure 5-7). In the current study, Kollidon® 17PF exhibited a similar precipitation inhibition effect as AS-LF with a slightly lower maximum solubility and the precipitation effect of PVP usually depends on different drugs and it most probably affects the crystal growth rate rather than the nucleation process [220]. Interestingly, beyond the

precipitation inhibition effect, HPMC E5 also increased the apparent solubility. The reason for this phenomenon is not yet clear. It seemed that cellulose derivatives have a better precipitation effect compared to synthetic polymers due to their bulky group in the structure[221]. HPMCAS-LF was selected into the final formulation, which was further investigated and the evaluation of HPMC E5 will be continued.

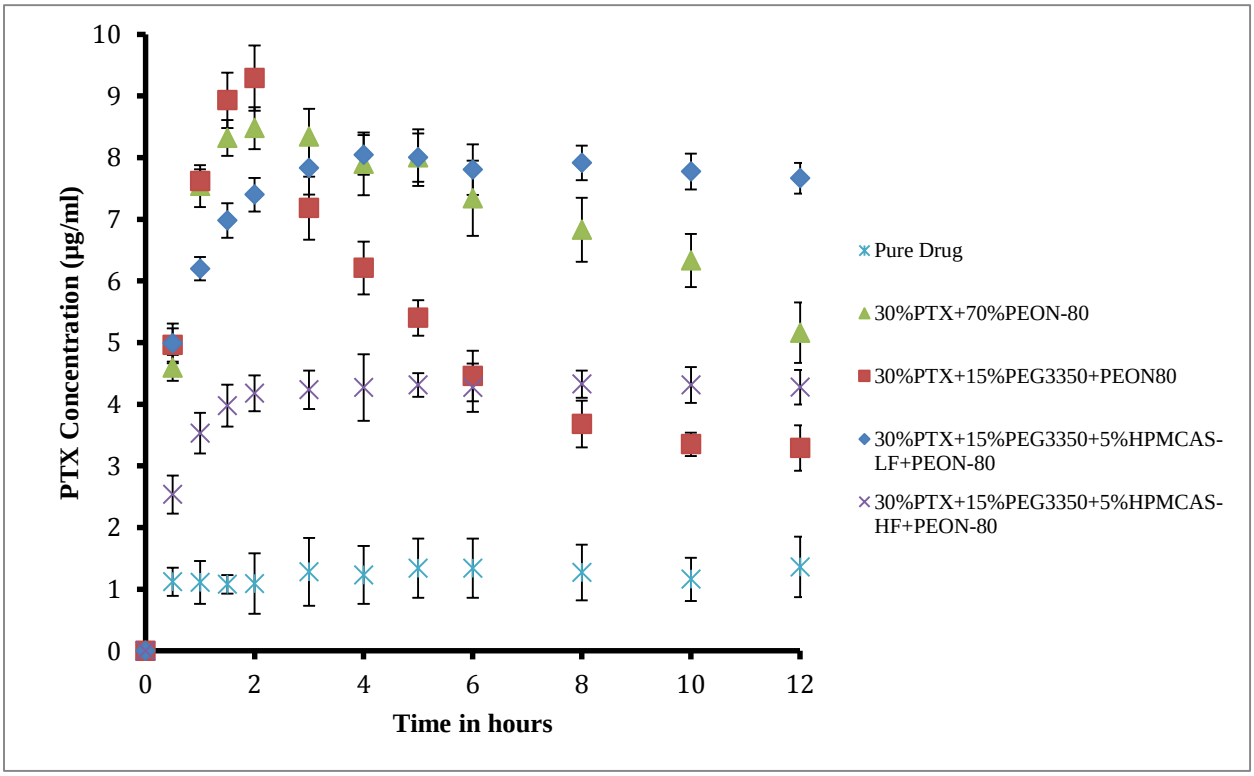

Figure 5-6: Effect of HPMCAS grade on the precipitation inhibition

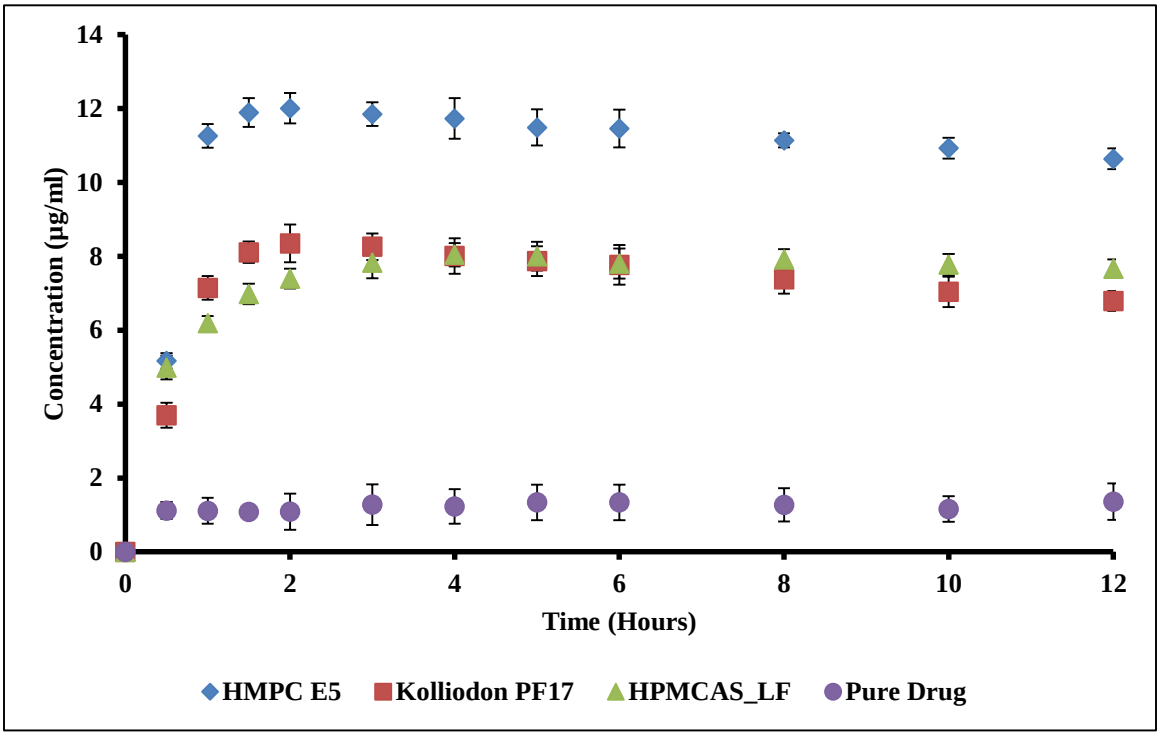

Figure 5-7: Effect of polymer type on the precipitation inhibition

5. 2. 5 Characterization of the final formulation

A. Dissolution in different pH medium

To confirm with phase solubility study conducted previously, the final formulation was subjected to dissolution study in different pH medium. As shown in Figure 5-8, the formulation demonstrated the highest solubility in pH 6.8 buffer solution, which is consistent with previous results. The formulation is subjected to a pH shift method as well which is usually performed as an alternative method for the investigation of supersaturation behavior of neutral compounds[222], in order to illustrate the release profile in the whole GI tract. As a result, the formulation also demonstrated an enhanced solubility and the solubility reduction at 3hrs is due to the volume change from 750mL to 1000mL, which changed the apparent solubility.

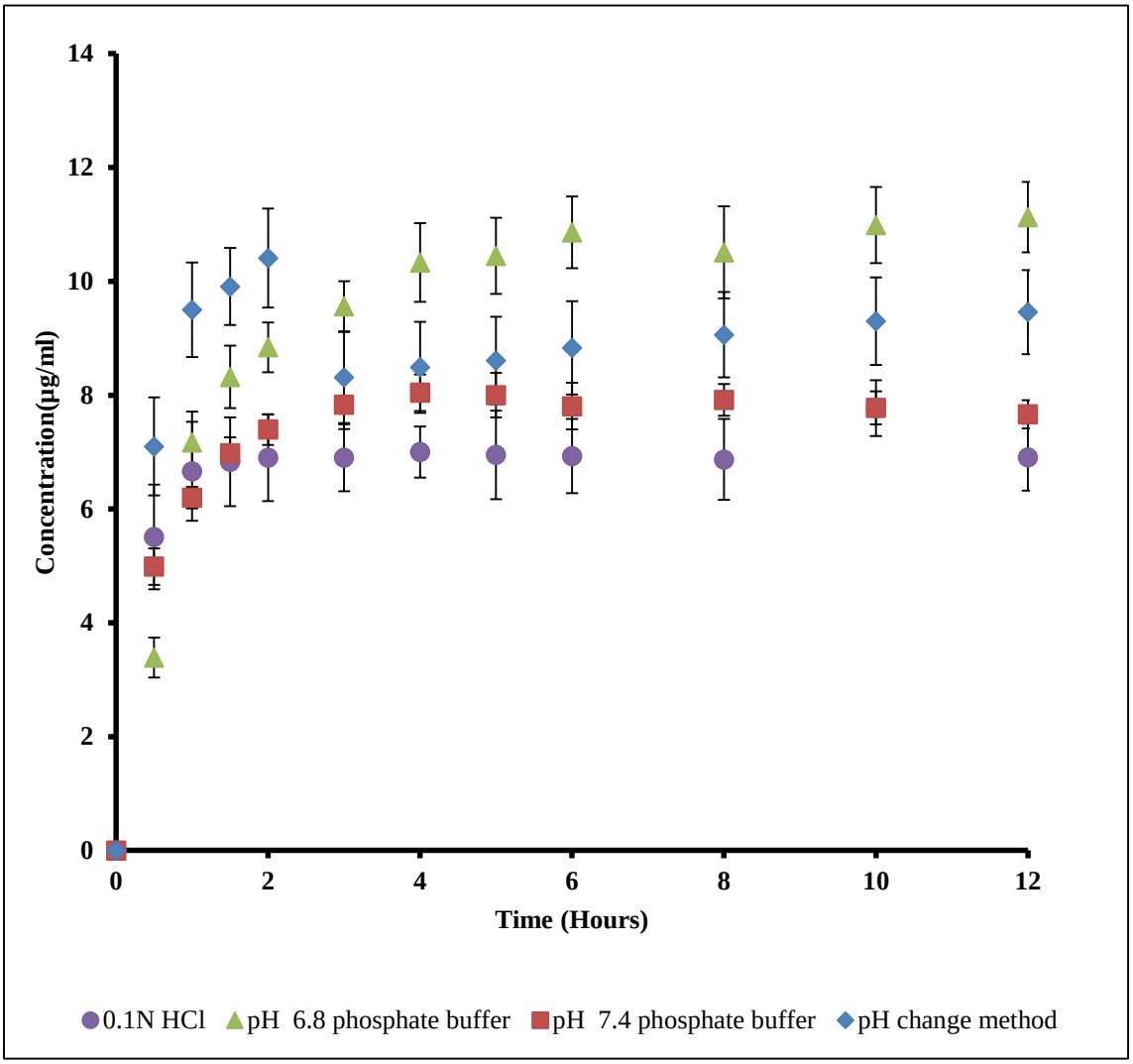

Figure 5-8: Dissolution of paclitaxel extrudates in different pH medium

B. Differential Scanning Calorimetry

No characteristic endothermic or degradation peak of paclitaxel was detected in the extrudates which indicated the existence of amorphous paclitaxel (Figure 5-9). PolyOx^{TM} WSR N-80 and PEG 3350 exhibited the same spectrum as expected due to the same monomer in their structures.

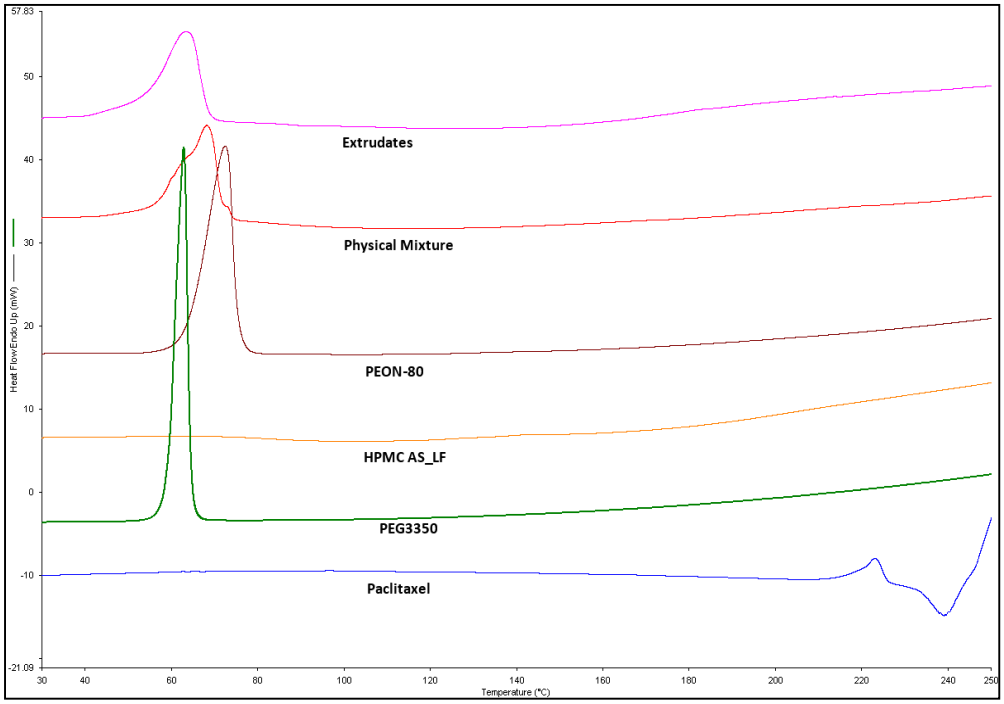

Figure 5-9: DSC of paclitaxel, PEG 3350, HPMCAS-LF, PolyOx^{TM} WSR N-80, physical mixture and extrudates

C. Fourier transform infrared spectroscopy (FT-IR)

PEO N 80 and PEG 3350 demonstrated the same spectra due to their same monomer. The stretch peak of the O-H group in pure paclitaxel at 3468.02 cm^{-1} as well as the stretch peak of the carbonyl group at 1703 cm^{-1} were absent in the spectrum of the extrudates (Figure 5-10), which is probably due to the hydrogen bonding formed between PTX and AS-LF, resulting in the inhibition of precipitation.

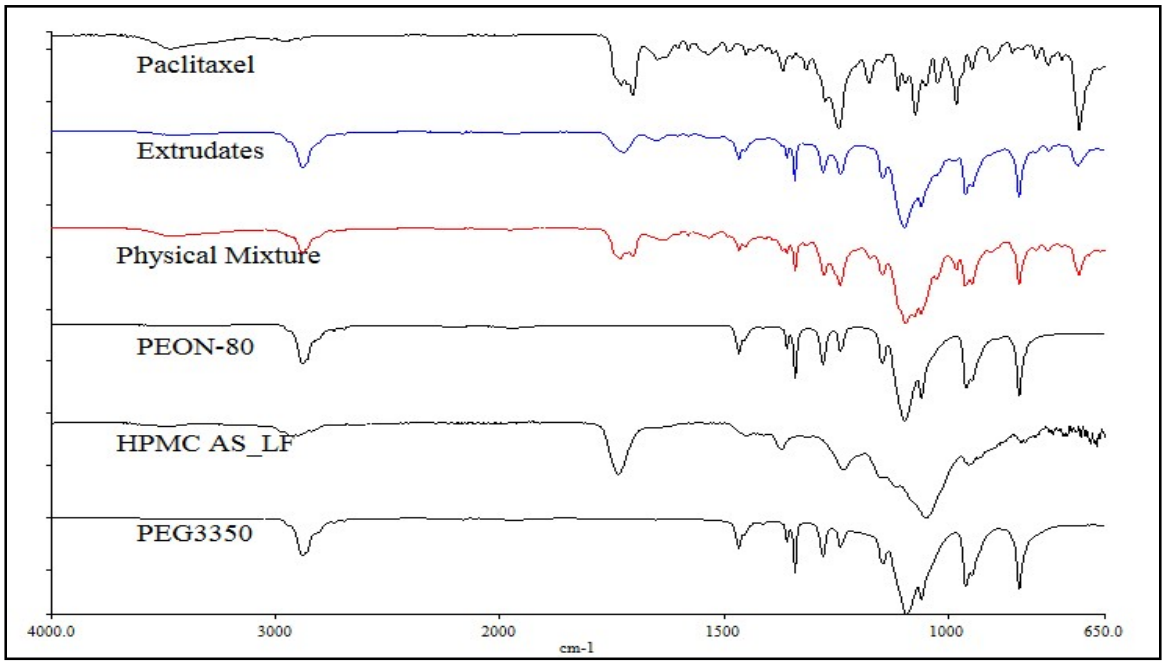

Figure 5-10: FT-IR of paclitaxel, PEG 3350, HPMCAS-LF, PolyOx^{TM} WSR N-80, physical mixture and extrudates

D. Stability

Stability is of paramount importance for formulation development, and therefore, the solid dispersion formulation was subjected to two storage conditions for three months, 25°C/60% RH and 40°C/75% RH per ICH guidelines. No crystallization evidence was detected in DSC thermograms indicating excellent physical stability (Figure 5-11), in addition the chemical stability was confirmed with the similar dissolution profile when compared to the fresh extrudates.

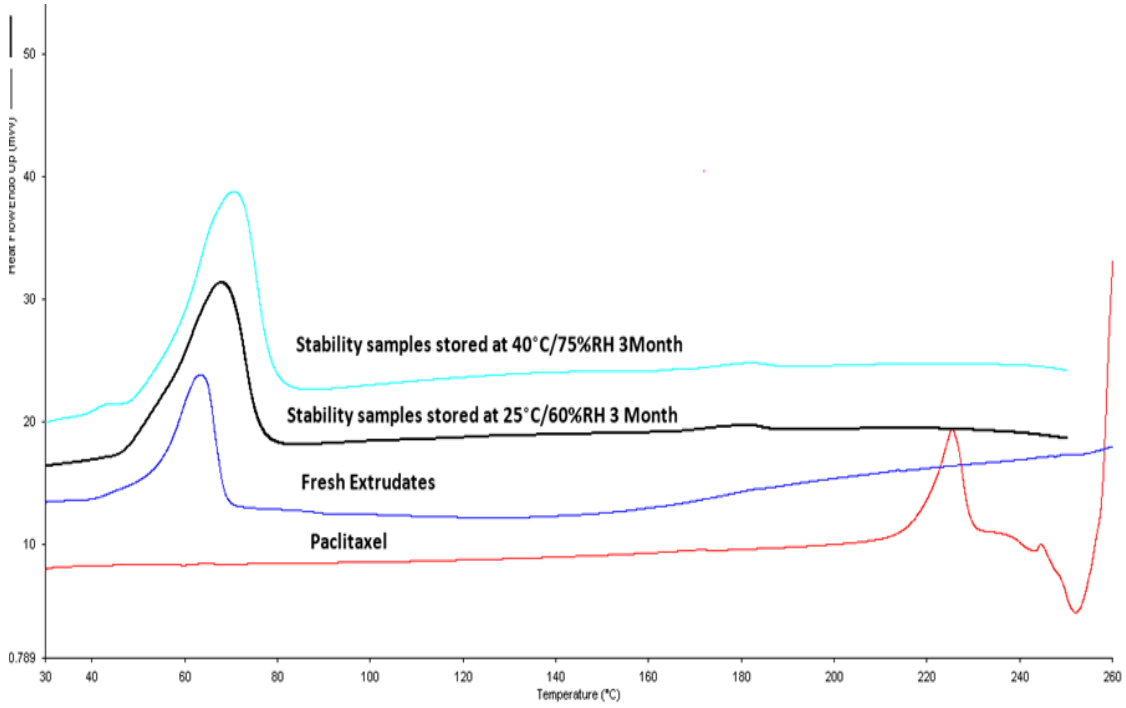

Figure 5-11: DSC of paclitaxel, fresh extrudates, and stability samples stored at 25°C/60% RH and 40°C/75% RH (at 3 month)

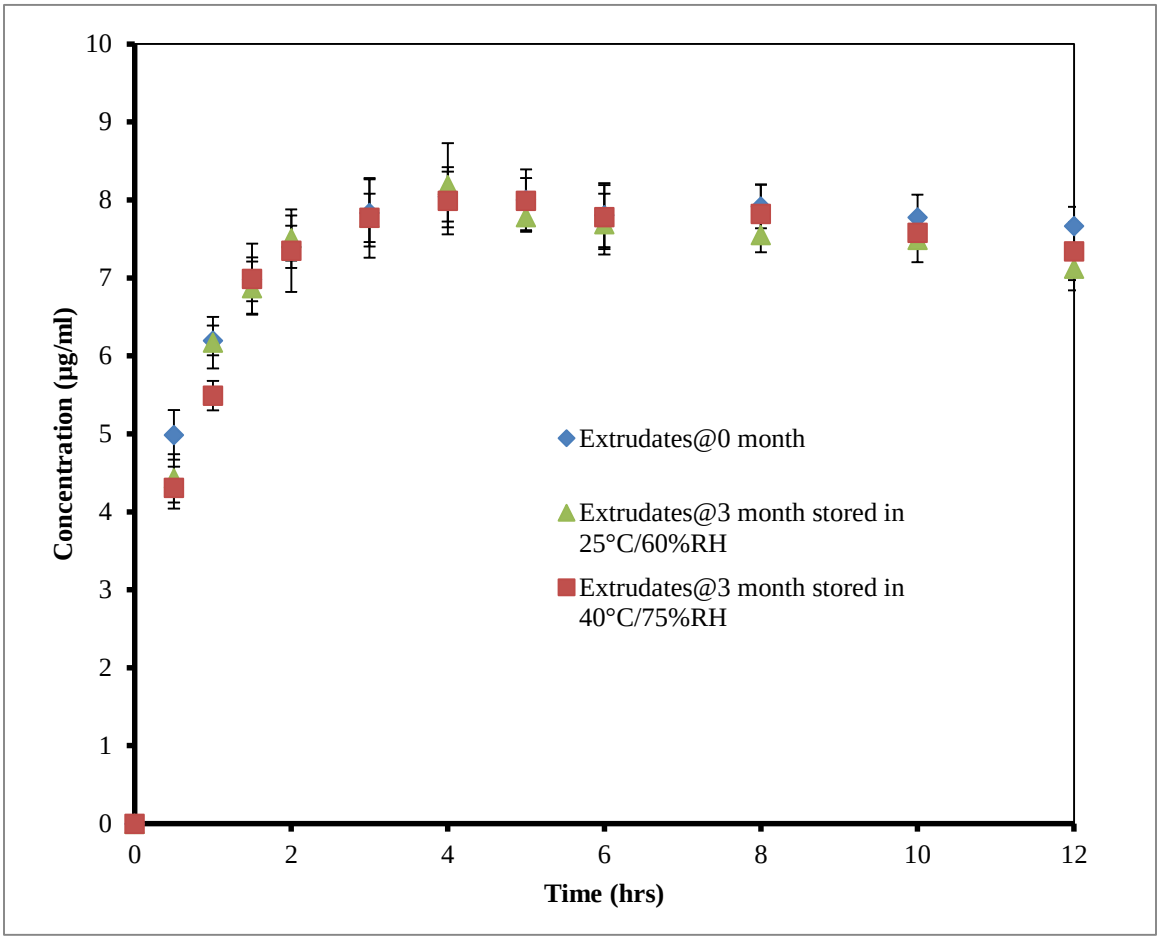

Figure 5-12: In vitro dissolution of fresh extrudates, and stability samples stored at 25°C/60% RH and 40°C/75% RH (at 3 month) in pH 7.4 buffer

CHAPTER 6

SUMMARY AND CONCLUSIONS

6.1 Summary

Over the last few decades, hot-melt extrusion (HME) has been well adapted into the pharmaceutical industry to enhance the solubility and bioavailability of poorly water soluble compounds by producing amorphous solid dispersions. It is critical to understand the miscibility/solubility of active pharmaceutical ingredient (API) within the polymeric carriers to determine the suitable drug load range. Additionally, processing parameters also play an important role in the formulation development utilizing HME.

In chapter 2, a melting point depression approach was applied to determine the miscibility/solubility of two poorly water soluble compounds felodipine and ketoconazole within an amphiphilic polymer Soluplus®. The plot of free energy of mixing vs concentration indicates felodipine is more miscible with Soluplus® than ketoconazole. Further, the Flory-Huggins phase diagrams of both systems confirmed the assumption with a predicted solubility 14% (w/w) of felodipine within Soluplus® compared to 4.3% (w/w) of ketoconazole at room temperature (298K).

In chapter 3, the utility of Soluplus® as a polymeric carrier for solubility enhancement of felodipine was investigated. Beyond the use of the melting point depression method, solubility parameters and heat of fusion were also employed in the present study to determine the miscibility of felodipine within Soluplus®. With the incorporation of pre-dissolved Soluplus®, the solubility of felodipine was further elevated which indicated the possible utility of Soluplus®

as a surfactant. Both of FT-IR and Raman spectroscopy studies demonstrated the formation of intermolecular interaction between felodipine and Soluplus®. In addition, morphology study indicated that felodipine could be molecularly dispersed within Soluplus® at a concentration of 10%.

In chapter 4, a center composite design (CCD) was applied to investigate the influence of formulation factors and processing parameters on the ketoconazole-Soluplus® melt extrudates. Finally, an optimized formulation containing 29.8% ketoconazole was extruded at 140°C/31rpm. The final formulation released 72.80±1.31% at 15min with an average post extrusion content of 97.68±4.38%. Furthermore, DSC and morphology studies indicated the amorphous state of ketoconazole. Collectively, these data suggested that considerable attention needs to be paid to both the formulation and processing factors developing hot melt extruded dosage forms.

In chapter 5, a novel formulation containing 30% paclitaxel, 15% PEG3350, 5% HPMCAS-LF and 50% PolyOx™ WSR N-80 was prepared utilizing hot-melt extrusion technology. The formulation maintained a minimum solubility of paclitaxel as 7.66µg/mL for 12 hours. Due to the absence of Cremophor® EL, the formulation is expected to avoid severe side effects. Moreover, the present study demonstrated the possible utility of hot-melt extrusion technology as an alternative approach for formulation development of high melting point compounds.

6.2 Future Prospective

- Employ melting point depression method to model more compounds and to understand the relationship between the physical properties of the model compounds and miscibility with Soluplus®
- Employ design of experiments to larger size twin screw extruder and investigate the scalability of the final formulation of ketoconazole
- Investigate the reason for the further solubility enhancement of paclitaxel with addition of HPMC E5

BIBLIOGRAPHY

1. Dressman, J.B., et al., *Estimating drug solubility in the gastrointestinal tract.* Adv Drug Deliv Rev, 2007. **59**(7): p. 591-602.
2. Kerns, E.H., *High throughput physicochemical profiling for drug discovery.* J Pharm Sci, 2001. **90**(11): p. 1838-58.
3. Bastin, R.J., M.J. Bowker, and B.J. Slater, *Salt selection and optimisation procedures for pharmaceutical new chemical entities.* Org. Proc. Res. Dev., 2000. **4**(5): p. 427-35.
4. Chemburkar, S.R., et al., *Dealing with the Impact of Ritonavir Polymorphs on the Late Stages of Bulk Drug Process Development.* Org. Proc. Res. Dev., 2000. **4**(5): p. 413-417.
5. Martin, F.A., et al., *Ketoconazole Salt and Co-crystals with Enhanced Aqueous Solubility.* Cryst. Growth Des., 2013. **13**(10): p. 4295-4304.
6. Law, D., et al., *Properties of rapidly dissolving eutectic mixtures of poly(ethylene glycol) and fenofibrate: the eutectic microstructure.* J Pharm Sci, 2003. **92**(3): p. 505-15.
7. Kossena, G.A., et al., *Low dose lipid formulations: effects on gastric emptying and biliary secretion.* Pharm Res, 2007. **24**(11): p. 2084-96.
8. Collnot, E.M., et al., *Mechanism of inhibition of P-glycoprotein mediated efflux by vitamin E TPGS: influence on ATPase activity and membrane fluidity.* Mol Pharm, 2007. **4**(3): p. 465-74.
9. Rawat, S. and S.K. Jain, *Solubility enhancement of celecoxib using beta-cyclodextrin inclusion complexes.* Eur J Pharm Biopharm, 2004. **57**(2): p. 263-7.
10. Behm, F.M., et al., *Low-nicotine regenerated smoke aerosol reduces desire for cigarettes.* J Subst Abuse, 1990. **2**(2): p. 237-47.
11. Chitkara, D. and N. Kumar, *BSA-PLGA-based core-shell nanoparticles as carrier system for water-soluble drugs.* Pharm Res, 2013. **30**(9): p. 2396-409.

12. Beak, I.H. and M.S. Kim, *Improved supersaturation and oral absorption of dutasteride by amorphous solid dispersions.* Chemical & pharmaceutical bulletin, 2012. **60**(11): p. 1468-73.

13. Frank, K.J., et al., *The amorphous solid dispersion of the poorly soluble ABT-102 forms nano/microparticulate structures in aqueous medium: impact on solubility.* International journal of nanomedicine, 2012. **7**: p. 5757-68.

14. Van den Mooter, G., *The use of amorphous solid dispersions: A formulation strategy to overcome poor solubility and dissolution rate.* Drug Discovery Today: Technologies, 2012. **9**(2): p. e79-w85.

15. Sinha, S., et al., *Solid Dispersion as an Approach for Bioavailability Enhancement of Poorly Water-Soluble Drug Ritonavir.* AAPS PharmSciTech, 2010. **11**(2): p. 518-527.

16. Modi, A. and P. Tayade, *Enhancement of dissolution profile by solid dispersion (kneading) technique.* AAPS PharmSciTech, 2006. **7**(3): p. E87-E92.

17. De Brabander, C., et al., *Bioavailability of ibuprofen from hot-melt extruded mini-matrices.* International journal of pharmaceutics, 2004. **271**(1-2): p. 77-84.

18. Kanaze, F.I., et al., *Dissolution enhancement of flavonoids by solid dispersion in PVP and PEG matrixes: A comparative study.* Journal of Applied Polymer Science, 2006. **102**(1): p. 460-471.

19. Chiou, W.L. and S. Riegelman, *Pharmaceutical applications of solid dispersion systems.* J Pharm Sci, 1971. **60**(9): p. 1281-302.

20. Shah, S., et al., *Melt extrusion with poorly soluble drugs.* Int J Pharm, 2013. **453**(1): p. 233-52.

21. DiNunzio, J., et al., *Melt Extrusion*, in *Formulating Poorly Water Soluble Drugs*, R.O. Williams III, A.B. Watts, and D.A. Miller, Editors. 2012, Springer: New York.

22. Janssens, S. and G. Van den Mooter, *Review: physical chemistry of solid dispersions.* J Pharm Pharmacol, 2009. **61**(12): p. 1571-86.

23. Thommes, M., et al., *Improvement of the dissolution rate of poorly soluble drugs by solid crystal suspensions.* Mol Pharm, 2011. **8**(3): p. 727-35.

24. Vo, C.L., C. Park, and B.J. Lee, *Current trends and future perspectives of solid dispersions containing poorly water-soluble drugs.* Eur J Pharm Biopharm, 2013. **85**(3): p. 799-813.

25. Vasconcelos, T., B. Sarmento, and P. Costa, *Solid dispersions as strategy to improve oral bioavailability of poor water soluble drugs.* Drug Discov Today, 2007. **12**(23-24): p. 1068-75.

26. Sekiguchi, K., N. Obi, and Y. Ueda, *Studies on Absorption of Eutectic Mixture. Ii. Absorption of Fused Conglomerates of Chloramphenicol and Urea in Rabbits.* Chem Pharm Bull (Tokyo), 1964. **12**: p. 134-44.

27. Seo, A., et al., *The preparation of agglomerates containing solid dispersions of diazepam by melt agglomeration in a high shear mixer.* Int J Pharm, 2003. **259**(1-2): p. 161-71.

28. Lakshman, J.P., et al., *Application of melt extrusion in the development of a physically and chemically stable high-energy amorphous solid dispersion of a poorly water-soluble drug.* Mol Pharm, 2008. **5**(6): p. 994-1002.

29. Yao, W., et al., *Thermodynamic properties for the system of silybin and poly(ethylene glycol) 6000.* Thermochimica Acta, 2005. **437**(1-2): p. 17-20.

30. Vippagunta, S.R., et al., *Factors affecting the formation of eutectic solid dispersions and their dissolution behavior.* J Pharm Sci, 2007. **96**(2): p. 294-304.

31. Emas, M. and H. Nyqvist, *Methods of studying aging and stabilization of spray-congealed solid dispersions with carnauba wax. 1. Microcalorimetric investigation.* Int J Pharm, 2000. **197**(1-2): p. 117-27.

32. Sarode, A.L., et al., *Hot melt extrusion (HME) for amorphous solid dispersions: Predictive tools for processing and impact of drug-polymer interactions on supersaturation.* Eur J Pharm Sci, 2012. **48**(3): p. 371-384.

33. Serajuddin, A.T., *Solid dispersion of poorly water-soluble drugs: early promises, subsequent problems, and recent breakthroughs.* J Pharm Sci, 1999. **88**(10): p. 1058-66.

34. Taylor, L.S. and G. Zografi, *Spectroscopic characterization of interactions between PVP and indomethacin in amorphous molecular dispersions.* Pharm Res, 1997. **14**(12): p. 1691-8.

35. Desai, J., K. Alexander, and A. Riga, *Characterization of polymeric dispersions of dimenhydrinate in ethyl cellulose for controlled release.* Int J Pharm, 2006. **308**(1-2): p. 115-23.

36. Karavas, E., E. Georgarakis, and D. Bikiaris, *Application of PVP/HPMC miscible blends with enhanced mucoadhesive properties for adjusting drug release in predictable pulsatile chronotherapeutics.* Eur J Pharm Biopharm, 2006. **64**(1): p. 115-26.

37. Yoshihashi, Y., et al., *Estimation of physical stability of amorphous solid dispersion using differential scanning calorimetry.* Journal of Thermal Analysis and Calorimetry, 2006. **85**(3): p. 689-92.

38. Ceballos, A., et al., *Influence of formulation and process variables on in vitro release of theophylline from directly-compressed Eudragit matrix tablets.* Farmaco, 2005. **60**(11-12): p. 913-8.

39. Van den Mooter, G., et al., *Evaluation of Inutec SP1 as a new carrier in the formulation of solid dispersions for poorly soluble drugs.* Int J Pharm, 2006. **316**(1-2): p. 1-6.

40. Chauhan, B., S. Shimpi, and A. Paradkar, *Preparation and evaluation of glibenclamide-polyglycolized glycerides solid dispersions with silicon dioxide by spray drying technique.* Eur J Pharm Sci, 2005. **26**(2): p. 219-30.

41. van Drooge, D.J., et al., *Characterization of the molecular distribution of drugs in glassy solid dispersions at the nano-meter scale, using differential scanning calorimetry and gravimetric water vapour sorption techniques.* Int J Pharm, 2006. **310**(1-2): p. 220-9.

42. Sun, N., et al., *In vitro evaluation and pharmacokinetics in dogs of solid dispersion pellets containing Silybum marianum extract prepared by fluid-bed coating.* Planta Med, 2008. **74**(2): p. 126-32.

43. Won, D.H., et al., *Improved physicochemical characteristics of felodipine solid dispersion particles by supercritical anti-solvent precipitation process.* Int J Pharm, 2005. **301**(1-2): p. 199-208.

44. Dong, Z., et al., *Evaluation of solid state properties of solid dispersions prepared by hot-melt extrusion and solvent co-precipitation.* Int J Pharm, 2008. **355**(1-2): p. 141-9.

45. Yu, D.G., et al., *Third generation solid dispersions of ferulic acid in electrospun composite nanofibers.* Int J Pharm, 2010. **400**(1-2): p. 158-64.

46. Van Drooge, D.J., et al., *Spray freeze drying to produce a stable Δ9-tetrahydrocannabinol containing inulin-based solid dispersion powder suitable for inhalation.* European Journal of Pharmaceutical Sciences, 2005. **26**(2): p. 231-40.

47. Overhoff, K.A., et al., *Solid dispersions of itraconazole and enteric polymers made by ultra-rapid freezing.* Int J Pharm, 2007. **336**(1): p. 122-32.

48. Breitenbach, J., *Melt extrusion can bring new benefits to HIV therapy.* American Journal of Drug Delivery, 2006. **4**(2): p. 61-64.

49. Shah, S. and M.A. Repka, *Melt Extrusion in Drug Delivery: Three Decades of Progress*, in *Melt Extrusion Materials, Technology and Drug Product Design*, M.A. Repka, N. Langley, and J. DiNunzio, Editors. 2013, Springer: New York Dordrecht Heidelberg London.

50. Repka, M.A., et al., *Melt extrusion: process to product.* Expert Opin Drug Deliv, 2012. **9**(1): p. 105-25.

51. Repka, M.A., et al., *Hot-melt extrusion technology*, in *Encyclopedia of pharmaceutical technology*, J. Swarbrick and J. Boylan, Editors. 2002, Marcel Decker: New York. p. 203-266.

52. Maniruzzaman, M., et al., *Taste masking of paracetamol by hot-melt extrusion: an in vitro and in vivo evaluation.* Eur J Pharm Biopharm, 2012. **80**(2): p. 433-42.

53. Gryczke, A., et al., *Development and evaluation of orally disintegrating tablets (ODTs) containing Ibuprofen granules prepared by hot melt extrusion.* Colloids Surf B Biointerfaces, 2011. **86**(2): p. 275-84.

54. Ma, D., et al., *Development of a HPMC-based controlled release formulation with hot melt extrusion (HME).* Drug Dev Ind Pharm, 2013. **39**(7): p. 1070-83.

55. Young, C.R., C. Dietzsch, and J.W. McGinity, *Compression of controlled-release pellets produced by a hot-melt extrusion and spheronization process.* Pharm Dev Technol, 2005. **10**(1): p. 133-9.

56. Guo, Z., et al., *The utilization of drug–polymer interactions for improving the chemical stability of hot-melt extruded solid dispersions.* Journal of Pharmacy and Pharmacology, 2013. **66**(2): p. 285-96.

57. Liu, X., et al., *Improving the chemical stability of amorphous solid dispersion with cocrystal technique by hot melt extrusion.* Pharm Res, 2012. **29**(3): p. 806-17.

58. Crowley, M.M., et al., *Stability of polyethylene oxide in matrix tablets prepared by hot-melt extrusion.* Biomaterials, 2002. **23**(21): p. 4241-8.

59. Breitenbach, J., *Melt extrusion: from process to drug delivery technology.* European Journal of PharmaceuticS and biopharmaceutics, 2002. **54**(2): p. 107-117.

60. Dreiblatt, A., *Process design*, in *Pharmaceutical extrusion technology*, I. Ghebre-Sellassie and C. Martin, Editors. 2003, Marcel Dekker, Inc.: New York. p. 153-169.

61. Schenck, L., et al., *Achieving a hot melt extrusion design space for the production of solid solutions*, in *Chemical Engineering in the Pharmaceutical Industry: R&D to Manufacturing*, D.J. Am Ende, Editor. 2010, John Wiley & Sons, Inc.,: Hoboken, New Jersey.

62. Zhu, Y., et al., *Solid-state plasticization of an acrylic polymer with chlorpheniramine maleate and triethyl citrate.* Int J Pharm, 2002. **241**(2): p. 301-10.

63. Follonier, N., E. Doelker, and E.T. Cole, *Evaluation of hot-melt extrusion as a new technique for the production of polymer-based pellets for sustained release capsules*

containing high loadings of freely soluble drugs. Drug Dev Ind Pharm, 1994. **20**(8): p. 1323-39.

64. Djuris, J., et al., *Preparation of carbamazepine-Soluplus solid dispersions by hot-melt extrusion, and prediction of drug-polymer miscibility by thermodynamic model fitting.* Eur J Pharm Biopharm, 2013. **84**(1): p. 228-37.

65. Song, Y., et al., *Physicochemical characterization of felodipine-kollidon VA64 amorphous solid dispersions prepared by hot-melt extrusion.* J Pharm Sci, 2013. **102**(6): p. 1915-23.

66. Sarode, A.L., et al., *Hot melt extrusion for amorphous solid dispersions: temperature and moisture activated drug-polymer interactions for enhanced stability.* Mol Pharm, 2013. **10**(10): p. 3665-75.

67. Nakamichi, K., et al., *Evaluation of a floating dosage form of nicardipine hydrochloride and hydroxypropylmethylcellulose acetate succinate prepared using a twin-screw extruder.* Int J Pharm, 2001. **218**(1-2): p. 103-12.

68. Repka, M.A. and J.W. McGinity, *Physical-mechanical, moisture absorption and bioadhesive properties of hydroxypropylcellulose hot-melt extruded films.* Biomaterials, 2000. **21**(14): p. 1509-17.

69. Forster, A., et al., *Selection of excipients for melt extrusion with two poorly water-soluble drugs by solubility parameter calculation and thermal analysis.* International journal of pharmaceutics, 2001. **226**(1-2): p. 147-61.

70. Crowley, M.M., et al., *The influence of guaifenesin and ketoprofen on the properties of hot-melt extruded polyethylene oxide films.* European journal of pharmaceutical sciences :

official journal of the European Federation for Pharmaceutical Sciences, 2004. **22**(5): p. 409-18.

71. Reitz, C. and P. Kleinebudde, *Solid lipid extrusion of sustained release dosage forms.* Eur J Pharm Biopharm, 2007. **67**(2): p. 440-8.

72. Guns, S., et al., *Upscaling of the hot-melt extrusion process: comparison between laboratory scale and pilot scale production of solid dispersions with miconazole and Kollicoat IR.* Eur J Pharm Biopharm, 2012. **81**(3): p. 674-82.

73. Windbergs, M., et al., *Two-Step Solid Lipid Extrusion as a Process to Modify Dissolution Behavior.* AAPS PharmSciTech, 2010. **11**(1): p. 2-8.

74. Miyagawa, Y., et al., *In vivo performance of wax matrix granules prepared by a twin-screw compounding extruder.* Drug Dev Ind Pharm, 1999. **25**(4): p. 429-35.

75. Crowley, M.M., et al., *Physicochemical properties and mechanism of drug release from ethyl cellulose matrix tablets prepared by direct compression and hot-melt extrusion.* Int J Pharm, 2004. **269**(2): p. 509-22.

76. Verreck, G., et al., *The effect of supercritical CO2 as a reversible plasticizer and foaming agent on the hot stage extrusion of itraconazole with EC 20cps.* The Journal of Supercritical Fluids, 2007. **40**(1): p. 153-162.

77. Zhang, F. and J.W. McGinity, *Properties of hot-melt extruded theophylline tablets containing poly(vinyl acetate).* Drug Dev Ind Pharm, 2000. **26**(9): p. 931-42.

78. Ozguney, I., D. Shuwisitkul, and R. Bodmeier, *Development and characterization of extended release Kollidon SR mini-matrices prepared by hot-melt extrusion.* Eur J Pharm Biopharm, 2009. **73**(1): p. 140-5.

79. Gosau, M. and B.W. Muller, *Release of gentamicin sulphate from biodegradable PLGA-implants produced by hot melt extrusion.* Pharmazie, 2010. **65**(7): p. 487-92.

80. Aharoni, S.M., *Increased glass transition temperature in motionally constrained semicrystalline polymers.* Polymers for Advanced Technologies, 1998. **9**(3): p. 169-201.

81. Schilling, S.U., et al., *Citric acid as a solid-state plasticizer for Eudragit RS PO.* J Pharm Pharmacol, 2007. **59**(11): p. 1493-500.

82. Wu, C. and J.W. McGinity, *Influence of methylparaben as a solid-state plasticizer on the physicochemical properties of Eudragit RS PO hot-melt extrudates.* Eur J Pharm Biopharm, 2003. **56**(1): p. 95-100.

83. Repka, M.A., et al., *Influence of plasticizers and drugs on the physical-mechanical properties of hydroxypropylcellulose films prepared by hot melt extrusion.* Drug Dev Ind Pharm, 1999. **25**(5): p. 625-33.

84. Ghebremeskel, A.N., C. Vemavarapu, and M. Lodaya, *Use of surfactants as plasticizers in preparing solid dispersions of poorly soluble API: stability testing of selected solid dispersions.* Pharm Res, 2006. **23**(8): p. 1928-36.

85. Repka, M.A. and J.W. McGinity, *Influence of vitamin E TPGS on the properties of hydrophilic films produced by hot-melt extrusion.* Int J Pharm, 2000. **202**(1-2): p. 63-70.

86. Andrews, G.P., et al., *Physicochemical characterization and drug-release properties of celecoxib hot-melt extruded glass solutions.* J Pharm Pharmacol, 2010. **62**(11): p. 1580-90.

87. Follonier, N., E. Doelker, and E.T. Cole, *Various ways of modulating the release of diltiazem hydrochloride from hot-melt extruded sustained release pellets prepared using polymeric materials.* Journal of Controlled Release, 1995. **36**(3): p. 243-250.

88. Shah, N., et al., *Structured Development Approach for Amorphous Systems*, in *Formulating Poorly Water Soluble Drugs*, R.O. Williams III, A.B. Watts, and D.A. Miller, Editors. 2012, Springer: New York Dordrecht Heidelberg London.

89. Riande, E., R. Diaz-Calleja, and M. Prolongo, *Crystalline and Amorphous States in Polymers*, in *Polymer Viscoelasticity: Stress and Strain in Practice*, E. Riande, R. Diaz-Calleja, and M. Prolongo, Editors. 1999, Marcel Dekker, Inc.: New York.

90. Hiemenz, P.C. and T.L. Lodge, *Polymer Chemistry*. 2nd ed. 2007, Boca Raton: CRC Press Taylor & Francis Group.

91. Rauwendall, C., ed. *Polymer Extrusion*. 3rd ed. 1994, Hanser Pulisher: Munich.

92. Mccrum, N.G. and C.P. Buckley, eds. *Principles of Polymer Engineering*. 1997, Oxford University Press: Oxford.

93. Kolter, K., M. Karl, and A. Gryczke, *Hot Melt Extrusion with BASF Pharma Polymers Compendium*, in *Extrusion Compendium*, K. Kolter, M. Karl, and A. Gryczke, Editors. 2012.

94. Van Krevelen, D.W. and K. Te Nijenhuis, eds. *Properties of Polymers*. Fourth ed. 2009, Elsevier B.V.

95. Chokshi, R.J., et al., *Stabilization of low glass transition temperature indomethacin formulations: impact of polymer-type and its concentration.* J Pharm Sci, 2008. **97**(6): p. 2286-98.

96. Hancock, B.C., P. York, and R.C. Rowe, *The use of solubility parameters in pharmaceutical dosage form design.* International Journal of Pharmaceutics, 1997. **148**: p. 1-21.

97. Mididoddi, P.K. and M.A. Repka, *Characterization of hot-melt extruded drug delivery systems for onychomycosis.* European journal of pharmaceutics and biopharmaceutics : official journal of Arbeitsgemeinschaft fur Pharmazeutische Verfahrenstechnik e.V, 2007. **66**(1): p. 95-105.

98. Greenhalgh, D.J., et al., *Solubility parameters as predictors of miscibility in solid dispersions.* Journal of pharmaceutical sciences, 1999. **88**(11): p. 1182-90.

99. Gupta, J., et al., *Prediction of solubility parameters and miscibility of pharmaceutical compounds by molecular dynamics simulations.* The journal of physical chemistry. B, 2011. **115**(9): p. 2014-23.

100. Hildebrand, J.H. and R.L. Scott, eds. *The Solubility of nonelectrolytes*. 3rd ed. 1950, Reinhold Pub. Corp: New York.

101. Hansen, C.M., ed. *Hansen Solubility Parameters A User's Handbook.* 2000, CRC Press, LLC.

102. Hoy, K.L., ed. *The Hoy tables of solubility parameters*. 1985, Union Carbide Corporation: South Charleston.

103. Rubinstein, M. and P.J. Marsac, eds. *Polymer Physics*. 2003, Oxford University Press: New York.

104. Nishi, T. and T.T. Wang, *Melting Point Depression and Kinetic Effects of Cooling on Crystallization in Poly(vinylidene fluoride)-Poly(methyl methacrylate) Mixtures.* Macromolecules, 1975. **8**(6): p. 909-915.

105. Rim, P.B. and J.P. Runt, *Melting point depression in crystalline/compatible polymer blends.* Macromolecules, 1984. **17**(8): p. 1520-1526.

106. Cortazar, M.M., M.E. Calahorra, and G.M. Guzmán, *Melting point depression in poly (ethylene oxide)-poly (methyl methacrylate) blends.* European Polymer Journal, 1982. **18**(2): p. 165-166.

107. Liberman, S.A., A. De S. Gomes, and E.M. Macchi, *Compatibility in poly(ethylene oxide)–poly(methyl methacrylate) blends.* Journal of Polymer Science: Polymer Chemistry Edition, 1984. **22**(11): p. 2809-2815.

108. DiNunzio, J. and D.A. Miller, *Formulation Development of Amorphous Solid Dispersion Prepared by Melt Extrusion*, in *Melt Extrusion Materials, Technology and Drug Product Design*, M.A. Repka, N. Langley, and J. DiNunzio, Editors. 2013, Springer: New York Dordrecht Heidelberg London. p. 161-203.

109. Marsac, P.J., S.L. Shamblin, and L.S. Taylor, *Theoretical and practical approaches for prediction of drug-polymer miscibility and solubility.* Pharmaceutical research, 2006. **23**(10): p. 2417-26.

110. Marsac, P.J., T. Li, and L.S. Taylor, *Estimation of drug-polymer miscibility and solubility in amorphous solid dispersions using experimentally determined interaction parameters.* Pharmaceutical research, 2009. **26**(1): p. 139-51.

111. Lin, D. and Y. Huang, *A thermal analysis method to predict the complete phase diagram of drug-polymer solid dispersions.* International journal of pharmaceutics, 2010. **399**(1-2): p. 109-15.

112. Zhao, Y., et al., *Prediction of the thermal phase diagram of amorphous solid dispersions by Flory-Huggins theory.* Journal of pharmaceutical sciences, 2011. **100**(8): p. 3196-207.

113. Amidon, G.L., et al., *A theoretical basis for a biopharmaceutic drug classification: the correlation of in vitro drug product dissolution and in vivo bioavailability.* Pharm Res, 1995. **12**(3): p. 413-20.

114. Brouwers, J., M.E. Brewster, and P. Augustijns, *Supersaturating drug delivery systems: the answer to solubility-limited oral bioavailability?* J Pharm Sci, 2009. **98**(8): p. 2549-72.

115. Xu, S. and W.G. Dai, *Drug precipitation inhibitors in supersaturable formulations.* Int J Pharm, 2013. **453**(1): p. 36-43.

116. Yamashita, K., et al., *Establishment of new preparation method for solid dispersion formulation of tacrolimus.* Int J Pharm, 2003. **267**(1-2): p. 79-91.

117. Tajarobi, F., et al., *The influence of crystallization inhibition of HPMC and HPMCAS on model substance dissolution and release in swellable matrix tablets.* Eur J Pharm Biopharm, 2011. **78**(1): p. 125-33.

118. Xie, S., et al., *Direct Precipitation of Micron-Size Salbutamol Sulfate: New Insights into the Action of Surfactants and Polymeric Additives.* Cryst. Growth Des., 2010. **10**(8): p. 3363-3371.

119. Zhang, N., et al., *Studies on preparation of carbamazepine (CBZ) supersaturatable self-microemulsifying (S-SMEDDS) formulation and relative bioavailability in beagle dogs.* Pharm Dev Technol, 2011. **16**(4): p. 415-421.

120. Overhoff, K.A., et al., *Effect of stabilizer on the maximum degree and extent of supersaturation and oral absorption of tacrolimus made by ultra-rapid freezing.* Pharm Res, 2008. **25**(1): p. 167-75.

121. Dai, W.G., et al., *Combination of Pluronic/Vitamin E TPGS as a potential inhibitor of drug precipitation.* Int J Pharm, 2008. **355**(1-2): p. 31-7.

122. Brewster, M.E., et al., *Comparative interaction of 2-hydroxypropyl-beta-cyclodextrin and sulfobutylether-beta-cyclodextrin with itraconazole: phase-solubility behavior and stabilization of supersaturated drug solutions.* Eur J Pharm Sci, 2008. **34**(2-3): p. 94-103.

123. Dias, M.M., et al., *The effect of beta-cyclodextrins on the permeation of diclofenac from supersaturated solutions.* Int J Pharm, 2003. **263**(1-2): p. 173-81.

124. Myers, R.H., D.C. Montgomery, and C.M. Anderson-Cook, eds. *Response Surface Methodology Process and Product Optimization Using Designed Experiments*. Third ed. 2009, Wiley: Hoboken, New Jersey.

125. Prodduturi, S., et al., *Solid-state stability and characterization of hot-melt extruded poly(ethylene oxide) films.* J Pharm Sci, 2005. **94**(10): p. 2232-45.

126. Saltiel, E., et al., *Felodipine. A review of its pharmacodynamic and pharmacokinetic properties, and therapeutic use in hypertension.* Drugs, 1988. **36**(4): p. 387-428.

127. Varkey, B., *Oral antifungal therapy. Current status of ketoconazole.* Postgrad Med, 1983. **73**(1): p. 52-3.

128. Wani, M.C., et al., *Plant antitumor agents. VI. The isolation and structure of taxol, a novel antileukemic and antitumor agent from Taxus brevifolia.* J Am Chem Soc, 1971. **93**(9): p. 2325-7.

129. Konno, T., J. Watanabe, and K. Ishihara, *Enhanced solubility of paclitaxel using water-soluble and biocompatible 2-methacryloyloxyethyl phosphorylcholine polymers.* J Biomed Mater Res A, 2003. **65**(2): p. 209-14.

130. Spencer, C.M. and D. Faulds, *Paclitaxel. A review of its pharmacodynamic and pharmacokinetic properties and therapeutic potential in the treatment of cancer.* Drugs, 1994. **48**(5): p. 794-847.

131. Scripture, C.D., W.D. Figg, and A. Sparreboom, *Peripheral neuropathy induced by paclitaxel: recent insights and future perspectives.* Curr Neuropharmacol, 2006. **4**(2): p. 165-72.

132. Roytta, M., S.B. Horwitz, and C.S. Raine, *Taxol-induced neuropathy: short-term effects of local injection.* J Neurocytol, 1984. **13**(5): p. 685-701.

133. Gelderblom, H., et al., *Cremophor EL: the drawbacks and advantages of vehicle selection for drug formulation.* Eur J Cancer, 2001. **37**(13): p. 1590-8.

134. Hoffman, H., *Polyoxythylenglycerol triricinoleat 35 DAC 1979.* Pharm Zeit, 1984. **129**: p. 1730-3.

135. Hamada, H., et al., *Enhancement of water-solubility and bioactivity of paclitaxel using modified cyclodextrins.* J Biosci Bioeng, 2006. **102**(4): p. 369-71.

136. Park, J.H., et al., *Preparation and evaluation of Cremophor-free paclitaxel solid dispersion by a supercritical antisolvent process.* J Pharm Pharmacol, 2011. **63**(4): p. 491-9.

137. Fox, T.G., *Influence of Diluent and of Copolymer Composition on the Glass Temperature of a Polymer System.* Bull. Am. Phys. Soc, 1956. **1**(123-135).

138. Gordon, M. and J.S. Taylor, *Ideal copolymers and the second-order transitions of synthetic rubbers. i. non-crystalline copolymers.* Journal of Applied Chemistry, 1952. **2**(9): p. 493-500.

139. Couchman, P.R. and F.E. Karasz, *A classical thermodynamic discussion of the effect of composition on glass transition temperatures.* Macromolecules, 1978. **11**(1): p. 117-9.

140. Flory, P.J., ed. *Principle of Polymer Chemistry*. 1953, Cornell University Press: Ithaca.

141. Sun, Y., et al., *Solubilities of crystalline drugs in polymers: an improved analytical method and comparison of solubilities of indomethacin and nifedipine in PVP, PVP/VA, and PVAc.* Journal of pharmaceutical sciences, 2010. **99**(9): p. 4023-31.

142. Gramaglia, D., et al., *High speed DSC (hyper-DSC) as a tool to measure the solubility of a drug within a solid or semi-solid matrix.* Int J Pharm, 2005. **301**(1-2): p. 1-5.

143. Barton, A.F.M., ed. *Handbook of Solubility Parameters and Other Cohesion Parameters*. 2nd ed. 1991, CRC Press, LLC.

144. Qiu, Z., T. Ikehara, and T. Nishi, *Miscibility and crystallization in crystalline/crystalline blends of poly(butylene succinate)/poly(ethylene oxide).* Polymer, 2003. **44**: p. 2799-2806.

145. Qian, F., J. Huang, and M.A. Hussain, *Drug-polymer solubility and miscibility: Stability consideration and practical challenges in amorphous solid dispersion development.* Journal of pharmaceutical sciences, 2010. **99**(7): p. 2941-7.

146. Cheng, S.Z.D., ed. *Phase Transitions in Polymers: The Role of Metastable States*. 1st ed. 2008, Elsevier Science: Amsterdam.

147. Iskandar, M. and S. Krause, *Phase separation instyrene-a-methyl styrene block copolymers.* Polymer Alloys Polymer Science and Technology, 1978. **10**: p. 231-243.

148. Newman, A. and E. Munson, *Characterizing Miscibility in Amorphous Solid Dispersions*, in *American Pharmaceutical Review*. 2012.

149. Ivanisevic, I., S. Bates, and P. Chen, *Novel methods for the assessment of miscibility of amorphous drug-polymer dispersions.* J Pharm Sci, 2009. **98**(9): p. 3373-86.

150. Rumondor, A.C., et al., *Evaluation of drug-polymer miscibility in amorphous solid dispersion systems.* Pharm Res, 2009. **26**(11): p. 2523-34.

151. Nollenberger, K., et al., *Pair distribution function X-ray analysis explains dissolution characteristics of felodipine melt extrusion products.* J Pharm Sci, 2009. **98**(4): p. 1476-86.

152. Newman, A., et al., *Characterization of amorphous API:Polymer mixtures using X-ray powder diffraction.* J Pharm Sci, 2008. **97**(11): p. 4840-56.

153. Pham, T.N., et al., *Analysis of Amorphous Solid Dispersions Using 2D Solid-State NMR and 1H T1 Relaxation Measurements.* Molecular Pharmaceutics, 2010. **7**(5): p. 1667-1691.

154. Vogt, F.G. and G.R. Williams, *Analysis of a nanocrystalline polymer dispersion of ebselen using solid-state NMR, Raman microscopy, and powder X-ray diffraction.* Pharm Res, 2012. **29**(7): p. 1866-81.

155. Ito, A., et al., *Prediction of recrystallization behavior of troglitazone/polyvinylpyrrolidone solid dispersion by solid-state NMR.* Int J Pharm, 2010. **383**(1-2): p. 18-23.

156. Brettmann, B.K., A.S. Myerson, and B.L. Trout, *Solid-state nuclear magnetic resonance study of the physical stability of electrospun drug and polymer solid solutions.* J Pharm Sci, 2012. **101**(6): p. 2185-93.

157. Schachter, D.M., J. Xiong, and G.C. Tirol, *Solid state NMR perspective of drug-polymer solid solutions: a model system based on poly(ethylene oxide).* Int J Pharm, 2004. **281**(1-2): p. 89-101.

158. Yang, M., et al., *Determination of acetaminophen's solubility in poly(ethylene oxide) by rheological, thermal and microscopic methods.* Int J Pharm, 2011. **403**(1-2): p. 83-9.

159. Brostow, W., et al., *Prediction of glass transition temperatures: Binary blends and copolymers.* Materials Letters, 2008. **62**: p. 3152-3155.

160. Seyler, R.J., ed. *Assignment of the glass transition*. 1994, American society for testing and materials: Philadelphia.

161. Menard, K.P., ed. *Dynamic Mechanical Analysis: An Introduction, Technique and Applications*. 1999, CRC Press, LLC.

162. Koike, T., *Determination of glass transition temperature from dielectric analysis for a series of epoxide oligomers.* Journal of Applied Polymer Science, 1992. **45**(5): p. 901-907.

163. Kwei, T.K., *The effect of hydrogen bonding on the glass transition temperatures of polymer mixtures.* Journal of Polymer Science: Polymer Letters Edition, 1984. **22**(6): p. 307-313.

164. Qian, F., et al., *Is a distinctive single Tg a reliable indicator for the homogeneity of amorphous solid dispersion?* International journal of pharmaceutics, 2010. **395**(1-2): p. 232-5.

165. Pinal, R., *Entropy of Mixing and the Glass Transition of Amorphous Mixtures.* Entropy, 2008. **10**: p. 207-233.

166. Baird, J.A. and L.S. Taylor, *Evaluation of amorphous solid dispersion properties using thermal analysis techniques.* Advanced drug delivery reviews, 2012. **64**(5): p. 396-421.

167. Reinemann, D.N., et al., *Vibrational spectroscopy of N-methyliminodiacetic acid (MIDA)-protected boronate ester: examination of the B-N dative bond.* J Phys Chem A, 2011. **115**(24): p. 6426-31.

168. Rubinstein, M. and R.H. Colby, *Thermodynamics of blends and solutions*, in *Polymer Physics*. 2003, Oxford University Press Inc.: New York. p. 137-170.

169. Gabbott, P., *A Practical Introduction to Differential Scanning Calorimetry*, in *Principles and Applications of Thermal Analysis*, P. Gabbott, Editor. 2008, Blackwell Publishing Ltd.

170. Haddadin, R., et al., *Estimation of drug solubility in polymers via differential scanning calorimetry and utilization of the fox equation.* Pharmaceutical development and technology, 2009. **14**(1): p. 18-26.

171. Mahieu, A., et al., *A new protocol to determine the solubility of drugs into polymer matrixes.* Molecular pharmaceutics, 2013. **10**(2): p. 560-6.

172. Oladiran, G.S. and H.K. Batchelor, *Determination of Flurbiprofen Solubility in a Wax-Based Matrix Using Hyperdsc, Higuchi Release Kinetics and Microscopy.* Chemical Engineering Research and Design, 2007. **85**(7): p. 1039-1043.

173. Ahmed, A., et al., *Penciclovir solubility in Eudragit films: a comparison of X-ray, thermal, microscopic and release rate techniques.* Journal of pharmaceutical and biomedical analysis, 2004. **34**(5): p. 945-56.

174. Theeuwes, F., A. Hussain, and T. Higuchi, *Quantitative analytical method for determination of drugs dispersed in polymers using differential scanning calorimetry.* Journal of pharmaceutical sciences, 1974. **63**(3): p. 427-9.

175. Jasti, B.R., et al., *A novel method for determination of drug solubility in polymeric matrices.* Journal of pharmaceutical sciences, 2004. **93**(8): p. 2135-41.

176. Tao, J., et al., *Solubility of small-molecule crystals in polymers: D-mannitol in PVP, indomethacin in PVP/VA, and nifedipine in PVP/VA.* Pharmaceutical research, 2009. **26**(4): p. 855-64.

177. Atkins, P. and J. De Paula, eds. *Physical Chemistry*. 8th ed. 2009, Oxford University Press: Oxford.

178. Friesen, D.T., et al., *Hydroxypropyl methylcellulose acetate succinate-based spray-dried dispersions: an overview.* Molecular pharmaceutics, 2008. **5**(6): p. 1003-19.

179. Rosenbaum, S.E., ed. *Basic Pharmacokinetics and Pharmacodynamics: An Integrated Textbook and Computer Simulations*. 1st ed. 2011, John Wiley & Sons, Inc.: Hoboken.

180. Raghavan, S.L., et al., *Membrane transport of hydrocortisone acetate from supersaturated solutions; the role of polymers.* International journal of pharmaceutics, 2001. **221**(1-2): p. 95-105.

181. Raghavan, S.L., et al., *Crystallization of hydrocortisone acetate: influence of polymers.* International journal of pharmaceutics, 2001. **212**(2): p. 213-21.

182. Rangel-Yagui, C.O., A. Pessoa, Jr., and L.C. Tavares, *Micellar solubilization of drugs.* Journal of pharmacy & pharmaceutical sciences : a publication of the Canadian Society for Pharmaceutical Sciences, Societe canadienne des sciences pharmaceutiques, 2005. **8**(2): p. 147-65.

183. Loftsson, T., M. Masson, and M.E. Brewster, *Self-association of cyclodextrins and cyclodextrin complexes.* Journal of pharmaceutical sciences, 2004. **93**(5): p. 1091-9.

184. Gilmore, C.J., *X-Ray Diffraction*, in *Solid State Characterization of Pharmaceuticals*, R.A. Storey and I. Ymen, Editors. 2011, Blackwell Publishing Ltd.

185. Nichols, G., S. Luk, and C. Roberts, *Microscopy*, in *Solid State Characterization of Pharmaceuticals*, R.A. Storey and I. Ymen, Editors. 2011, Blackwell Publishing Ltd.

186. Hifiker, R., ed. *Polymorphism: in the Pharmaceutical Industry*. 2006, Wiley-VCH Verlag GmbH & Co. KGaA: Weinheim.

187. Marsac, P.J., et al., *Effect of temperature and moisture on the miscibility of amorphous dispersions of felodipine and poly(vinyl pyrrolidone).* Journal of pharmaceutical sciences, 2010. **99**(1): p. 169-85.

188. Karavas, E., et al., *Effect of hydrogen bonding interactions on the release mechanism of felodipine from nanodispersions with polyvinylpyrrolidone.* European journal of pharmaceutics and biopharmaceutics : official journal of Arbeitsgemeinschaft fur Pharmazeutische Verfahrenstechnik e.V, 2006. **63**(2): p. 103-14.

189. Konno, H. and L.S. Taylor, *Influence of different polymers on the crystallization tendency of molecularly dispersed amorphous felodipine.* Journal of pharmaceutical sciences, 2006. **95**(12): p. 2692-705.

190. Teberekidis, V.I. and M.P. Sigalas, *Theoretical study of hydrogen bond interactions of felodipine with polyvinylpyrrolidone and polyethyleneglycol.* Journal of Molecular Structure: THEOCHEM, 2007. **803**(1-3): p. 29-38.

191. Saerens, L., et al., *Raman spectroscopy for the in-line polymer-drug quantification and solid state characterization during a pharmaceutical hot-melt extrusion process.*

European journal of pharmaceutics and biopharmaceutics : official journal of Arbeitsgemeinschaft fur Pharmazeutische Verfahrenstechnik e.V, 2011. **77**(1): p. 158-63.

192. Tumuluri, V.S., et al., *Off-line and on-line measurements of drug-loaded hot-melt extruded films using Raman spectroscopy.* International journal of pharmaceutics, 2008. **357**(1-2): p. 77-84.

193. Triggs, N.E. and J.J. Valentini, *An investigation of hydrogen bonding in amides using Raman spectroscopy.* The journal of physical chemistry, 1992. **96**(17): p. 6922-31.

194. Bellantone, R.A., et al., *A method to predict the equilibrium solubility of drugs in solid polymers near room temperature using thermal analysis.* J Pharm Sci, 2012. **101**(12): p. 4549-58.

195. Henrist, D. and J.P. Remon, *Influence of the process parameters on the characteristics of starch based hot stage extrudates.* Int J Pharm, 1999. **189**(1): p. 7-17.

196. Ghosh, I., et al., *Key considerations for optimization of formulation and melt-extrusion process parameters for developing thermosensitive compound.* Pharm Dev Technol, 2012. **17**(4): p. 502-10.

197. Liu, H., et al., *Effects of extrusion process parameters on the dissolution behavior of indomethacin in Eudragit E PO solid dispersions.* Int J Pharm, 2010. **383**(1-2): p. 161-9.

198. Verhoeven, E., et al., *Influence of formulation and process parameters on the release characteristics of ethylcellulose sustained-release mini-matrices produced by hot-melt extrusion.* Eur J Pharm Biopharm, 2008. **69**(1): p. 312-9.

199. Bley, H., B. Fussnegger, and R. Bodmeier, *Characterization and stability of solid dispersions based on PEG/polymer blends.* Int J Pharm, 2010. **390**(2): p. 165-73.

200. El-Banna, H.M., N.A. Daabis, and S.A. El-Fattah, *Aspirin stability in solid dispersion binary systems.* J Pharm Sci, 1978. **67**(11): p. 1631-3.

201. Hancock, B.C., S.L. Shamblin, and G. Zografi, *Molecular mobility of amorphous pharmaceutical solids below their glass transition temperatures.* Pharm Res, 1995. **12**(6): p. 799-806.

202. Straubinger, R.M., *Biopharmaceutics of paclitaxel (taxol): formulation, activity, and pharmacokinetics*, in *Taxol: Science and Applications*, M. Suffness, Editor. 1995, CRC Press: New York. p. 237-254.

203. Singla, A.K., A. Garg, and D. Aggarwal, *Paclitaxel and its formulations.* Int J Pharm, 2002. **235**(1-2): p. 179-92.

204. Lee, S.C., et al., *Hydrotropic polymeric micelles for enhanced paclitaxel solubility: in vitro and in vivo characterization.* Biomacromolecules, 2007. **8**(1): p. 202-8.

205. Pawar, R., et al., *Intravenous and regional paclitaxel formulations.* Curr Med Chem, 2004. **11**(4): p. 397-402.

206. Terwogt, J.M., et al., *Alternative formulations of paclitaxel.* Cancer Treat Rev, 1997. **23**(2): p. 87-95.

207. Hennenfent, K.L. and R. Govindan, *Novel formulations of taxanes: a review. Old wine in a new bottle?* Annals of Oncology 2006. **17**(5): p. 735-749.

208. Liggins, R.T., W.L. Hunter, and H.M. Burt, *Solid-state characterization of paclitaxel.* J Pharm Sci, 1997. **86**(12): p. 1458-63.

209. Liu, H., et al., *Preparation of budesonide-poly (ethylene oxide) solid dispersions using supercritical fluid technology.* Drug Dev Ind Pharm, 2007. **33**(9): p. 959-66.

210. Li, L., O. AbuBaker, and Z.J. Shao, *Characterization of poly(ethylene oxide) as a drug carrier in hot-melt extrusion.* Drug Dev Ind Pharm, 2006. **32**(8): p. 991-1002.

211. Perissutti, B., et al., *Preparation of extruded carbamazepine and PEG 4000 as a potential rapid release dosage form.* Eur J Pharm Biopharm, 2002. **53**(1): p. 125-32.

212. Biswal, S., et al., *Enhancement of dissolution rate of gliclazide using solid dispersions with polyethylene glycol 6000.* AAPS PharmSciTech, 2008. **9**(2): p. 563-70.

213. Betageri, G.V. and K.R. Makarla, *Enhancement of dissolution of glyburide by solid dispersion and lyophilization techniques.* Int J Pharm, 1995. **126**(1): p. 155-160.

214. Dahlberg, C., A. Millqvist-Fureby, and M. Schuleit, *Surface composition and contact angle relationships for differently prepared solid dispersions.* Eur J Pharm Biopharm, 2008. **70**(2): p. 478-85.

215. Van den Mooter, G., et al., *Physico-chemical characterization of solid dispersions of temazepam with polyethylene glycol 6000 and PVP K30.* Int J Pharm, 1998. **164**(1-2): p. 67-80.

216. Crison, J.R., N.D. Weiner, and G.L. Amidon, *Dissolution media for in vitro testing of water-insoluble drugs: effect of surfactant purity and electrolyte on in vitro dissolution of carbamazepine in aqueous solutions of sodium lauryl sulfate.* J Pharm Sci, 1997. **86**(3): p. 384-8.

217. Curatolo, W., J.A. Nightingale, and S.M. Herbig, *Utility of hydroxypropylmethylcellulose acetate succinate (HPMCAS) for initiation and maintenance of drug supersaturation in the GI milieu.* Pharm Res, 2009. **26**(6): p. 1419-31.

218. Tanno, F., et al., *Evaluation of hypromellose acetate succinate (HPMCAS) as a carrier in solid dispersions.* Drug Dev Ind Pharm, 2004. **30**(1): p. 9-17.

219. Jachowicz, R. and A. Czech, *Preparation and evaluation of piroxicam-HPMCAS solid dispersions for ocular use.* Pharm Dev Technol, 2008. **13**(6): p. 495-504.

220. Lindfors, L., et al., *Nucleation and crystal growth in supersaturated solutions of a model drug.* Journal of colloid and interface science, 2008. **325**(2): p. 404-13.

221. Ilevbare, G.A., et al., *Maitaining Supersaturaton in Aqueous Drug Solutions: Impact of Different Polymer on Induction Times.* Cryst. Growth Des., 2013. **13**(2): p. 740-751.

222. Bevernage, J., et al., *Evaluation of gastrointestinal drug supersaturation and precipitation: strategies and issues.* Int J Pharm, 2013. **453**(1): p. 25-35.

VITA

Jiannan Lu, son of Mrs. Meihua Wang and Mr. Ye Lu, was born on July 23, 1987 in Suqian, Jiangsu, China. In 2004, he received his high school Diploma from Suqian Middle School (Suqian, Jiangsu, China). Thereafter, he received his Bachelor's degree in Pharmaceutical Science emphasized in Basic Pharmacy from China Pharmaceutical University (Nanjing, Jiangsu, China) in 2008.

After graduating with a Bachelor's degree, Mr. Lu was accepted into the Ph.D. program of Pharmaceutical Science with an emphasis on Pharmaceutics in University of Mississippi. He is a member of American Association of Pharmaceutical Sciences (AAPS) and American Chemical Society (ACS). He is also a member of Rho Chi Pharmacy Honor Society. He was the recipient of Center of Research Excellence in Natural Products Neuroscience (CORE-NPN) fellowship (2010). He served as the Chair of American Association of Pharmaceutical Scientists – University of Mississippi Student Chapter (AAPS-UMSC), from 2011-2012. He also completed two internships during his Ph.D. in Abbott Laboratories, Inc. (Chicago, IL, 2012) and SE Tylose USA, Inc. (Totowa, NJ, 2014), respectively.